Das BEM46 Protein in *Neurospora crassa*: Eisosomale Lokalisation und Verknüpfung mit der Tryptophan-abhängigen Auxin-Biosynthese

Dissertation zur Erlangung des Doktorgrades
der Mathematisch-Naturwissenschaftlichen Fakultät
der Christian-Albrechts-Universität zu Kiel

vorgelegt von
Krisztina Kolláth-Leiß
aus Salgótarján (Ungarn)

Kiel, 2014

Referent/in: Prof. Dr. Frank Kempken……...

Korreferent/in: Prof. Dr. Karin Krupinska……..

Tag der mündlichen Prüfung: 14.01.2015……

Zum Druck genehmigt: Kiel, 14.01.2015……..

Der Dekan

„Ausdauer wird früher oder später belohnt. Meist später.“

Wilhelm Busch (1832 - 1908)

für meine Familie

Die unten aufgeführten Publikationen sind Bestandteile der Dissertation. In der vorliegenden Arbeit wird durch römische Nummerierung auf die aufgelisteten Veröffentlichungen verwiesen. Alle diese Arbeiten finden sich im Anhang.

Referierte

(I) **Mercker M, Kollath-Leiß K, Allgaier S, et al.** (2009) The BEM46-like protein appears to be essential for hyphal development upon ascospore germination in Neurospora crassa and is targeted to the endoplasmic reticulum. Curr Genet 55:151–161.

(II) **Kumar A, Kollath-Leiß K, Kempken F** (2013) Characterization of bud emergence 46 (BEM46) protein: sequence, structural, phylogenetic and subcellular localization analyses. Biochem Biophys Res Commun 438:526–32. doi: 10.1016/j.bbrc.2013.07.103

(III) **Kollath-Leiß K, Bönniger C, Sardar P, Kempken F** (2014) BEM46 shows eisosomal localization and association with tryptophan-derived auxin pathway in Neurospora crassa. Eukaryot Cell 13:1051–63. doi: 10.1128/EC.00061-14

Andere

(IV) **Kolláth-Leiß K, Kempken F** (2012) Bem46-Homologe: bekannte Proteine mit unbekannter Funktion. Biospektrum 18:251–253. doi: 10.1007/s12268-012-0170-3

Darlegung des eigenen Anteils an den aufgeführten Schriften

zu (I)

Nachweis der ER-Lokalisation: vollständige Methodenentwicklung, Versuchsdesign, Versuchsdurchführung und Auswertung der Ergebnisse, Erstellen der diesbezüglichen Teile des Manuskripts

zu (II)

Experimenteller Nachweis der Funktionalität des ER-Retentionssignals: vollständige Entwicklung der Konzeption, Methodenentwicklung, Versuchsdesign, Versuchsdurchführung, Auswertung und Diskussion der Ergebnisse, Erstellen der diesbezüglichen Teile des Manuskripts

zu (III)

Phänotypanalysen: vollständige Durchführung der Ascosporen-Keimungsversuche, Datenerhebung, Auswertung, Ergebnisdiskussion, vollständige Konzeptentwicklung der Untersuchungskriterien des vegetativen Myzels, vollständige Durchführung, Auswertung und Diskussion der Ergebnisse, Literaturrecherche

Alternatives Spleißen: phänotypische Untersuchung der die alternativen Fragmente exprimierenden Stämme, vollständige Versuchsdurchführung, Datenerhebung und Auswertung; überwiegende Durchführung, vollständige Datenerhebung, Auswertung und Diskussion der Lokalisationsstudien

Nachweis der eisosomalen Lokalisation: vollständige Konzeptentwicklung, Literaturrecherchen, überwiegende Versuchsdurchführung und Auswertung, vollständige Diskussion

Identifizierung möglicher Interaktionspartner: überwiegende Versuchsdurchführung der *Y2H*-Analysen, vollständige Datenerhebung, Auswertung und Diskussion, vollständige Konzeptentwicklung der *split*-YFP-Analyse, Literaturrecherche, Methodenentwicklung, Versuchsdurchführung, Datenerhebung und Auswertung, Diskussion

Nachweis der Auxin-Produktion von *N. crassa*: vollständige Konzeptentwicklung, Literaturrecherche, überwiegende Methodenentwicklung, vollständige Versuchsdurchführung, Datenerhebung und Auswertung, Diskussion

Quantitativer Indolnachweis: vollständige Konzeptentwicklung, Literaturrecherche, Methodenentwicklung, Versuchsdurchführung, Datenerhebung und Auswertung, Diskussion

Identifizierung des Biosyntheseweges: überwiegende Entwicklung der Konzeption mit Literaturrecherche und ersten Datenbankanalysen, in Teilen Durchführung und Auswertung der Ergebnisse

MTR-Lokalisation: vollständige Konzeptentwicklung mit Literaturrecherche, mehrheitliche Durchführung, überwiegende Auswertung und Diskussion

Erstellen des Manuskripts: (überwiegend)

zu (IV)

Überprüfung der Kolokalisation des BEM46 Proteins mit dem Aktin-Zytoskelett: Vollständige Entwicklung der Konzeption, Literaturrecherche, Methodenentwicklung, Versuchsdesign, Versuchsdurchführung, Auswertung und Diskussion der Ergebnisse, überwiegender Anteil an Erstellung des Manuskripts

Inhaltsverzeichnis

Abbildungsverzeichnis

Abkürzungen

A	Adenin
aa	*amino acid* / Aminosäure
ABHD	α/β-Hydrolase-Domäne
AS	Anthranilat-Synthase
BAR-Domäne	Bin–Amphiphysin–Rvs-Domäne
bem1	Bezeichnung eines Gens (*bud emergence 1*)
bem46	Bezeichnung eines Gens (*bud emergence 46)*
BIFC	Bimolekulare Fluoreszenzkomplementation (*bimolecular fluorescence complementation*)
BLAST	*Basic Local Alignment Search Tool*
bp	Basenpaare
bud5	Bezeichnung eines Gens (*bud emergence 5*)
C	Cytosin
cAMP	zyklisches Adenosinmonophosphat
CAT	*conidial anastomosis tube*
ccg1	Bezeichnung eines Gens (*clock controlled gene*)
cdc24	Bezeichnung eines Gens (*cell division cycle 24*)
cDNA	komplementäre DNA (*copy* DNA)
CLSM	konfokale Laser-Raster-Mikroskopie (*confocal laser scanning microscopy*)
DNA	Desoxyribonukleinsäure
DR5	sythetisches Auxin-responsives Element
eGFP	*enhanced* GFP

ER	Endoplasmatisches Retikulum
FGSC	*Fungal Genetics Stock Center*
G	Guanin
GDP	Guanosindiphosphat
GFP/RFP/YFP	*green/red/yellow fluorescent protein*
GTP	Guanosintriphosphat
GTPase	Guanosintriphosphatase
GUS	β-Glucuronidase
HDEL	Aminosäure-Sequenzmotiv: Histidin-Asparaginsäure-Glutaminsäure-Leucin
his-3	Bezeichnung eines Gens der Histidin-Biosynthese (Imidazoleglycerol-Phosphate-Dehydratase)
HPLC	*high pressure liquide chromatography*
HTAM	N-Hydroxyl-Tryptamin
IAA	Indol-3-Essigsäure
IAAld	Indol-3-Acetaldehyd
iad	Bezeichnung eines Gens (IAAld-Dehydrogenase)
IAM	Indol-3-Acetamid
IAN	Indol-3-Acetonitril
IAOx	Indol-3-Acetaldoxim
IPA	Indol-3-Pyruvat
ipd	Bezeichnung eines Gens (IPA-Decarboxylase)
kb	Kilobasenpaare / Kilobasen
KDEL	Aminosäure-Sequenzmotiv: Lysin-Asparaginsäure-Glutaminsäure-Leucin

ko	*knock-out*
MCC	Plasmamembran-Domäne (*membrane compartment of CAN1)*
mRNA	messenger RNA
mtr	Bezeichnung eines Gens (methyl-Tryptophan resistent)
NMD	*nonsense-mediated mRNA decay*
nt	Nukleotide
PCR	Polymerase-Kettenreaktion *(polymerase chain reaction)*
PHARC	Neurodegenerative Krankheit (*polyneuropathy, hearing loss, ataxia, retinitis pigmentosa, and cataract*)
qRT-PCR	quantitative RT-PCR
RIP	Wiederholung-induzierte Punktmutation (*Repeat-induced point mutation*)
RNA	Ribonukleinsäure
RNAi	RNA-Interferenz
RNase	Ribonuklease
RT-PCR	PCR unter Verwendung des Enzyms reverse Transkriptase
SNARE	Proteinkomplex *(soluble N-ethylmaleimide-sensitive-factor attachment receptor)*
T	Thymin
tam	Bezeichnung eines Gens (Trp-Aminotransferase)
TAM	Tryptamin
TAT	Tryptophan-Permease
TLC	Dünnschicht-Chromatographie *(thin layer chromatography)*
Tol	Indol-3-Ethanol
Trp	Tryptophan

t-SNARE	Transmembran Protein (*target synaptosome-associated protein receptor*)
U	Uracyl
ÜE / OE	Überexpression / *overexpression*
v-SNARE	Transmembran Protein (*vesicle synaptosome-associated protein receptor*)
wt	Wildtyp
Y2H	Hefe-Zwei-Hybrid-System (*Yeast Two-Hybrid System*)

Zusammenfassung

In allen Genomen von eukaryotischen Organismen wird mindestens ein BEM46-Homolog kodiert, jedoch ist die genaue Funktion des Proteins bisher weitgehend unklar. Die geringe über das BEM46 Protein publizierte Datenmenge lässt vermuten, dass BEM46 eine Rolle im polaren Wachstum spielt. Da Ascomyceten als Modellsystem für polares Wachstum fungieren, konzentrieren sich die Untersuchungen der vorliegenden Arbeit auf das BEM46 Protein in *Neurospora crassa*.

In früheren Studien wurden zwei *bem46*-transformante *N. crassa*-Stämme (RNAi-vermittelte *knock-down*- und Überexpressions-Transformante) hergestellt und zum Teil phänotypisch untersucht. Die Transformanten zeigten eine auf 0% reduzierte Ascosporen-Keimungsrate mit einzelnen so genannten *survival* Meiosporen, die ihre Fähigkeit zum polaren Wachstum verloren haben. Nach erfolgreicher Herstellung einer *knock-out*-Mutante wurden die phänotypischen Analysen aller transformanten und mutanten Stämme wiederholt und ausgeweitet. Die Ascosporen-Keimungsrate der *knock-out*-Linie ist um 50% reduziert. Das vegetative Myzelium der Transformanten und der Mutante zeigt normales Hyphenwachstum und Konidiophor-Bildung, jedoch sind die Konidienkeimung und das Wachstum der jungen Hyphen von der *bem46*-Expression beeinflusst. Die Anthranylat-Synthase Komponent II (*trp-1*), die als Enzym einen Schritt der Tryptophan-Biosynthese katalysiert, wurde als Interaktionspartner des BEM46 Proteins in *N. crassa* identifiziert. Die Interaktion wurde durch bimolekulare Fluoreszenzkomplementation (*split-YFP*) *in vivo* bestätigt. Tryptophan dient als Vorläufer diverser Botenstoffe darunter Auxin. Da die Publikationen zur Auxin-Produktion in *N. crassa* nicht über die herkömmlichen Datenbanken erhältlich sind, waren die Ergebnisse in der gegenwärtigen Forschung nicht bekannt. Folglich wurde im ersten Schritt die Fähigkeit des *N. crassa* Wildtyp-Stammes zur Auxin-Biosynthese untersucht und mit Hilfe von indirektem (mit Hilfe von DR5::GUS *A. thaliana* Pflanzen) und direktem (mit Hilfe von Dünnschichtchromatographie) Verfahren nachgewiesen. Durch bioinformatische Analysen wurde ein putativer Auxin-Biosyntheseweg in *N. crassa* identifiziert. Die relative Indolproduktion der *Δtrp-1*- (erhal-

ten über FGSC) und *Δbem46*-Mutante sowie der *bem46*-Transformanten wurde in diversen Entwicklungsstadien ermittelt. Während der Keimungsphase der Asco- und Konidiosporen produzieren die mutanten und transformanten Stämme Auxin in signifikant unterschiedlichen Mengen. Die Expression der für die Enzyme des putativen Biosyntheseweges kodierenden Gene ist auch signifikant abweichend (Bönniger 2013). Die Untersuchungen führen zu dem Ergebnis, dass das BEM46 Protein mit der Auxin-Biosynthese von *N. crassa* verknüpft ist. Obwohl die Ergebnisse eine Verbindung zwischen BEM46 und der Auxin-Biosynthese in *N. crassa* postulieren, scheint die Interaktion komplex und der Wirkungsmechanismus bleibt unbekannt.

Mit Hilfe von PCR und einer anschließenden Sequenzierung wurden Hinweise auf alternatives Spleißen des *bem46*-Transkripts in *N. crassa* gewonnen. Die Wirkung der alternativen Fragmente wurde untersucht und es wurde gezeigt, dass sie für die Reduktion der Ascosporenkeimung in den Transformanten und in der Mutante verantwortlich sind. Der Einfluss der kleinen Transkripte auf die Indolproduktion wurde auch beobachtet.

Es wurde gezeigt, dass das BEM46 Protein von *N. crassa* in dem endoplasmatischen Retikulum sowie in den Eisosomen lokalisiert ist. Auch der neutrale Aminosäuren-Transporter MTR wurde in den Eisosomen von *N. crassa* nachgewiesen.

Die Ergebnisse der vorliegenden Arbeit deuten darauf hin, dass das BEM46 Protein von *N. crassa* an dem Kreuzungspunkt von Tryptophan-Aufnahme und intrazellulärer Tryptophan-abhängiger Auxin-Biosynthese agiert und über die Auxin-Produktion das polare Wachstum des Pilzes abhängig von den Entwicklungsstadien beeinflusst.

Summary

Although every eukaryotic organism possesses at least one gene coding for a BEM46 homologues protein, the function of BEM46 is not fully understood. Limited information has been published about BEM46 in different organisms, but all of these suggest a function of BEM46 in maintaining polar growth. Hence, ascomycetes serve as a model system for polar growth: Our investigations focus on the BEM46 protein of *Neurospora crassa*.

In former studies, two *bem46* transformant strains (RNAi mediated knock-down and overexpression transformants) were generated and partly phenotypically analysed. The transformants show a loss of ascospore germination with a typical loss-of-polarity phenotype, observed by single survival ascospores. After successfully generating the *bem46*-knock-out mutant strain, the phenotypical analyses were extended and repeated. The *bem46* mutant strain shows only a slight reduction of ascospore germination. Vegetative mycelia of *bem46* transformant and mutant strains show normal hyphal and conidiophore development. However, conidial germination and elongation of young hyphae is influenced by *bem46* expression. The anthranilate synthase component II (*trp-1*), an enzyme that catalyses a step in the tryptophan-biosynthesis, was identified as an interacting partner of BEM46 in *N. crassa*. The interaction was confirmed by bimolecular fluorescence complementation (split-YFP) assay. Tryptophan acts amongst others as a precursor for several messenger substances including auxin. As the publications about auxin production in *N. crassa* are not available in common databases, the results of these studies have not been established in actual scientific research. Therefore, the auxin biosynthetic capability of *N. crassa* wild type strain was verified by direct (thin layer chromatography) and indirect (using *A. thaliana* DR5::GUS seedlings) approaches. A putative biosynthetic pathway was identified using bioinformatics tools. The relative indole production of the Δ*trp-1* (available at FGSC) and Δ*bem46* mutants, as well as the *bem46* transformant strains, was determined in different developmental stages of *N. crassa*. During the germination of asco- and conidiospores, the auxin production significantly varied in the different strains. The expression of the genes coding for the enzymes of the putative biosynthetic pathway was also significantly altered (Bönniger 2013). The analyses

led to the result that there is a connection between BEM46 and auxin biosynthesis in *N. crassa*. Although, an influence of BEM46 on the auxin production of *N. crassa* seems to be evident, the way in which it reacts appears to be complex and remains elusive.

Evidence for an alternative splicing of the *bem46* transcript in *N. crassa* was provided by PCR and subsequent sequencing. The influence of the alternative spliced products was investigated and results showed that the alternative fragments are responsible for the loss of ascospore germination in the transformant strain. In addition, their influence on the indole production was observed.

It was shown that BEM46 of *N. crassa* is localised to the perinuclear endoplasmic reticulum and to the eisosomes. An additional protein, the neutral amino acid transporter MTR, was also detected in the eisosomes.

Based on the results of the investigations, it is hypothesised that BEM46 acts at the crossing point of indole uptake and biosynthesis in *N. crassa.* Additionally, it influences polar growth in different developmental stages, by affecting the auxine production of the fungus.

1. Einführung

1.1 Das *bud emergence 46* (BEM46) Protein

Das BEM46 Protein gehört zu der Superfamilie der α/β-Hydrolasen, die durch die α/β-Hydrolase-Domäne charakterisiert wird (Ollis et al. 1992; Nardini and Dijkstra 1999). Sie besteht aus fünf bis acht β-Faltblättern, die durch α-Helices zu einem α/β/α-Sandwich verbunden werden. Die zu der Superfamilie gehörigen Proteine sind sowohl hinsichtlich ihrer Enzymaktivität als auch ihrer Substratspezifität sehr vielfältig. So befinden sich unter anderem Carboxysäureesther-Hydrolasen, Lipid-Hydrolasen, Halo-Peroxidasen oder Dehalogenasen unter den Mitgliedern, von denen mehr als 30000 in der ESTHER-Datenbank aufgeführt sind (Lenfant et al. 2013).

Die Tertiärstruktur des BEM46 Proteins von *N. crassa* wurde durch bioinformatische Analysen modelliert (Arbeit II). Das Protein besitzt eine α/β-Hydrolase-Domäne, die aus acht β-Faltblättern aufgebaut ist, und eine zusätzliche Region am N-terminalen Ende aus jeweils zwei β-Faltblättern und α-Helices aufweist. Die Aminosäuren 186G-189L wurden als putative Ligand-Bindestellen, 188S, 262D und 292H als kritische Aminosäurereste des Reaktionszentrums identifiziert.

Die BEM46 Proteine sind innerhalb des eukaryotischen Reiches konserviert, das heißt das Genom jedes eukaryotischen Organismus' kodiert für mindestens ein Homolog des Proteins (Harris and Momany 2004; Arbeit II). Durch Sequenzvergleich-Analysen der Proteine wurden *Indels* (Insertions-/Deletions-Polymorphismen) identifiziert, die für die Diversität der BEM46-Homologe verantwortlich sind, wobei der wesentliche Aufbau der BEM46-Struktur konserviert bleibt (Arbeit II). Vertebraten besitzen mehrere *bem46*-Paraloge, die durch Duplikationsereignisse entstanden sind. Die BEM46-Homologe in Säugetieren gehören zu der ABHD (*α/β-hydrolase domain*)-Familie und spielen eine wichtige Rolle im Lipid-Stoffwechsel und in der Lipid–Signaltransduktion (Holmquist 2000). Mutationen im menschlichen *abhd12* Gen, die zum vollständigen Funktionsverlust des kodierten Proteins führen, verursachen die selte-

ne neurodegenerative Erbkrankheit PHARC (*polyneuropathy, hearing loss, ataxia, retinitis pigmentosa, and cataract*, Fiskerstrand et al. 2010).

Trotz ihres universellen Vorkommens gibt es lediglich Hinweise auf die exakte Funktion von BEM46, weshalb das für das Protein kodierende Gen zu den TOP10 der bekannten Genen mit unbekannter Funktion zählt (Galperin and Koonin 2004; Galperin and Koonin 2010).

Es gibt bisher nur wenige Arbeiten, die sich mit dem BEM46 Protein befassen, die nachfolgend zusammenfassend dargestellt werden. In der **Abbildung 1** ist der Aufbau von fünf BEM46-Homologen in verschiedenen Organismen schematisch abgebildet (Mochizuki et al. 2005a). Alle Proteine besitzen eine α/β-Hydrolase- und, mit Ausnahme des BEM46 Proteins aus *N. crassa,* auch eine Transmembran-Domäne. Die Proteine in den Organismen *A. thaliana*, *N. crassa* und *M. musculus* verfügen darüber hinaus über ein Signalpeptid.

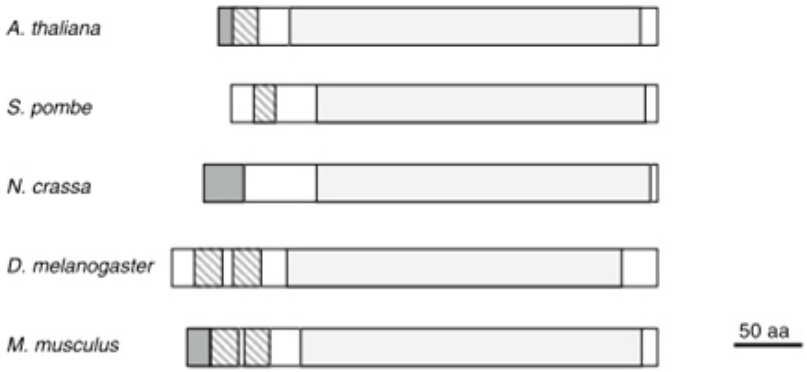

Abbildung 1: Schematische Darstellung der BEM46-Aminosäuresequenz in unterschiedlichen Organismen (verändert nach Mochizuki *et al.*, 2005). Hellgrau: α/β-Hydrolase-Domäne, dunkelgrau: Signalpeptid, gestreift: Transmembran-Domäne

Das *bem46* Gen von *Schizosaccharomyces pombe* wurde als Supressor einer *bem1*/*bud5* Doppelmutante von *Saccharomyces cerevisiae* beschrieben (Valencik and Pringle 1995). BEM1 ist ein Gerüstprotein mit mehreren Interaktionspartnern, darunter Actin, CDC42, BUD5 und BUD1 (Chant et al. 1991; Chenevert et al. 1992; Park et al. 1997; Cabib et al. 1998; Irazoqui et al. 2003). Das Protein spielt eine wichtige Rolle in der Positionierung des Polarisom-Proteinkomplexes während der Keimung (Cabib et al. 1998). BUD5, das eine essentiel-

le Rolle in der Festlegung der Position der Keimungsstelle spielt, ist ein GDP-GTP-Austausch-Faktor für BUD1 (Chant et al. 1991). Die *bem1*/*bud5* Doppelmutante zeigt eine fehlerhafte Zellpolarisation und Keimung (Cabib et al. 1998; Madden and Snyder 1998). Das zu BEM46 homologe Protein in *S. cerevisiae* (YNL320W) wurde als nicht essentiell beschrieben (Giaever et al. 2002).

In *Drosophila melanogaster* wurde das RAPSYNOID Protein als Interaktionspartner für das BEM46-Homolog durch das Hefe-Zwei-Hybrid-System (Y2H) identifiziert (Giot et al. 2003). RAPSYNOID ist ein GDP-GTP-Austausch-Faktor für das Protein Gα. Es ist in der Kontrolle der asymmetrischen Zellteilung involviert (Parmentier et al. 2000).

Das WAVY GROWTH2 (*At5g20520*) Protein ist das BEM46-Homolog von *Arabidopsis thaliana*. Die *Δwavy growth2*-Mutante entwickelt kürzere Wendungen an der Wurzelspitze (Okada and Shimura 1990), wodurch die Wurzel etwas kürzer als die von der Wildtyp Pflanze erscheint. Das Protein besitzt sowohl eine Transmembran-Domäne als auch ein Signalpeptid und ist intrazellulär in der Plasmamembran und in den Membranen anderer Kompartimente lokalisiert (Mochizuki et al. 2005b). Es wird hauptsächlich in jungen Keimlingen und in der Wurzel adulter Pflanzen exprimiert. WAVY GROWTH2 gilt als ein allgemeiner Regulator, der als Reaktion auf mechanische Reize, Licht- oder Gravitationsstimuli die Wurzelspitzenrotation negativ kontrolliert.

Die genannten Literaturdaten deuten darauf hin, dass das BEM46 Protein in der Aufrechterhaltung der Zellpolarität eine Rolle spielt.

1.2 Die Ausbildung der Zellpolarität

Die Asymmetrie der Zellform, der Zellfunktionen oder der Verteilung intrazellulärer Komponenten wird als Zellpolarität bezeichnet. Die meisten Zellen von einfachen Bakterien bis hin zu multizellulären Vertebraten sind in der Lage, sich polar zu entwickeln. Dabei dient die entstandene Polarität unterschiedlichen Zwecken, darunter der Kommunikation über lange Stre-

cken (Neuronen (Cáceres et al. 2012)), der Entstehung ungleicher Tochterzellen (Stomata-Entwicklung (Facette and Smith 2012)) oder der Aufrechterhaltung einer Barriere zwischen unterschiedlichen biologischen Räumen (Epithelien (Wang et al. 1990)). Obwohl die Resultate sehr unterschiedlich sein können, sind die Kernmechanismen der Entwicklung der Polarität unter allen Organismen evolutionär konserviert (Nelson 2003). Hierzu gehört die Determinierung des Ortes der auszubildenden Polarität an der Plasmamembran mittels spezifischen kortikalen Marker, die Anordnung des Zytoskeletts mit Hilfe von Gerüstproteinen und die Mobilisierung sowie Transport benötigter Proteine zur Plasmamembran.

Die genaue Maschinerie des polaren Wachstums wurde in den Hefen *S. cerevisiae* und *S. pombe* detailliert studiert. Kortikale Positionsmarker der Ras-GTPase-Familie bestimmen die Position der auszubildende Polarität während der Knospung und der Paarung (*mating*). Das konservierte CDC42 Protein spielt eine zentrale Rolle in der Übertragung der Positionsinformation an verschiedene Effektoren - darunter an dem Polarisom -, die für die Organisation der morphogenetischen Maschinerie, welche das Zytoskelett und den sekretorischen Apparat umfasst, verantwortlich sind. Die sekretorischen Vesikel werden entlang den Bahnen des Actin-Zytoskeletts zu dem Proteinkomplex Exocyst transportiert, bevor sie schließlich mit der Plasmamembran mittels v-SNARE/t-SNARE-Interaktion fusionieren (Chang and Peter 2003; Park and Bi 2007).

1.3 Der Mechanismus des polaren Wachstums filamentöser Pilzhyphen

Polares apikales Spitzenwachstum ist ein Charakteristikum filamentöser Pilzhyphen. Es findet in zwei distinkten Entwicklungsstadien des vegetativen Lebenszyklus statt: erstens während der Auskeimung der Hyphen aus den Konidio- und Ascosporen, zweitens während der Entstehung einer neuen Verzweigung im Pilzmyzelium (Harris and Momany 2004). Wird die Polarität erst einmal ausgebildet, wird sie kontinuierlich aufrechterhalten (Steinberg 2007). Obwohl die konservierten Mechanismen der polaren Entwicklung, die für Hefen im Detail beschrieben wurden, auch für Hyphenpilze zutreffen, gibt es zwei Besonderheiten; nämlich

die Fähigkeit der multiplen Achsenentwicklung und die extrem hohe Elongationsgeschwindigkeit, die mit dem Hefe-Modell nicht zu erklären sind. Die in Hefe wirkenden Positionsmarker sind in Ascomyceten wenig konserviert oder gar nicht vorhanden (Harris and Momany 2004). Welche Mechanismen den Ort der auszubildenden Polarität in Hyphenpilzen festlegen, bleibt weiterhin unklar. Die Positionsinformation wird zunächst auf das Polarisom-Proteinkomplex (Steinberg 2007), das neben Formine diverse Gerüstproteine enthält, übertragen und durch die konservierte Rho-GTPase CDC42 auf die morphogenetische Maschinerie transferiert. Die Regulierung des Prozesses erfolgt mit Hilfe von Lipid-Rafts (Fischer et al. 2008). Das rapide Spitzenwachstum der Hyphen, das in *N. crassa* 1µm/s (Seiler and Plamann 2003) beträgt, wird vom Spitzenkörper angetrieben (Sudbery 2008). Der Spitzenkörper ist eine dynamische Struktur aus mehreren Proteinkomplexen, darunter das Polarisom (Harris et al. 2005). Der Myosin-basierte Vesikeltransport entlang der Aktin-Bahnen endet im Spitzenkörper, der somit als Vesikel-Reservoir für die kontinuierlich wachsende Hyphenspitze fungiert (Harris and Momany 2004). Da der Spitzenkörper am Hyphenspitze fixiert ist (Bartnicki-Garcia et al. 1989; Bartnicki-Garcia et al. 1995; Sudbery 2008), reicht gemäß mathematischer Modelle ein räumlich gleichmäßiger Fluss sekretorischer Vesikel vom Spitzenkörper zur Plasmamembran aus, um die Polarität am apikalen Ende aufrechtzuerhalten. Die Wiederverwertung der Positionsmarker bzw. der Elemente der morphogenetischen Maschinerie erfolgt über Endozytose. In diesem Prozess wird die Rolle von *actin patches* diskutiert (Engqvist-Goldstein and Drubin 2003; Read and Kalkman 2003; Harris and Momany 2004).

2. Charakterisierung des BEM46 Proteins aus *Neurospora crassa*

Im Rahmen einer vorherigen Diplomarbeit (Mercker 2006a) wurden verschiedene *Neurospora crassa*-Stämme mit unterschiedlichem *bem46*-Hintergrund hergestellt, die in weiteren Experimenten der vorliegenden Arbeit verwendet wurden. Die Erzeugung der RNAi-vermittelten *knock-down*- (Nct289) und Überexressions- (Nct288) Transformanten ist in der Arbeit I beschrieben. Darüber hinaus lag ein GFP-gekoppelter BEM46-Überexpressions-Stamm (Nct293) für Lokalisationsstudien zur Verfügung (s. Arbeit I).

2.1 Phänotypische Analysen der *bem46*-Transformanten und der mutanten Stämme

Die ersten phänotypischen Analysen der *bem46-knock-down*- und Überexpressions-Stämme wurden im Rahmen einer vorherigen Diplomarbeit durchgeführt ((Mercker 2006b); Arbeit I). Die Untersuchungen führten zu dem Ergebnis, dass sowohl die Überexpression als auch die Herunterregulierung der *bem46*-Transkriptmenge die Ascosporenkeimung beeinflusst. Die Keimungsrate der beiden Stämme war, verglichen mit dem Wildtyp, auf 0% reduziert (Arbeit I, Abbildung 6b; Arbeit III, Abbildung 1). Hellfeldaufnahmen zeigten vereinzelt Ascosporen, bei denen die Keimungsschläuche zwar ausgetreten sind, aber nicht die für den Wildtyp spezifischen langen, polar wachsenden Hyphen bildeten, sondern als blasenartige Strukturen blieben und kurz nach dem Austreten das Wachstum einstellten (Arbeit I, Abbildung 5a-b), was auf die verlorene Fähigkeit der transformanten Hyphen zum polaren, gerichteten Wachstum hindeutet (*loss-of-polarity phenotype*).

Da eine *Δbem46* Mutante im *Fungal Genetics Stock Center* (FGSC, Kansas City, Missouri, USA) nicht erhältlich war, wurde diese in der Arbeitsgruppe selbst hergestellt (Arbeit III, *supplementary*). Nachdem die Mutante zur Verfügung stand, wurden die phänotypischen Analysen mit allen drei Stämmen (RNAi (NcT289), Überexpression (NcT288) und *knock-out* (Nct411)) wiederholt (Arbeit III). Die Abwesenheit des *bem46*-Transkripts führte lediglich zu einer um 50% reduzierten Ascosporenkeimung (Arbeit III, Abbildung 1; **Abbildung 2A**), wobei einzelne Ascosporen den oben beschriebenen *loss-of-polarity*-Phänotyp zeigten (**Abbildung 2B**).

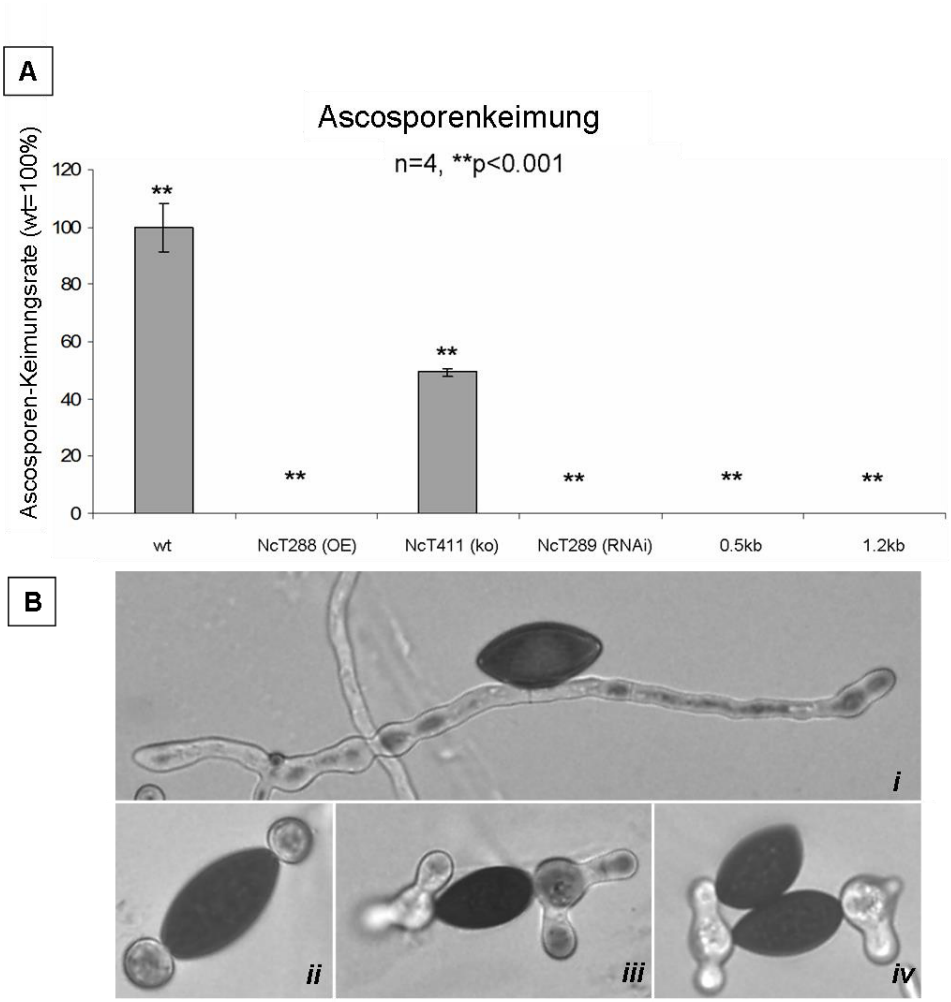

Abbildung 2: Unterschiede in der Ascosporen-Keimungsrate (**A**) und in der Morphologie der keimenden Ascosporen (**B**) des Wildtyps (***i***) und der Transformanten (***ii-iv***). wt, Wildtyp; NcT288 (OE), *bem46*-Überexpressionsstamm; NcT289 (RNAi), *bem46-knock-down*-Stamm; NcT411 (ko), *bem46-knock-out*-Stamm; 0.5kb, der Stamm überexprimiert ein 0,5kb-großes alternativ gespleißtes *bem46*-Fragment; 1.2kb, der Stamm überexprimiert ein 1,2kb-großes alternativ gespleißtes *bem46*-Fragment

Weiterhin wurden Unterschiede hinsichtlich der Morphologie des vegetativen Myzels festgestellt (**Abbildung 3A-B**). Die Konidien der *knock-out*-Mutante und der RNAi-Transformante keimten früher als der Wildtyp aus und die zum Wildtyp relative Wachstumsrate der jungen Hyphen war erhöht. Dagegen zeigten die Konidien des Überexpressions-Stammes eine verzögerte Keimung und die Elongation der jungen Hyphen war deutlich reduziert (Arbeit III, Abbildung 9D). Darüber hinaus führte die Überexpression des *bem46*-Transkripts zu weniger gebildeten aeralen Hyphen und eine veränderte Morphologie des Myzels im Flüssigmedium.

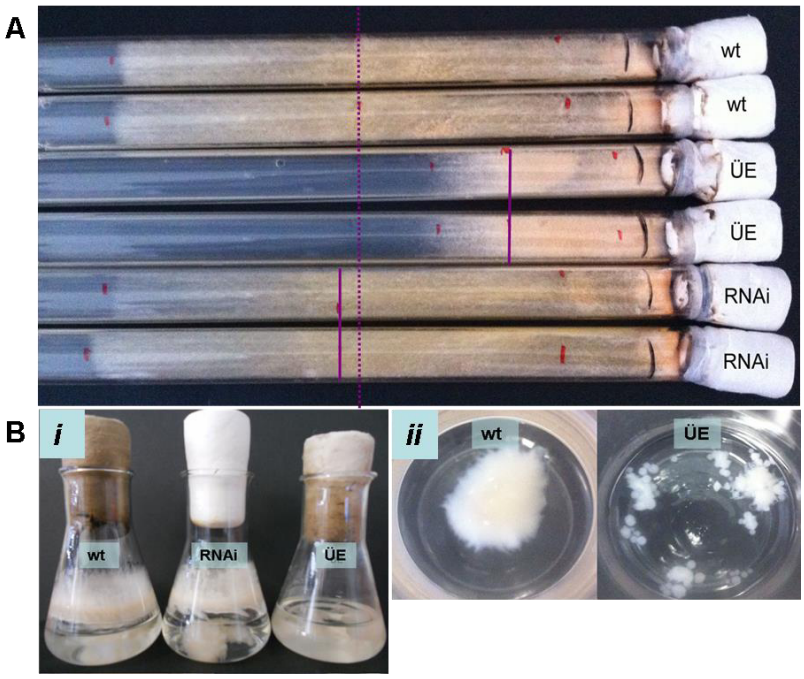

Abbildung 3: Phänotypische Veränderungen des vegetativen Myzels der *bem46*-Transformanten auf Fest- (**A**) und im Flüssigmedium (**B**). (**A**) Die Wachstumsgeschwindigkeit der Hyphen wurde mit Hilfe von Laufrohren bestimmt. Die Pilze wuchsen auf festem Minimalmedium drei Tage. Die violettfarbenen Linien markieren die Wachstumsfront nach zwei Tagen. Zu diesem Zeitpunkt waren die Unterschiede in der Wachstumsrate der jungen Hyphen zwischen den einzelnen Transformanten am größten. Die gestrichelte Linie repräsentiert das Wachstum des Wildtyps nach zwei Tagen. (**B*i***) Das Myzel der Überexpressions-Transformante bildet keine aerale Hyphen; es ist nicht in der Lage, an der Flaschenwand hochzuwachsen. (**B*ii***) Das Myzel der Überexpressions-Transformante bildet im Unterschied zum Wildtyp mehrere feste runde Kolonien.

2.2 Die intrazelluläre Lokalisation des BEM46 Proteins *in N. crassa*

Um die intrazelluläre Lokalisation des BEM46 Proteins zu untersuchen, wurde ein *N. crassa*-Ausgangsstamm (FGSC #6103)[1] mit einem Expressionsvektor transformiert, der die *egfp* gekoppelte *bem46*-Gensequenz unter der Kontrolle des starken *ccg1*-Promotors enthält (pMM536). Die Transformante wurde mittels konfokalem Laser-Raster-Mikroskop (CLSM) untersucht (Arbeit I).

[1] Die Histidin-auxotrophen Stämme FGSC #6103 und FGSC #9716 fungierten als Ausgangsstämme für Transformationsexperimente und wurden in der vorliegenden Arbeit als „Wildtyp"-Kontrolle verwendet.

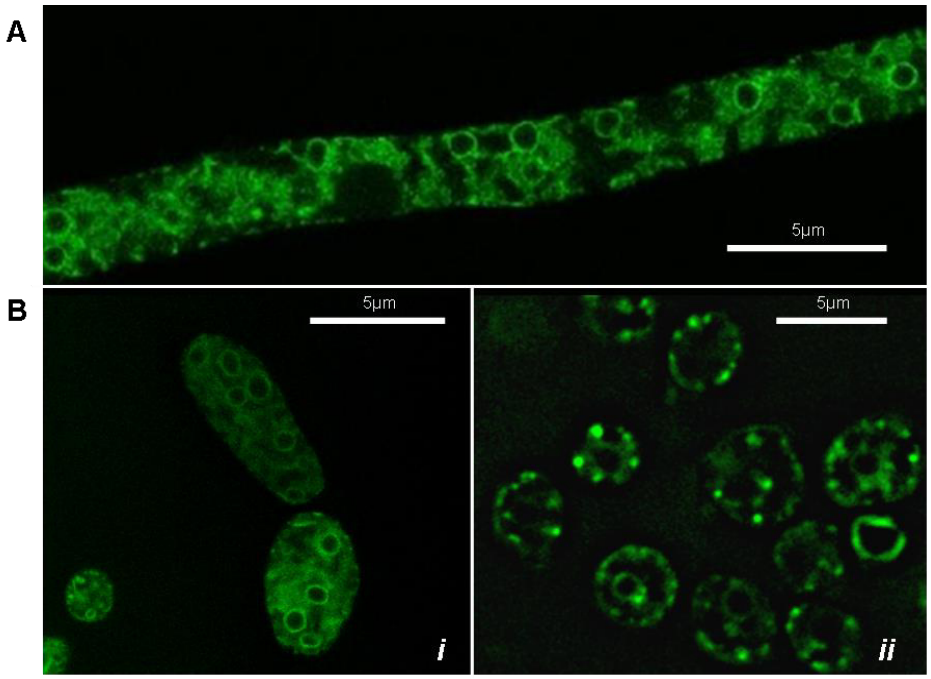

Abbildung 4: Die intrazelluläre Lokalisation des BEM46::eGFP Proteins. CLSM-Aufnahmen von einer jungen Hyphe (**A**) bzw. von Makrokonidien (**B**). Die Fokusebene der Aufnahmen wurde entweder im Bereich der perinukleären-ER (***i***) oder im Bereich der kortikalen, punktförmigen Strukturen (***ii***) eingestellt.

Das BEM46::eGFP Protein ist in ringförmigen Strukturen um den Kern und punktuell nahe der Plasmamembran (**Abbildung 4A-B**) lokalisiert. Mit Hilfe von für das endoplasmatische Retikulum spezifischem Farbstoff ER-Tracker Red wurden die ringförmigen Strukturen als das perinukleäre ER identifiziert (Arbeit I, Abbildung 7). Da für die Lokalisation im ER ein ER-Retentionssignal am C-terminalen Ende der Proteinsequenz notwendig ist, wurde die primäre Aminosäuresequenz des BEM46 Proteins bioinformatisch untersucht (Arbeit II). Das typische Signal ist nach dem Muster [KRHQSA]-[DENQ]-E-L (Lewis and Pelham 1990) aufgebaut, wobei auch weitere, hiervon abweichende Aminosäurekombinationen vorkommen (Raykhel et al. 2007). Am C-terminalen Ende der Aminosäuresequenz des BEM46 Proteins wurde zunächst ein putatives Retentionssignal (PEKK) identifiziert, das aber weder den typischen noch den neu identifizierten Aminosäureabfolgen entspricht (Arbeit II). Um die Funktionsfähigkeit der PEKK-Sequenz als Retentionssignal zu überprüfen, wurde der für die Lokalisationsstudien verwendete Vektor pMM536 mittels *in vitro*-Deletion modifiziert (Arbeit II, Abbildung 3A). Der so entstandene Vektor, der für das eGFP-gekoppelte BEM46 Protein

ohne das putative Retentionssignal kodiert, wurde in *N. crassa* transformiert und die intrazelluläre Lokalisation des Fusionsproteins wurde mit Hilfe von CLSM analysiert (Arbeit II, Abbildung 3C-D). Das BEM46 Protein ohne das putative Retentionssignal wurde nicht im perinukleären ER detektiert, was die Funktionsfähigkeit der PEKK-Aminosäureabfolge als ER-Retentionssignal bestätigt.

Färbungen mit dem Membranfarbstoff SynaptoRed lieferten keine Hinweise darauf, dass die punktförmigen Strukturen Vesikel sein könnten (Arbeit I, Abbildung 7a*iii*). Da das BEM46 Protein in Hefe eine putative Rolle im polaren Wachstum spielt (s. Einleitung 1.1) und das Aktin-Zytoskelett ebenfalls in diesem Prozess involviert ist, wurde vermutet, dass die kortikalen Punkte *actin patches*, welche Strukturen die Anknüpfungspunkte des Zytoskeletts an der Plasmamembran sind (Berepiki et al. 2010), sein könnten. Um diese Hypothese zu überprüfen, wurde ein heterokaryotischer *N. crassa*-Stamm hergestellt, der sowohl das BEM46::eGFP als auch das Lifeact::tRFP (Berepiki et al. 2010) Protein überexprimiert. Die Lokalisation der beiden Proteine wurde mit Hilfe von CLSM analysiert (Arbeit IV).

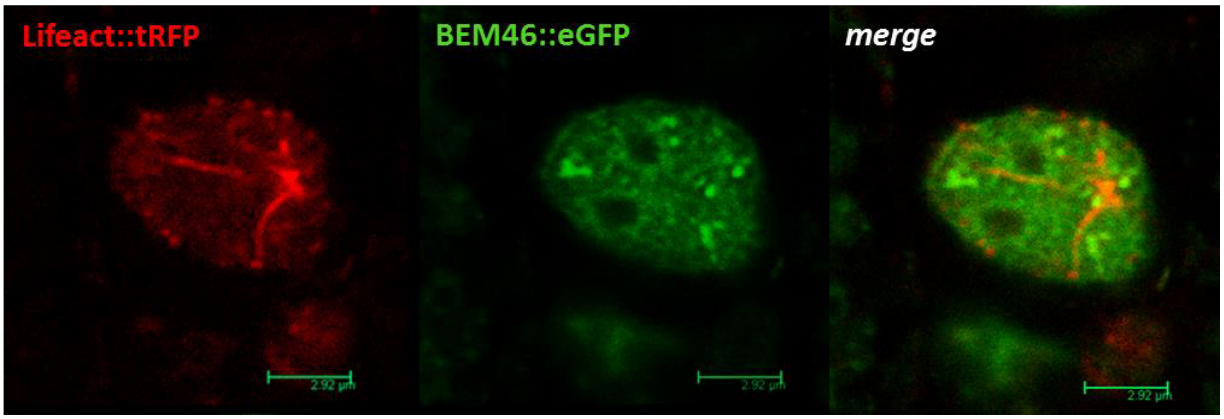

Abbildung 5: CLSM-Aufnahmen eines Makrokonidiums, das sowohl das tRFP-gekoppelte Lifeact (**Lifeact::tRFP**) als auch das eGFP-gekoppelte BEM46 (**BEM46::eGFP**) Protein überexprimiert. Die Überlagerung beider Fluoreszenzsignale (***merge***) zeigt keine Kolokalisation des Aktin-Zytoskeletts und des BEM46 Proteins.

Wie **Abbildung 5** zeigt, wurde keine Kolokalisation der beiden Signale beobachtet, was die Identität der punktförmigen Strukturen als *actin patches* ausschließt. Als weitere Möglichkeiten wurden *lipid rafts* oder Eisosomen in Betrachtung gezogen. *Lipid rafts* sind sehr dynamische Mikrodomänen in der Plasmamembran, die einen selektiven Transport von Lipiden und Proteinen ermöglichen (Edidin 2003). Sie beeinflussen diverse inter- und intrazelluläre Prozesse, darunter die Zell-Zell Interaktion, den Membran-Transport, die Stressreaktion und das polarisierte Wachstum (Malinsky et al. 2013). Im Gegensatz zu *lipid rafts* sind Eisosomen sehr stabile Proteinkomplexe am Zellkortex. Um die Stabilität der kortikalen Strukturen zu untersuchen, wurden Langzeitaufnahmen von quellenden Macroconidien des BEM46::eGFP überexprimierenden Stammes angefertigt (Arbeit III, Abbildung 3A). Da die kortikalen Punkte über einen Zeitraum von 15 Minuten stabil waren, wurden *lipid rafts* ausgeschlossen und die folgenden Experimente fokussierten sich auf die putative eisosomale Identität der Strukturen.

2.3 Die eisosomale Lokalisation des BEM46 Proteins von *N. crassa*

Eisosomen (εισω: griech. für „hinein“) wurden zuerst in der Hefe *Saccharomyces cerevisiae* (Walther et al. 2006) als stabile, kortikale, mit der MCC (*membrane compartment of CAN1*)-Domäne der Plasmamembran assoziierte Proteinkomplexe beschrieben (Grossmann et al. 2008). Die MCC-Domäne bildet furchenähnliche Invaginationen von 50 nm Tiefe und 200-300 nm Länge (Strádalová et al. 2009) und enthält außer dem Arginin-Transporter CAN1 weitere Symporter wie FUR4 (Uracil-Kation-Symporter (Jund et al. 1988)) oder TAT2 (Tryptophan- und Tyrosin-Permease (Schmidt et al. 1994)). Proteine, die im Bereich der MCC-Domänen lokalisiert sind, bleiben geschützt vor Endozytose, die ausschließlich an MCC-freien Orten stattfindet. Die Verbindung zwischen den MCC-Domänen und den Eisosomen wird über das Transmembranprotein SUR7 realisiert. Die Eisomen von *S. cerevisiae* sind in allen Stadien des Zellzyklus als stabile, kortikale, punktförmige Strukturen vorhanden (Walther et al. 2006). Die Hauptkomponenten des Proteinkomplexes sind die zytosolischen PIL1 und LSP1 Proteine. Obwohl die primären Aminosäuresequenzen dieser Proteine zu 72% identisch sind, erfüllen sie keine redundanten Funktionen. In *S. cerevisiae* ist PIL1 essentiell für die Lokalisation von LSP1 und SUR7 und dadurch für die Organisation der Eiso-

somen. Das Protein NCE102 beeinflusst die Stabilität des Proteinkomplexes. Walther et al. (2006) postulierten eine direkte Beteiligung der Eisosomen an der Festlegung der Endozytose-Orte. Diese These wurde jedoch in späteren Studien nicht bestätigt bzw. widerlegt (Grossmann et al. 2008; Vangelatos et al. 2010; Reijnst et al. 2011; Seger et al. 2011). Untersuchungen der Eisosomen von *Schizosaccharomyces pombe* (Kabeche et al. 2011), *Candida albicans* (Reijnst et al. 2011), *Ashbya gossypii* (Seger et al. 2011) und *Aspergillus nidulans* (Vangelatos et al. 2010) haben ergeben, dass PIL1 und LSP1 im gesamten Reich der Pilze konserviert sind und PIL1 eine wichtige, aber nicht immer essentielle Rolle in der Eisosom-Bildung spielt. Während die Δ*pil1*-Mutation in *C. albicans* letal ist, führt sie in *S. pombe* zu keinen erkennbaren phänotypischen Veränderungen, obwohl die Überexpression des Proteins die Zellteilung und die Ausbildung der Zellpolarität negativ beeinflusst. Eisosomen wurden bisher in allen untersuchten Organismen als sehr stabile, fast statische, kortikale Punkte charakterisiert, dennoch kommen sie in unterschiedlichen Stadien des Generationswechsels der einzelnen Pilze vor. In *S. cerevisiae* und *C. albicans* sind Eisosomen kontinuierlich vorhanden. Dagegen wurden sie in *A. gossypii* und in *A. nidulans* lediglich in gequollenen bzw. keimenden Konidien beobachtet. In den zuletzt genannten Pilzen korrespondiert die Genexpression des PIL1 Proteins mit der Eisosomen-Formation. Die höchste *pil1*-Transkript-Menge wurde in Konidien gemessen. Neue Untersuchungen haben in den PIL1- und LSP1-Orthologen eine sogenannte BAR-Domäne (*Bin/amphiphysin/Rrs*) identifiziert (Ziółkowska et al. 2011; Olivera-Couto et al. 2011). Die bananenförmige Domäne besteht aus drei langen α-Helices und besitzt einen positiv geladenen Fleck an der konkaven Oberfläche, der die Interaktion mit der negativ geladenen Plasmamembran ermöglicht. Als Dimere verursachen BAR-Domänen eine Krümmung der Membran, was zur Clusterbildung von Lipiden und Proteinen in der Membran führt.

Die putative eisosomale Lokalisation des BEM46::eGFP Proteins wurde durch Kolokalisationsstudien mit einem RFP-gekoppelten eisosomalen Protein überprüft (Arbeit III). Das PILA Protein ist in dem mit *N. crassa* verwandten Ascomyceten *Aspergillus nidulans* als PIL1-Homolog (s. o.) beschrieben (Vangelatos et al. 2010). Entsprechend wurde das PILA-

Homolog in *N. crassa* mit Hilfe von pBLAST-Analysen bioinformatisch identifiziert. Das für das Protein kodierende Gen wurde an *trfp* gekoppelt in einen Überexpressionsvektor für *N. crassa* unter der Kontrolle des *ccg1*-Promotors kloniert und in den *N. crassa*-Stamm FGSC #6103 transformiert. Um die Kolokalisation mehrerer fluoreszent markierten Proteine zu überprüfen, gibt es in *N. crassa* neben der Möglichkeit der Kotransformation eine einfachere Methode, die Heterokaryonbildung. Da die Septi der Hyphen diskontinuierlich sind, die sogar den Transport von Zellkernen erlauben, ist das cönozytische Myzel als eine einzige, mehrkernige Zelle zu betrachten. Darüber hinaus sind Hyphen des gleichen Paarungstyps in der Lage, ungeachtet deren genetischen Identität, miteinander zu fusionieren. Bringt man die Konidien unterschiedlicher Transformanten des gleichen Paarungstyps gleichzeitig auf das Nährmedium, werden die auskeimenden Hyphen miteinander fusionieren. Es entsteht ein heterokaryotisches Myzel, das das Proteom beider Transformanten gleichzeitig exprimiert (Fleissner et al. 2009). Mittels Heterokaryonbildung wurden Myzelien erzeugt, die die Proteine BEM46::eGFP und PILA::tRFP gleichzeitig exprimierten. Die Lokalisation der fluoreszenten Fusionsproteine wurde mit Hilfe von CLSM untersucht. Die CLSM-Aufnahmen (Arbeit III, Abbildung 3B; **Abbildung 6A-B**) zeigen die Kolokalisation beider Proteine in kortikalen, punktförmigen Strukturen, die somit als Eisosomen identifiziert wurden.

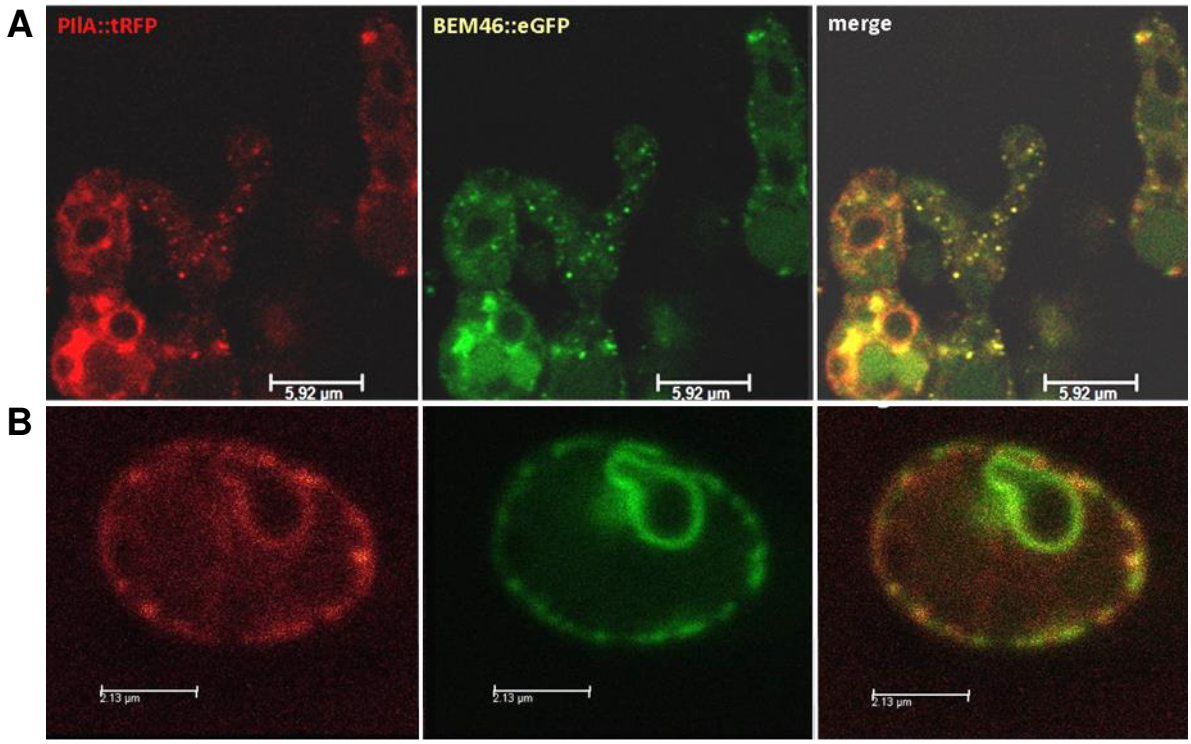

Abbildung 6: Die eisosomale Lokalisation des BEM46::eGFP Proteins. CLSM-Aufnahmen von keimenden (**A**) und gequollenen Konidien (**B**) eines Heterokaryons, das sowohl das eisosomal lokalisierte PILA::tRFP als auch das BEM46::eGFP Protein überexprimiert. *merge*: Überlagerung der im roten und grünen Bereich detektierten Signale

2.4 Die Spleißformen des *bem46*-Transkripts von *N. crassa*

Alternatives Spleißen ist ein Mechanismus, der multizellulären Organismen eine Regulation der Genexpression auf RNA-Ebene erlaubt (Roy et al. 2013). Dabei kommt es sowohl zu qualitativen u.a. durch den Abbau gespleißter Fragmente über *nonsense-mediated mRNA decay* (NMD) (McGlincy and Smith 2008; Nicholson and Mühlemann 2010) als auch zu quantitativen Veränderungen des Transkriptoms, die wiederum die Funktionalität des Proteoms beeinflussen (Roy et al. 2013). Die alternativ gespleißten Fragmente können translatiert werden, wodurch diverse Proteine mit unterschiedlichen Primär- und/oder Tertiärstrukturen entstehen (Syed et al. 2012), die als dominante Kompetitoren für das ursprüngliche Protein wirken können (Seo et al. 2011). Alternatives Spleißen selbst wird durch *riboswitches* reguliert und kann durch Veränderungen der Umweltbedingungen ausgelöst werden (Brunner and Diernfellner 2006; Leal et al. 2009), wodurch es ein flexibles Werkzeug für Umweltadap-

tation darstellt (Kazan 2003). In Ascomyceten tritt alternatives Spleißen seltener als bei Säugetieren auf (Kempken 2013): In *N. crassa* wird die Expression von 162 aus 9733 für Protein-kodierende Gene durch den Mechanismus beeinflusst. Die am häufigsten auftretende Form des alternativen Spleißens in Ascomyceten ist das Beibehalten von Introns (*intron retention*).

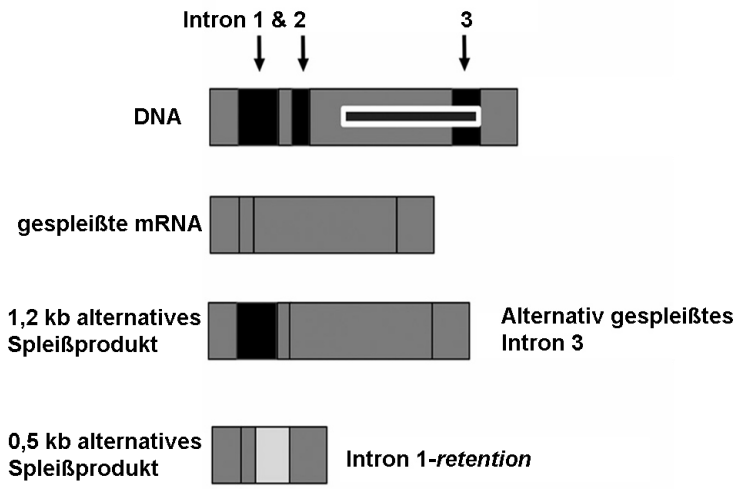

Abbildung 7: Schematische Darstellung der möglichen *bem46*-mRNA-Fragmente, die durch Spleißen entstehen. Die DNA kodiert für drei Exonen und drei Intronen (Intron 1, 2 und 3). Die gewöhnlich gespleißte mRNA (gespleißte mRNA) besteht aus den drei Exonen. Durch alternatives Spleißen im Bereich des dritten Introns entsteht ein 1,2 kb großes mRNA-Fragment (1,2 kb alternatives Spleißprodukt). Das 0,5 kb große alternative Spleißprodukt enthält das Intron 1 und wird zusätzlich modifiziert.

Durch RT-PCR und anschließende Sequenzierung wurden im Wildtyp und im RNAi-Stamm zwei alternativ gespleißte Fragmente des *bem46*-Transkripts identifiziert (Arbeit III, Abbildung 2A; **Abbildung 7**): ein größeres, 1,2 kb langes Fragment, das durch *intron retention* entsteht, und ein kleineres, 0,5 kb langes Fragment, in dem das dritte Exon des ursprünglichen *bem46*-Transkripts fehlt. Nimmt man an, dass für die Initiation der Proteinsynthese immer das gleiche AUG-Startkodon verwendet wird, können zwei alternative Peptide von 40 (kodiert vom 1,2 kb Fragment) bzw. 123 (kodiert vom 0,5 kb Fragment) Aminosäuren entstehen. Um die Wirkung der alternativen Spleißprodukte zu untersuchen, wurden diese jeweils in Überexpressionsvektoren kloniert und die Vektoren in den *N. crassa* Wildtyp-Stamm trans-

formiert (Arbeit III). Die Ascosporenkeimung der so entstandenen Stämme lag, genau wie die der Überexpressions- und RNAi-Transformanten, bei 0% (Arbeit III, Abbildung 1). Dieses Ergebnis deutet darauf hin, dass die 0%ige Ascosporenkeimungsrate der RNAi-Transformante in erster Linie nicht das Resultat der Herunterregulierung des ursprünglichen *bem46*-Transkripts ist, sondern vielmehr von der Akkumulation der alternativ gespleißten Fragmente ausgelöst wurde. Dabei könnten die alternativ entstandenen Peptide als Kompetitor des ursprünglichen BEM46-Proteins wirken, oder die modifizierte, fehlerhafte Lokalisation der Peptide führte zu einer Fehlfunktion. Um letztere Hypothese zu überprüfen, wurde das für das 123 Aminosäuren lange Peptid kodierende 0,5 kb Fragment in einen Überexpressionsvektor an *egfp*-gekoppelt kloniert, und der Vektor wurde in den *N. crassa* Wildtyp-Stamm transformiert (Arbeit III). Untersuchungen der intrazellulären Lokalisation des GFP-Konstrukts mit Hilfe von CLSM zeigten eine vom nativen BEM46 abweichende Lokalisation des Peptids. So wurde das alternative Produkt nicht im perinukleären-ER, sondern ausschließlich in kortikalen, punktförmigen Strukturen detektiert (Arbeit III, Abbildung 3C).

2.5 Interaktionspartner des BEM46 Proteins von *N. crassa*

Mit Hilfe des Hefe-Zwei-Hybrid-(*Y2H)*-Systems konnte die Anthranilat-Synthase (*trp-1*) als einziger Interaktionspartner des BEM46 Proteins identifiziert werden (Arbeit III). Die Interaktion wurde durch bimolekulare Fluoreszenzkomplementation (BiFC (Hoff and Kück 2005)) *in vivo* bestätigt (Arbeit III, Abbildung 4-5). Die Anthranilat-Synthase ist ein multifunktionales Enzym der Tryptophan-Biosynthese (**Abbildung 8**). Das Protein in *N. crassa* besteht aus den α-(*trp-1*) und β-(*trp-2*) Untereinheiten. Die β-Untereinheit ist aus den G-, F- und C-Domänen aufgebaut. Die α-Untereinheit katalysiert die Umwandlung von Chorismat zu Anthranilat. Die trifunktionale β-Untereinheit ist zuständig für die Bindung von Glutamin und besitzt Amidotransferase- (G-Domäne), InGP2-Synthase- (C-Domäne) und PRA-isomerase- (F-Domäne) Aktivität (Walker and DeMoss 1983; Walker and Demoss 1986).

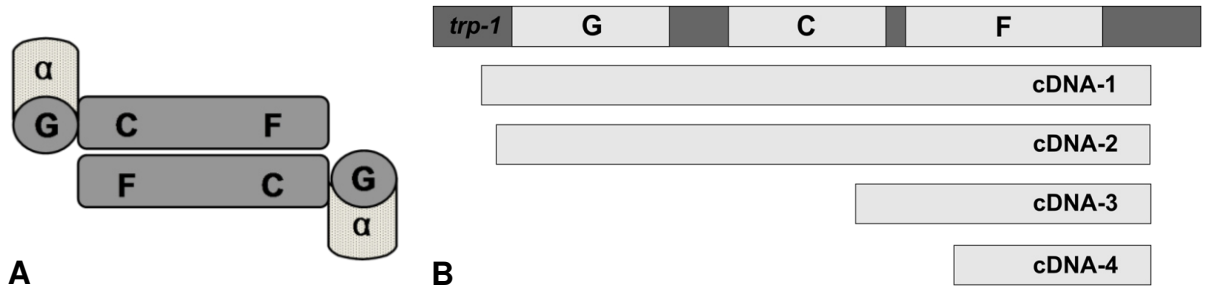

Abbildung 8: Die Anthranilat-Synthase interagiert mit dem BEM46 Protein in *N. crassa*. (**A**) Aufbau des Proteinkomplexes. (**B**) Schematische Darstellung der interagierenden cDNA-Fragmente.

Wie **Abbildung 8B** zeigt, enthalten alle cDNA-Fragmente, die zu einer positiven Interaktion im *Y2H*-Assay führten, den für die F-Domäne kodierenden Teil des *trp-1* Gens. Daraus lässt sich schließen, dass die Interaktion über die eben genannte Domäne stattfindet.

Das *trp-1 knock-out N. crassa*-Stamm (erhalten über die *Fungal Genetics Stock Center*) wurde phänotypisch untersucht (Arbeit III). Die Ascosporenkeimung der *Δtrp-1*-Mutante war relativ zu dem Wildtyp um ca. 50% reduziert (Arbeit III, Abbildung 6C). Dieses Ergebnis ist vergleichbar mit der Keimungsrate der *Δbem46*-Mutante. Auch der oben beschriebene *loss-of-polarity*-Phänotyp war bei den Ascosporen des *Δtrp-1*-Stammes wiederzufinden (Arbeit III, Abbildung 6A). Ähnliche Ergebnisse wurden in dem Modellorganismus *A. thaliana* beschrieben, in dem sowohl die *Δtrp*- als auch die *Δwavy growth2*-Mutante die gleiche fehlerhafte Wurzelspitzenkrümmung aufweisen (Mochizuki et al. 2005a). Diese Resultate deuten darauf hin, dass der Zusammenhang von BEM46 mit der Tryptophan-Biosynthese nicht nur in *N. crassa* besteht. Tryptophan erfüllt in der eukaryotischen Zelle vielfältige Funktionen. Unter anderem ist es ein wichtiger Präkursor für eine Reihe von Metaboliten, darunter Auxin (Radwanski and Last 1995; Mano and Nemoto 2012). In *N. crassa* agiert Tryptophan selbst als Signalmolekül, das die Ausbildung von Hyphenverbindungen (*conidial anastomosis tubes (CAT)*) inhibiert (Fischer-Harman et al. 2012).

Die Untersuchungen des vegetativen Myzels haben gezeigt, dass Konidien des *Δtrp-1* Stammes früher auskeimen und die jungen Hyphen eine schnellere Elongationsrate haben

als der Wildtyp. Da beide Effekte durch Auxinzugabe (Indolessigsäure, IAA) hervorgerufen werden (Nakamura et al. 1982; Tomita et al. 1984), wurde die Indolproduktion von keimenden Asco- und Konidiosporen der *Δtrp-1*-Mutante bestimmt. Die Ascosporen der Mutante produzierten mit dem Wildtyp vergleichbare Mengen an Auxin. Dagegen war die Auxinproduktion der Konidiosporen der Mutante während der Keimung circa zehnfach erhöht (Arbeit III, Abbildung D-E). Diese Resultate lassen die Hypothese zu, dass BEM46 über die Tryptophan-abhängige Auxin-Biosynthese Einfluss auf das Wachstum der Hyphen nimmt.

2.6 Der Einfluss des BEM46 Proteins auf die Auxinbildung in *N. crassa*

2.6.1 Die Auxinbildung der Pilze

Auxine sind natürliche oder synthetische pflanzliche Wachstumsregulatoren (Woodward and Bartel 2005), die eine Vielzahl an biologischen Effekten darunter das Zellwachstum, die Zellteilung, die Bildung von Adventivwurzeln, die Kontrolle der Apikaldominanz und diverse Tropismen beeinflussen (Klee and Estelle 1991). Zu der Gruppe der Auxine gehören chemisch unterschiedliche Substanzen, die alle ein aromatisches Ringsystem und einen Rest mit terminaler Carboxygruppe besitzen. Der meist verbreitete natürliche Vertreter ist die Indol-3-Essigsäure (IAA).

Kurz nach der Entdeckung von Auxin als Wachstumshormon in höheren Pflanzen (Kögl and Kostermans 1934) wurde die Substanz in verschiedenen Pilzen identifiziert und untersucht. Bis Ende der 1950er Jahre lagen diverse Studien zur fungalen Auxin-Synthese und ihrer Wirkung vor. Eine Zusammenfassung der Forschungsergebnisse wurde 1959 von Hans E. Grün vorgenommen (Gruen 1959). Er beschreibt über 90 Pilze aus verschiedenen taxonomischen Gruppen, die in der Lage sind, Auxin *in vitro* im Minimalmedium zu synthetisieren, wobei die Synthese meist an extern zugefügtem Tryptophan gekoppelt ist. Die Wirkung von Auxin auf das Wachstum, die Keimung oder die Myzelbildung wurde meistens als inhibitorisch beschrieben, wobei in einigen Spezies (darunter *Candida albicans*, *Saccharomyces cerevisiae* oder *Neurospora tetrosperma*) ein konzentrationsabhängiger Effekt beobachtet wurde. Solange Auxin (in den Studien wird am häufigsten IAA verwendet) in niedriger Kon-

zentration fördernd wirkt, hemmen hohe Konzentrationen sowohl Wachstum als auch Konidienkeimung. Diese Ergebnisse gerieten später in Vergessenheit.

Da die gegenwärtige Forschung sich auf die Auxinbildung in Interaktionen zwischen Pilzen und Pflanzen konzentriert, wird in erster Linie über phytopathogene oder Mycorrhizabildende Arten publiziert (Strzelczyk and Pokojska-Burdziej 1984; Furukawa et al. 1996; Basse et al. 1996; Hasan 2002; Chung et al. 2003; Reineke et al. 2008). In diesem Zusammenhang wird Auxin als ein Vermittler der Interaktion beschrieben (Prusty et al. 2004).

In *N. crassa* wurde die Produktion des Auxins Indol-3-Essigsäure (IAA) mit Hilfe von HPLC-Analysen nachgewiesen (Tomita et al. 1987), und der Einfluss von extern zugefügtem Auxin auf die unterschiedlichen asexuellen Entwicklungsstadien des Pilzes untersucht. Die oben beschriebene konzentrationsabhängige Wirkung von Auxin wurde auch in *N. crassa* nachgewiesen. Die optimale Konzentration der extern zugefügten IAA liegt bei 10^{-6} M. In hohen Konzentrationen (10^{-4} M) wirkt IAA inhibitorisch (Nakamura et al. 1978). Dabei beeinflusst sie sowohl die konidiale Keimungsrate (Nakamura et al. 1978; Nakamura et al. 1982) als auch die Elongation der jungen Keimungsschläuche (Tomita et al. 1984). Da die oben genannten Publikationen nicht in den einschlägigen Literaturdatenbanken erhältlich sind, gerieten diese Ergebnisse in Vergessenheit. Die Biosynthese von IAA kann entweder Tryptophan-abhängig (Tryptophan fungiert als Prekursor für den Syntheseprozess), oder Tryptophan-unabhängig erfolgen (Baca and Elmerich 2003). Da die meisten Auxinproduzierenden Organismen mehrere Biosynthesewege gleichzeitig nutzen, ist die Aufklärung des Biosynthese-Netzwerkes erschwert. Obwohl die Schlüsselenzyme der Synthese in Pflanzen bekannt sind, ist ihre Zuordnung zu den einzelnen Wegen unklar. In der Literatur werden verschiedene putative Netzwerke beschrieben (Woodward and Bartel 2005; Quittenden et al. 2009; Mashiguchi et al. 2011; Mano and Nemoto 2012). Welche Biosynthesewege in Pilzen funktionieren, ist im Allgemeinen wenig untersucht. Eine Ausnahme bildet *Ustilago maydis*, in dem einzelne Biosynthesewege genauer charakterisiert sind (Reineke et al. 2008). Die Untersuchungen der

vorliegenden Arbeit orientierten sich an dem von Mashiguchi *et al.* (2011) erstellten Modell, modifiziert nach den für *U. maydis* publizierten Ergebnissen (**Abbildung 9**).

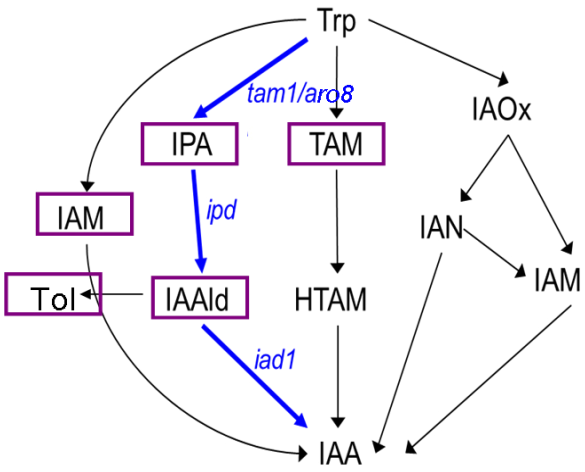

Abbildung 9: Schematische Darstellung der Tryptophan-abhängigen IAA-Biosynthese (nach Mashiguchi et al., 2011 und Reineke et al., 2008). Die in Pilzen nachgewiesenen Zwischenprodukte sind violett markiert. Der in der vorliegenden Arbeit untersuchte Weg ist blau dargestellt. *tam1*, Trp-Aminotransferase; *ipd*, IPA-Decarboxylase; *iad1*, IAAld-Dehydrogenase; Trp, Tryptophan; IPA, Indol-3-pyruvat; IAAld, Indol-3-Acetaldehyd; IAA, Indole-3-Essigsäure; Tol, Indol-3-Ethanol; TAM, Tryptamin; HTAM, N-Hydroxyl-Tryptamin; IAOx, Indol-3-Acetaldoxim; IAN, Indol-3-Acetonitril; IAM, Indol-3-Acetamid

2.6.2 Identifizierung eines putativen Auxin-Biosyntheseweges in *N. crassa*

In Pilzen wurden bisher IAAld (Indol-3-Acetaldehyd), IPA (Indol-3-pyruvat), TAM (Tryptamin) und IAM (Indol-3-Acetamid) als putative Intermediate der Auxin-Biosynthese nachgewiesen. Daraus lässt sich schließen, dass die fungale IAA-Produktion über den IPA, TAM oder IAM nicht aber über den IAN Weg stattfindet (Robinson et al. 1998; Chung et al. 2003; Chung and Tzeng 2004; Reineke et al. 2008). Für *U. maydis* wurde die Biosynthese über den IPA-Weg mit den beteiligten Enzymen TAM1 (Tryptophan-Aminotransferase), IPD (Indol-3-Pyruvat-Decarboxylase) und IAD1/2 (Indol-3-Acetaldehyd-Dehydrogenase) näher charakterisiert (Basse et al. 1996; Zuther et al. 2008). Mit Hilfe von bioinformatischen pBLAST-Analysen wurden die homologen Proteine aller in dem IPA-Biosyntheseweg beteiligten Enzyme (NCU09166.7 (*tam1*), NCU02397.7 (*ipd*) NCU03415 (*iad1*)) in *N. crassa* identifiziert (Arbeit III, *supplementary*). Die Aminosäuresequenzen der orthologen Enzyme in *U. maydis* und *N. crassa* wurden miteinander verglichen, und die für die Funktion von IAD1/2 essentiellen Ami-

nosäurereste (Yoshida et al. 1998; Reineke et al. 2008) wurden identifiziert. Die Ergebnisse deuten darauf hin, dass *N. crassa* die genetischen Grundlagen dafür besitzt, über den IPA-Weg Auxin zu synthetisieren.

Mit Hilfe von quantitativen *real time PCR* (qRT-PCR)-Analysen sollte die Frage geklärt werden, ob die Expression der putativen Auxin-Biosynthesegene (*tam1*, *ipd* und *iad1*) in den verschiedenen *bem46*-Transformanten und in der *knock-out*-Mutante beeinflusst ist, d.h. ob sich die unterschiedliche *bem46*-Transkriptmenge auf die Expression der Auxin-Biosynthesegene auswirkt (Bönniger 2013). Die Ergebnisse zeigten, dass die Herunterregulierung des *bem46*-Transkripts in den RNAi-und *knock-out*-Stämmen zu einer Reduktion der *tam1*-Expression führt, was wiederum eine leichte Erhöhung der *iad1*-Expression bewirkt (Arbeit III, Abbildung 7; **Abbildung 10A-C**). Dagegen wird in dem *bem46*-Überexpressions-Stamm die *tam1*-Expression nicht negativ beeinflusst, was in einer leichten Erhöhung der *ipd*-Expression und einer sehr starken Erhöhung der *iad1*-Expression resultiert.

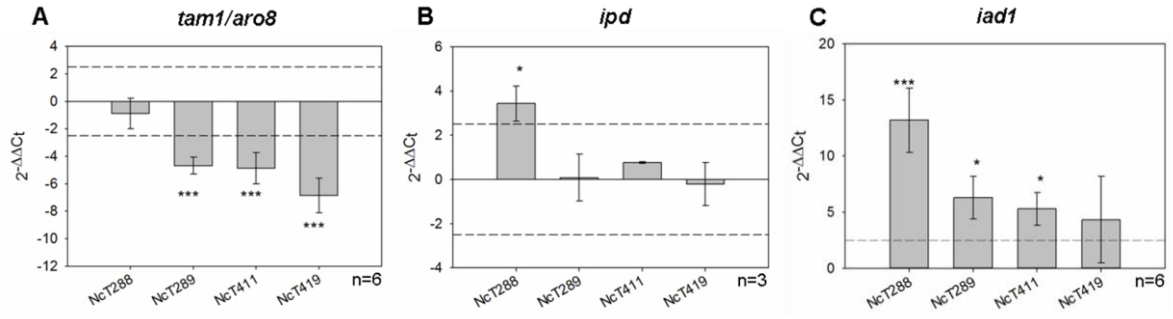

Abbildung 10: Auswertung der qRT-PCR-Analysen. Die Expression der drei putativen Auxin-Biosynthesegene *tam1* (**A**), *ipd* (**B**) und *iad1* (**C**) wurde in unterschiedlichen *N. crassa*-Stämmen bestimmt und verglichen. (Mit freundlicher Genehmigung von C. Bönniger.) NcT288, *bem46*-Überexpressionsstamm; NcT289, *bem46-knock-down*-Stamm; NcT411, *bem46-knock-out*-Stamm; NcT419, der Stamm überexprimiert ein alternativ gespleißtes *bem46*-Fragment (weitere Erklärung s. Text)

2.6.3 Qualitativer und quantitativer Nachweis der Auxinproduktion von *N. crassa*

Die Ergebnisse der qRT-PCR-Analysen unterstützten die Hypothese, dass BEM46 einen Einfluss auf die Auxin-Biosynthese in *N. crassa* hat. Im Weiteren wurde die Auxinproduktion des Pilzes qualitativ nachgewiesen und in den unterschiedlichen *bem46*-Transformanten und

in der *knock-out*-Mutante quantitativ untersucht. Der qualitative Auxin-Nachweis erfolgte indirekt mit Hilfe von *A. thaliana* DR5::GUS Pflanzen, die auf die Anwesenheit von Auxin als Indikator reagieren, und direkt mit Hilfe von dünnschichtchromatographischer Aufteilung der von dem Pilz produzierten Indolprodukte (Arbeit III, Abbildung 8). Beide Methoden führten zu dem Ergebnis, dass *N. crassa* in der Lage ist, im tryptophanhaltigen Medium Auxin zu synthetisieren. Die quantitative Bestimmung der Auxinproduktion der verschiedenen Transformanten und der Mutante wurde durchgeführt, um herauszufinden, ob die mit Hilfe der qRT-PCR-Analyse nachgewiesenen Unterschiede in der Genexpression der Biosynthesegene sich auch in der Biosynthese des Endprodukts Auxin zeigen. Da als Matrize für die qRT-PCR-Analysen aus vegetativen Myzelien isolierte RNA diente, wurde zunächst die Indolproduktion dieses Stadiums bestimmt. Es wurden jedoch keine Unterschiede in der Auxinproduktion in diesem Entwicklungsstadium ermittelt.

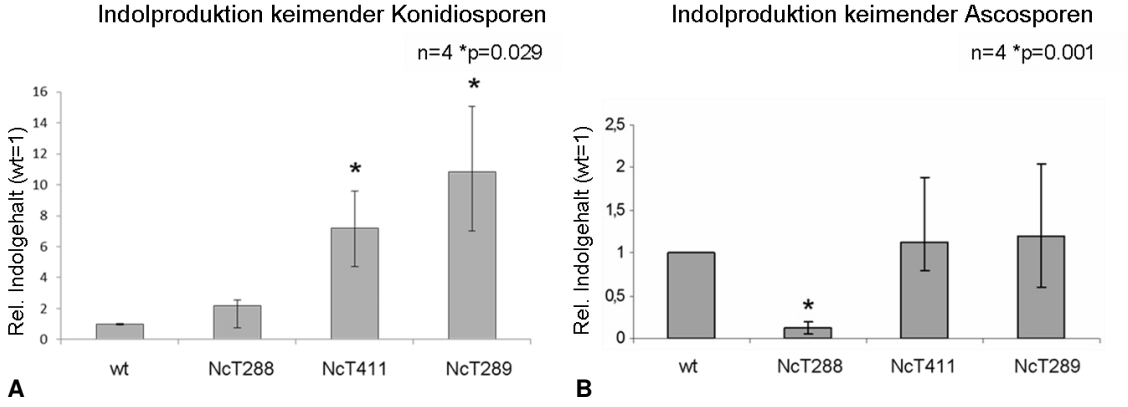

Abbildung 11: Auxinproduktion keimender Konidiosporen (**A**) und Ascosporen (**B**). Die Sporen verschiedener Pilzstämme wurden im tryptophanhaltigen Flüssigmedium inkubiert. Der Indolgehalt des Mediums wurde mit Hilfe der Salkowsky-Methode bestimmt und die relative Indolproduktion der einzelnen Stämme wurde auf die Indolproduktion des Wildtyps bezogen ermittelt. NcT288, *bem46*-Überexpressionsstamm; NcT289, *bem46-knock-down*-Stamm; NcT411, *bem46-knock-out*-Stamm; NcT419

Die phänotypischen Analysen haben gezeigt, dass BEM46 eine Rolle in der Keimung von sowohl Asco- als auch Konidiosporen spielt. Darüber hinaus ist die Wirkung von Auxin auf die Konidienkeimung und auf das Wachstum junger Hyphen in *N. crassa* bekannt (Nakamura et al. 1982; Tomita et al. 1984). Um einen eventuellen Zusammenhang zwischen BEM46,

Keimung und Auxin herzustellen, wurde die Indolproduktion der keimenden Konidio- und Ascosporen bestimmt (Arbeit III, Abbildung 9A-B; **Abbildung 11A-B**). In Konidiosporen führt die Herunterregulierung der *bem46*-Transkriptmenge zu erhöhter Indolproduktion, was wiederum in früherer Konidienkeimung und schnellerem Hyphenwachstum resultiert (Arbeit III, Abbildung 9C-D). Die in ihrer Keimung und im Hyphenwachstum stark beeinträchtigte Überexpressionstransformante produziert jedoch Auxin-Mengen, die der Auxinproduktion des Wildtyps entsprechen. Dieses Ergebnis ist umso unerwarteter, als die Expression des für das letzte Enzym des Biosyntheseweges kodierenden Gens in diesem Stamm stark hochreguliert ist. Ein ähnlich kontroverses Bild zeigt die Indolproduktion der keimenden Ascosporen. Solange die Herunterregulierung des *bem46*-Transkripts zu keiner signifikanten Veränderung in der Indolproduktion führt, ist die von der Überexpressions-Transformante produzierte Auxinmenge im Vergleich zum Wildtyp in etwa um das Zehnfache reduziert. Diese Ergebnisse deuten darauf hin, dass die Keimung von Konidio- und Ascosporen unterschiedlich reguliert wird, und dass BEM46 in den zwei Stadien eine unterschiedliche Rolle spielen könnte. Darüber hinaus muss berücksichtigt werden, dass in der vorliegenden Arbeit die Genexpression nur eines putativen Auxin-Biosyntheseweges untersucht wurde. Da aber die meisten Organismen ein Netzwerk mit mehreren unterschiedlichen Wegen nutzen (Baca and Elmerich 2003), ist davon auszugehen, dass *N. crassa* über mehrere, vom IPA-Weg abweichende, evtl. auch von Tryptophan unabhängige Synthesemöglichkeiten verfügt. Letzteres könnte erklären, warum die deutliche Überexpression von *iad1* in der *bem46*-überexpressions-Transformante nicht zwingend eine hohe Indolproduktion zur Folge hat. Darüber hinaus könnten Regulationsmechanismen auf höherer Ebene die Auxinproduktion beeinflussen. Solche Mechanismen, wie z.B. die Inaktivierung des Endprodukts über Ringoxidation oder Konjugatbildung, sind für *A. thaliana* belegt (Woodward and Bartel 2005). Die Bestimmung der Auxinproduktion der keimenden Ascosporen wird im Weiteren deswegen verfälscht, weil auch bei einer Keimungsrate von 0% einige wenige Sporen (ca. 1 in 2000) auskeimen und zur Indolproduktion beitragen.

2.7 Der Tryptophan-Transporter MTR in *N. crassa*: "*The missing link*"?

In *Saccharomyces cerevisiae* ist die Tryptophan- und Tyrosin-Permease TAT2 (YOL020W) in den Eisosomen lokalisiert (Grossmann et al. 2008). In der vorliegenden Arbeit wurde das neutrale Aminosäure-Transportprotein MTR (NCU06619) (Stadler 1967; Kinsey and Stadler 1969) als das TAT2-Homolog in *N. crassa* identifiziert (Arbeit III) und die Genexpression mit Hilfe einer qRT-PCR in den *bem46*-Transformanten sowie in der *knock-out*-Mutante untersucht (Bönniger 2013). Die Expression des *mtr*-Gens wies eine starke Hochregulierung im *bem46*-Überexpressionsstamm auf (Arbeit III, Abbildung 10A). Auch die intrazelluläre Lokalisation des MTR-Proteins wurde mit Hilfe von Reportergenkonstrukten untersucht. In Heterokaryen, die das *egfp*-gekopplete *mtr*-Gen zusammen mit dem für das eisosomale Protein kodierende *pila::trfp* Genkonstrukt exprimierten, wurde das MTR::eGFP Fusionsprotein in den Eisosomen detektiert (Arbeit III, Abbildung 10B). Die Kolokalisation des BEM46 Proteins mit dem MTR Protein in den Eisosomen von *N. crassa* und die Hochregulierung des *mtr*-Transkripts in dem *bem46*-Überexpressionsstamm deuten darauf hin, dass eine Verbindung zwischen BEM46 und der Tryptophan-Aufnahme des Pilzes besteht.

Die bisherigen Ergebnisse legen eine Verbindung zwischen BEM46, Tryptopan-Aufnahme und -Synthese, Auxinbiosynthese sowie Keimung in *N. crassa* nahe (**Abbildung 12**). Es bleibt aber weiterhin ungeklärt, welche genaue Rolle das Protein in diesen Prozessen spielt. Das BEM46 Protein interagiert mit der PRA-Isomerase-Domäne der Anthranilat-Synthase, wodurch es die Tryptophan–Biosynthese direkt beeinflussen könnte. Die Untersuchungen der Genexpression des für die Anthranilat-Synthase (AS) kodierenden Genes *trp-1* zeigten jedoch keine Unterschiede in den *bem46*-Transformanten, was auf die *bem46*-Unabhängigkeit der Synthese hindeutet, schließt aber die Möglichkeit einer gegensätzlichen Regulation nicht aus. Obwohl Tryptophan selbst als Signalmolekül fungieren kann (Fischer-Harman et al. 2012), konzentriert sich die vorliegende Arbeit auf seine Rolle als Vorstufe der Auxin-Biosynthese. Die bioinformatischen Untersuchungen haben gezeigt, dass das Genom von *N. crassa* für die Enzyme TAM1, IPD und IAD1 des Auxin-Biosyntheseweges über das Zwischenprodukt Indol-3-Pyruvat (IPA) kodiert. Darüber hinaus gibt es einen Zusammen-

hang zwischen der *bem46*-Genexpression und der Expression der Gene des putativen Auxin-Biosyntheseweges, welche Verbindung sich auf die Indolproduktion des Pilzes auswirkt. Die Tatsache, dass die alternativ gespleißten *bem46*-Fragmente in Ascosporen und in Konidiosporen unterschiedliche Wirkung zeigen, deutet darauf hin, dass die Prozesse, in denen BEM46 involviert ist, in dem sexuellen und asexuellen Stadium verschieden sind.

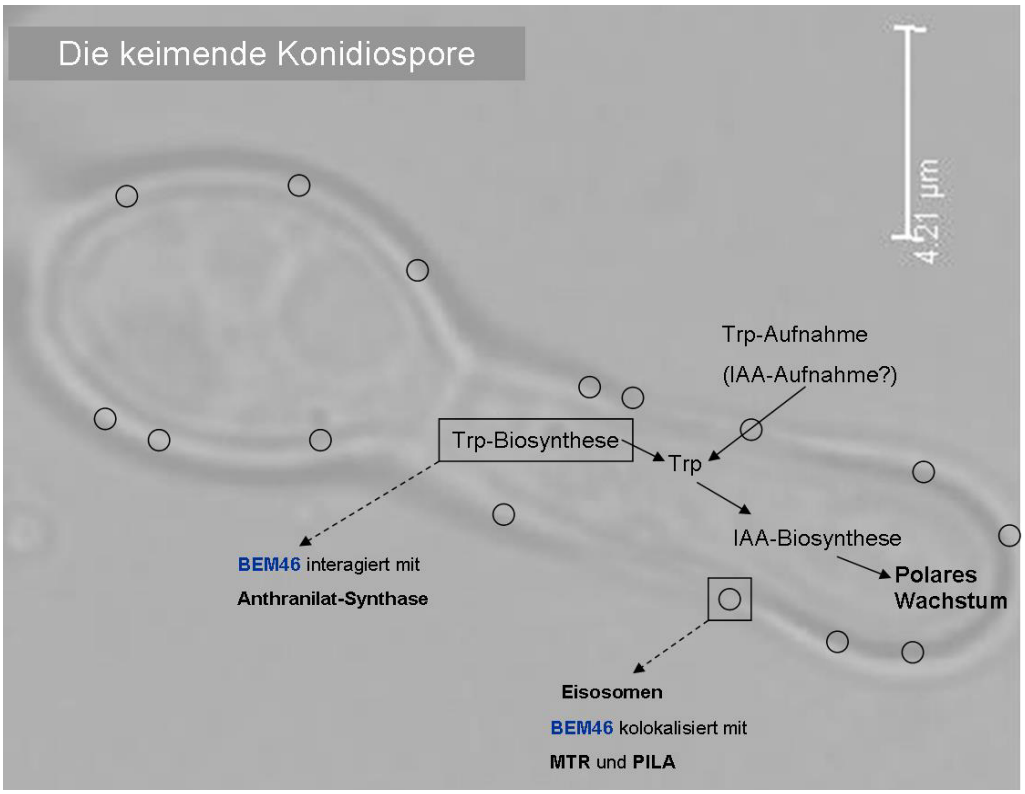

Abbildung 12: Modell des möglichen Zusammenhangs zwischen dem BEM46 Protein und dem polaren Hyphenwachstum einer keimenden Konidiospore von *N. crassa*. Trp; Tryptophan, IAA; Indol-3-Essigsäure

Eine mögliche Rolle könnte BEM46 in der Koordinierung der Tryptophan-Synthese über alternatives Spleißen und die Aufnahme von Tryptophan über MTR spielen und somit den intrazellulären Tryptophan-Gehalt kontrollieren. Da die Auxin-Biosynthese des Pilzes von Tryptophan abhängt, würde BEM46 somit indirekt auch den internen Auxin-Spiegel mitbestimmen oder überwachen. Eine präzise Regulation des Auxin-Gehalts ist umso wichtiger, als die Wirkung von Auxin abhängig von der Konzentration inhibierend oder aktivierend sein kann. *Microarray*-Daten deuten darauf hin, dass Auxin und BEM46 auch in der allgemeinen Ant-

wort auf Stressfaktoren eine Rolle spielen: Phytosphingosin-Behandlung -eine Substanz, die in *N. crassa* den programmierten Zelltod auslöst- führt zur Hochregulierung der Gene *iad1* und *bem46* (Videira et al. 2009).

Es bleibt weiterhin zu klären, durch welche Mechanismen BEM46 das polare Wachstum beeinflusst, und welche genaue Rolle Auxin in dem Prozess spielt. In *A. thaliana* führt die polare Verteilung von Auxin-Transportproteine der PIN-Familie in der Plasmamembran zum polaren Auxin-Transport und schließlich zum polaren Wachstum (Sassi and Vernoux 2013). Die polare Verteilung der PIN-Proteine wird dadurch erreicht, dass solange die Phosphoryllierung der apikal positionierten Transporter zur Endozytose und damit zur Wiederverwertung der Proteine führt, die basalen Transporter dephosphorylliert und dadurch von der Endozytose geschützt bleiben (Vanneste and Friml 2009). Eisosomen beeinflussen das Auftreten von Endozytose-Ereignissen (Walther et al. 2006). Ihre BAR-Domäne führt zur Krümmung der Membran, was wiederum die Clusterbildung bestimmter Membrankomponenten, darunter Transportproteine bewirkt, die somit vor Internalisierung geschützt werden (Ziółkowska et al. 2011; Olivera-Couto et al. 2011). Die eisosomale Lokalisation des Tryptophan-Transporters MTR und von BEM46 könnte bewirken, dass die Endozytose der Proteine verhindert wird. Die zeitliche oder räumliche Regulation der Endozytose, ähnlich der Phosphoryllierung der PIN-Proteine, könnte zur polaren Verteilung und als Folge dessen zum polaren Wachstum führen. In *N. crassa* konnten zwar keine Homologe der PIN-Familie identifiziert werden (persönliche Mitteilung P. Sardar), der Pilz besitzt jedoch den Auxin-*efflux carrier* Ncu00589. Die intrazelluläre Lokalisation des Proteins wird gegenwärtig untersucht.

Die Bestimmung des Zeitpunkts der Keimung und der Wachstumsrichtung der jungen Hyphen ist ein entscheidender Prozess in der Entwicklung eines Ascomyceten. Der Vorgang ist stark abhängig von den ständig wechselnden Umweltbedingungen des Pilzes, was eine präzise und flexible Regulation voraussetzt. Ein entscheidender Aspekt dieses Prozesses könnte die Kontrolle des internen Auxin-Spiegels sein, in dessen Regulation vermutlich BEM46

eine Rolle übernimmt. Die Möglichkeit für die Entstehung modifizierter BEM46-Peptide durch alternatives Spleißen könnte zur Flexibilität des Prozesses beitragen.

3. Literatur

Baca BE, Elmerich C (2003) Microbial production of plant hormones. In: Elmerich C, Newton WE (eds) Assoc. Endophytic Nitrogen-Fixing Bact. Cyanobacterial Assoc. Springer, Dordrecht, pp 113–143

Bartnicki-Garcia S, Bartnicki DD, Gierz G, et al. (1995) Evidence that spitzenkörper behavior determines the shape of a fungal hypha: A test of the hyphoid model. Exp Mycol 19:153–159.

Bartnicki-Garcia S, Hergert F, Gierz G (1989) Computer simulation of fungal morphogenesis and the mathematical basis for hyphal (tip) growth. Protoplasma 153:46–57.

Basse CW, Lottspeich F, Steglich W, Kahmann R (1996) Two potential indole-3-acetaldehyde dehydrogenases in the phytopathogenic fungus Ustilago maydis. Eur J Biochem 242:648–56.

Berepiki A, Lichius A, Shoji J-Y, et al. (2010) F-actin dynamics in Neurospora crassa. Eukaryot Cell 9:547–57. doi: 10.1128/EC.00253-09

Bönniger C (2013) Funktionelle Analysen des BEM46-Proteins aus Neurospora crassa. Christian-Albrechts-Universität zu Kiel

Brunner M, Diernfellner A (2006) How temperature affects the circadian clock of Neurospora crassa. Chronobiol Int 23:81–90. doi: 10.1080/07420520500545805

Cabib E, Drgonova J, Drgon T (1998) Role of small G proteins in yeast cell polarization and wall biosynthesis. Annu Rev Biochem 67:307–333.

Cáceres A, Ye B, Dotti CG (2012) Neuronal polarity: demarcation, growth and commitment. Curr Opin Cell Biol 24:547–53. doi: 10.1016/j.ceb.2012.05.011

Chang F, Peter M (2003) Yeasts make their mark. Nat Cell Biol 5:294–9. doi: 10.1038/ncb0403-294

Chant J, Corrado K, Pringle JR, Herskowitz I (1991) Yeast BUD5 , encoding a putative GDP-GTP exchange factor , is necessary for bud site selection and interacts with bud formation gene BEM1. Cell 65:1213–1224.

Chenevert J, Corrado K, Bender A, et al. (1992) A yeast gene (BEM1) necessary for cell polarization whose product contains two SH3 domains. Nature 356:77–79.

Chung K-R, Shilts T, Ertürk Üœ, et al. (2003) Indole derivatives produced by the fungus Colletotrichum acutatum causing lime anthracnose and postbloom fruit drop of citrus. FEMS Microbiol Lett 226:23–30. doi: 10.1016/S0378-1097(03)00605-0

Chung KR, Tzeng DD (2004) Biosynthesis of Indole-3-Acetic Acid by the Gall-inducing Fungus Ustilago esculenta. J Biol Sci 4:744–750. doi: 10.3923/jbs.2004.744.750

Edidin M (2003) The state of lipid rafts: from model membranes to cells. Annu Rev Biophys Biomol Struct 32:257–83. doi: 10.1146/annurev.biophys.32.110601.142439

Engqvist-Goldstein AEY, Drubin DG (2003) Actin assembly and endocytosis: from yeast to mammals. Annu Rev Cell Dev Biol 19:287–332. doi: 10.1146/annurev.cellbio.19.111401.093127

Facette MR, Smith LG (2012) Division polarity in developing stomata. Curr Opin Plant Biol 15:585–92. doi: 10.1016/j.pbi.2012.09.013

Fischer R, Zekert N, Takeshita N (2008) Polarized growth in fungi-interplay between the cytoskeleton, positional markers and membrane domains. Mol Microbiol 68:813–26. doi: 10.1111/j.1365-2958.2008.06193.x

Fischer-Harman V, Jackson KJ, Muñoz A, et al. (2012) Evidence for tryptophan being a signal molecule that inhibits conidial anastomosis tube fusion during colony initiation in Neurospora crassa. Fungal Genet Biol 49:896–902. doi: 10.1016/j.fgb.2012.08.004

Fiskerstrand T, H'mida-Ben Brahim D, Johansson S, et al. (2010) Mutations in ABHD12 cause the neurodegenerative disease PHARC: An inborn error of endocannabinoid metabolism. Am J Hum Genet 87:410–7. doi: 10.1016/j.ajhg.2010.08.002

Fleissner A, Diamond S, Glass NL (2009) The Saccharomyces cerevisiae PRM1 homolog in Neurospora crassa is involved in vegetative and sexual cell fusion events but also has postfertilization functions. Genetics 181:497–510. doi: 10.1534/genetics.108.096149

Furukawa T, Koga J, Adachi T, et al. (1996) Efficient Conversion of L-Tryptophan to Indole-3-Acetic Acid and/or Tryptophol by Some Species of Rhizoctonia. Plant Cell Physiol 37:899–905.

Galperin MY, Koonin E V (2004) "Conserved hypothetical" proteins: prioritization of targets for experimental study. Nucleic Acids Res 32:5452–63. doi: 10.1093/nar/gkh885

Galperin MY, Koonin E V (2010) From complete genome sequence to "complete" understanding? Trends Biotechnol 28:398–406. doi: 10.1016/j.tibtech.2010.05.006

Giaever G, Chu AM, Ni L, et al. (2002) Functional profiling of the Saccharomyces cerevisiae genome. Nature 418:387–91. doi: 10.1038/nature00935

Giot L, Bader JS, Brouwer C, et al. (2003) A protein interaction map of Drosophila melanogaster. Science 302:1727–36. doi: 10.1126/science.1090289

Grossmann G, Malinsky J, Stahlschmidt W, et al. (2008) Plasma membrane microdomains regulate turnover of transport proteins in yeast. J Cell Biol 183:1075–88. doi: 10.1083/jcb.200806035

Gruen EH (1959) Auxin and fungi. Annu Rev Plant Physiol 10:405–440.

Harris SD, Momany M (2004) Polarity in filamentous fungi: moving beyond the yeast paradigm. Fungal Genet Biol 41:391–400. doi: 10.1016/j.fgb.2003.11.007

Harris SD, Read ND, Roberson RW, et al. (2005) MINIREVIEWS Polarisome Meets Spitzenko ¨ rper : Microscopy , Genetics , and Genomics Converge. 4:225–229. doi: 10.1128/EC.04.2.225

Hasan H a H (2002) Gibberellin and auxin-indole production by plant root-fungi and their biosynthesis under salinity-calcium interaction. Acta Microbiol Immunol Hung 49:105–18. doi: 10.1556/AMicr.49.2002.1.11

Hoff B, Kück U (2005) Use of bimolecular fluorescence complementation to demonstrate transcription factor interaction in nuclei of living cells from the filamentous fungus Acremonium chrysogenum. Curr Genet 47:132–8. doi: 10.1007/s00294-004-0546-0

Holmquist M (2000) Alpha/beta-hydrolase fold enzymes: structures, functions and mechanisms. Curr Protein Pept Sci 1:209–235.

Irazoqui JE, Gladfelter AS, Lew DJ (2003) Scaffold-mediated symmetry breaking by Cdc42p. Nat Cell Biol 5:1062–70. doi: 10.1038/ncb1068

Jund R, Weber E, Chevallier M (1988) Primary structure of the uracil transport protein of Saccharomyces cerevisiae. Eur J Biochem 171:417–424.

Kabeche R, Baldissard S, Hammond J, et al. (2011) The filament-forming protein Pil1 assembles linear eisosomes in fission yeast. Mol Biol Cell 22:4059–67. doi: 10.1091/mbc.E11-07-0605

Kazan K (2003) Alternative splicing and proteome diversity in plants: the tip of the iceberg has just emerged. Trends Plant Sci 8:468–71. doi: 10.1016/j.tplants.2003.09.003

Kempken F (2013) Alternative splicing in ascomycetes. Appl Microbiol Biotechnol 97:4235–41. doi: 10.1007/s00253-013-4841-x

Kinsey J a, Stadler DR (1969) Interaction between analogue resistance and amino acid auxotrophy in Neurospora. J Bacteriol 97:1114–7.

Klee H, Estelle M (1991) Molecular genetic approaches to plant hormone biology. Annu Rev Plant Physiol Plant Mol Biol 42:529–551.

Kögl F, Kostermans DGFR (1934) Hetero-auxin als Stoffwechselprodukt niederer pflanzlicher Organismen. Isolierung aus Hefe. XIII. Z Physiol Chem 228:113–121.

Kolláth-Leiß K, Kempken F (2012) Bem46-Homologe: bekannte Proteine mit unbekannter Funktion. Biospektrum 18:251–253. doi: 10.1007/s12268-012-0170-3

Leal J, Squina FM, Freitas JS, et al. (2009) A splice variant of the Neurospora crassa hex-1 transcript, which encodes the major protein of the Woronin body, is modulated by extracellular phosphate and pH changes. FEBS Lett 583:180–4. doi: 10.1016/j.febslet.2008.11.050

Lenfant N, Hotelier T, Velluet E, et al. (2013) ESTHER, the database of the α/β-hydrolase fold superfamily of proteins: tools to explore diversity of functions. Nucleic Acids Res 41:D423–9. doi: 10.1093/nar/gks1154

Lewis MJ, Pelham HRB (1990) A human homologue of the yeast HDEL receptor. Lett to Nat 348:162–163.

Madden K, Snyder M (1998) Cell polarity and morphogenesis in budding yeast. Annu Rev Microbiol 52:687–744. doi: 10.1146/annurev.micro.52.1.687

Malinsky J, Opekarová M, Grossmann G, Tanner W (2013) Membrane microdomains, rafts, and detergent-resistant membranes in plants and fungi. Annu Rev Plant Biol 64:501–29. doi: 10.1146/annurev-arplant-050312-120103

Mano Y, Nemoto K (2012) The pathway of auxin biosynthesis in plants. J Exp Bot 63:2853–72. doi: 10.1093/jxb/ers091

Mashiguchi K, Tanaka K, Sakai T, et al. (2011) The main auxin biosynthesis pathway in Arabidopsis. PNAS 108:18512–18517. doi: 10.1073/pnas.1108434108/-/DCSupplemental.www.pnas.org/cgi/doi/10.1073/pnas.1108434108

McGlincy NJ, Smith CWJ (2008) Alternative splicing resulting in nonsense-mediated mRNA decay: what is the meaning of nonsense? Trends Biochem Sci 33:385–93. doi: 10.1016/j.tibs.2008.06.001

Mercker M (2006a) Funtionsanalyse des bem46-Homologs bei Neurospora crassa. Christian Albrechts Universität zu Kiel

Mercker M (2006b) Funtionsanalyse des bem46-Homologs bei Neurospora crassa. Christian Albrechts Universität zu Kiel

Mochizuki S, Harada A, Inada S, et al. (2005a) The Arabidopsis WAVY GROWTH 2 protein modulates root bending in response to environmental stimuli. Plant Cell 17:537–547. doi: 10.1105/tpc.104.028530.2

Mochizuki S, Harada A, Inada S, et al. (2005b) The Arabidopsis WAVY GROWTH 2 protein modulates root bending in response to environmental stimuli. Plant Cell 17:537–47. doi: 10.1105/tpc.104.028530

Nakamura T, Kawanabe Y, Takiyama E, Takahashi N (1978) Effects of auxin and gibberellin on conidial germination in Neurospora crassa. 19:705–709.

Nakamura T, Tomita K, Kawanabe Y (1982) Effect of auxin and gibberellin on conidial germination in Neurospora crassa II . “ Conidial density effect ” and auxin. 23:1363–1369.

Nardini M, Dijkstra BW (1999) α / β Hydrolase fold enzymes : the family keeps growing Marco Nardini and Bauke W Dijkstra *. Curr Opin Struct Biol 9:732–737.

Nelson WJ (2003) Adaptation of core mechanisms to generate cell polarity. Nature 422:766–774. doi: 10.1038/nature01602.Adaptation

Nicholson P, Mühlemann O (2010) Cutting the nonsense: the degradation of PTC-containing mRNAs. Biochem Soc Trans 38:1615–20. doi: 10.1042/BST0381615

Okada K, Shimura Y (1990) Reversible root tip rotation in Arabidopsis seedlings induced by obstacle-touching stimulus. Science 250:274–6. doi: 10.1126/science.250.4978.274

Olivera-Couto A, Graña M, Harispe L, Aguilar PS (2011) The eisosome core is composed of BAR domain proteins. Mol Biol Cell 22:2360–72. doi: 10.1091/mbc.E10-12-1021

Ollis DL, Cheah E, Cygler M, et al. (1992) The α / β hydrolase fold. "Protein Eng Des Sel 5:197–211. doi: 10.1093/protein/5.3.197

Park H-O, Bi E (2007) Central roles of small GTPases in the development of cell polarity in yeast and beyond. Microbiol Mol Biol Rev 71:48–96. doi: 10.1128/MMBR.00028-06

Park HO, Bi E, Pringle JR, Herskowitz I (1997) Two active states of the Ras-related Bud1/Rsr1 protein bind to different effectors to determine yeast cell polarity. Proc Natl Acad Sci U S A 94:4463–8.

Parmentier ML, Woods D, Greig S, et al. (2000) Rapsynoid/partner of inscuteable controls asymmetric division of larval neuroblasts in Drosophila. J Neurosci 20:RC84.

Prusty R, Grisafi P, Fink GR (2004) The plant hormone indoleacetic acid induces invasive growth in Saccharomyces cerevisiae. Proc Natl Acad Sci U S A 101:4153–7. doi: 10.1073/pnas.0400659101

Quittenden LJ, Davies NW, Smith J a, et al. (2009) Auxin biosynthesis in pea: characterization of the tryptamine pathway. Plant Physiol 151:1130–8. doi: 10.1104/pp.109.141507

Radwanski ER, Last RL (1995) Tryptophan biosynthesis and metabolism: Biochemical and molecular genetics. Plant Cell 7:921–934.

Raykhel I, Alanen H, Salo K, et al. (2007) A molecular specificity code for the three mammalian KDEL receptors. J Cell Biol 179:1193–204. doi: 10.1083/jcb.200705180

Read ND, Kalkman ER (2003) Does endocytosis occur in fungal hyphae? Fungal Genet Biol 39:199–203. doi: 10.1016/S1087-1845(03)00045-8

Reijnst P, Walther A, Wendland J (2011) Dual-colour fluorescence microscopy using yEmCherry- / GFP-tagging of eisosome components Pil1 and Lsp1 in Candida albicans. Yeast 28:331–338. doi: 10.1002/yea

Reineke G, Heinze B, Schirawski J, et al. (2008) Indole-3-acetic acid (IAA) biosynthesis in the smut fungus Ustilago maydis and its relevance for increased IAA levels in infected tissue. Mol Plant Pathol 9:339–355. doi: 10.1111/J.1364-3703.2008.00470.X

Robinson M, Riov J, Sharon a (1998) Indole-3-acetic acid biosynthesis in colletotrichum gloeosporioides f. sp. aeschynomene. Appl Environ Microbiol 64:5030–2.

Roy B, Haupt LM, Griffiths LR (2013) Review: Alternative splicing (AS) of genes as an approach for generating protein complexity. Curr Genomics 14:182–94. doi: 10.2174/1389202911314030004

Sassi M, Vernoux T (2013) Auxin and self-organization at the shoot apical meristem. J Exp Bot 64:2579–92. doi: 10.1093/jxb/ert101

Schmidt A, Hall MN, Koller A (1994) Two FK506 resistance-conferring genes in Saccharomyces cerevisiae , TAT1 and TAT2 , encode amino acid permeases mediating tyrosine and tryptophan uptake. Mol Cell Biol 14:6597–6606.

Seger S, Rischatsch R, Philippsen P (2011) Formation and stability of eisosomes in the filamentous fungus Ashbya gossypii. J Cell Sci 124:1629–34. doi: 10.1242/jcs.082487

Seiler S, Plamann M (2003) The genetic basis of cellular morphogenesis in the filamentous fungus Neurospora crassa. Mol Biol Cell 14:4352–4364. doi: 10.1091/mbc.E02

Seo PJ, Kim MJ, Ryu J-Y, et al. (2011) Two splice variants of the IDD14 transcription factor competitively form nonfunctional heterodimers which may regulate starch metabolism. Nat Commun 2:303. doi: 10.1038/ncomms1303

Stadler DR (1967) Suppressors of amino acid uptake mutants of Neurospora. Genetics 57:935–942.

Steinberg G (2007) Hyphal growth: a tale of motors, lipids, and the Spitzenkörper. Eukaryot Cell 6:351–60. doi: 10.1128/EC.00381-06

Strádalová V, Stahlschmidt W, Grossmann G, et al. (2009) Furrow-like invaginations of the yeast plasma membrane correspond to membrane compartment of Can1. J Cell Sci 122:2887–94. doi: 10.1242/jcs.051227

Strzelczyk E, Pokojska-Burdziej A (1984) Production of auxins and gibberellin-like substances by mycorrhizal fungi, bacteria and actinomycetes isolated from soil and the mycorrhizosphere of pine (Pinus silvestris L.)*. Plant Soil 81:185–194.

Sudbery PE (2008) Regulation of polarised growth in fungi. Fungal Biol Rev 22:44–55. doi: 10.1016/j.fbr.2008.07.001

Syed NH, Kalyna M, Marquez Y, et al. (2012) Alternative splicing in plants-coming of age. Trends Plant Sci 17:616–23. doi: 10.1016/j.tplants.2012.06.001

Tomita et al. (1987) Identification of Indol-3-acetic acid in Neurospora crassa. Agric Biol Chem 51:2633–2634.

Tomita K, Murayama T, Nakamura T (1984) Effects of Auxin and Gibberellin on Elongation of Young Hyphae in Neurospora crassa. Plant Cell Physiol 25:355–358.

Valencik M, Pringle J (1995) Schizosaccharomyces pombe bem1/ bud5 suppressor (bem46) mRNA. In: In. EMBL database, Access. number U29892.

Vangelatos I, Roumelioti K, Gournas C, et al. (2010) Eisosome organization in the filamentous ascomycete Aspergillus nidulans. Eukaryot Cell 9:1441–54. doi: 10.1128/EC.00087-10

Vanneste S, Friml J (2009) Auxin: a trigger for change in plant development. Cell 136:1005–16. doi: 10.1016/j.cell.2009.03.001

Videira A, Kasuga T, Tian C, et al. (2009) Transcriptional analysis of the response of Neurospora crassa to phytosphingosine reveals links to mitochondrial function. Microbiology 155:3134–41. doi: 10.1099/mic.0.029710-0

Walker MS, DeMoss J a (1983) Purification and characterization of the trifunctional beta-subunit of anthranilate synthase from Neurospora crassa. J Biol Chem 258:3571–5.

Walker MS, Demoss JA (1986) Organization of the Functional Domains of Anthranilate Synthase from. 261:

Walther TC, Brickner JH, Aguilar PS, et al. (2006) Eisosomes mark static sites of endocytosis. Nature 439:998–1003. doi: 10.1038/nature04472

Wang AZ, Ojakian GK, Nelson WJ (1990) Steps in the morphogenesis of a polarized epithelium. J Cell Sci 95:137–151.

Woodward AW, Bartel B (2005) Auxin: regulation, action, and interaction. Ann Bot 95:707–35. doi: 10.1093/aob/mci083

Yoshida A, Rzhetsky A, Hsu LC, Chang C (1998) Human aldehyde dehydrogenase gene family. Eur J Biochem 251:549–557.

Ziółkowska NE, Karotki L, Rehman M, et al. (2011) Eisosome-driven plasma membrane organization is mediated by BAR domains. Nat Struct Mol Biol 18:854–6. doi: 10.1038/nsmb.2080

Zuther K, Mayser P, Hettwer U, et al. (2008) The tryptophan aminotransferase Tam1 catalyses the single biosynthetic step for tryptophan-dependent pigment synthesis in Ustilago maydis. Mol Microbiol 68:152–72. doi: 10.1111/j.1365-2958.2008.06144.x

Kongressbeiträge

Kolláth-Leiß, K und Kempken, F (2009) The BEM46 homolog in *Neurospora crassa* appears to play an essential role in the hyphal development upon ascospore germination. 9th VAAM Symposium: Molecular Biology of Fungi, **Münster**

Kempken, F und Kolláth-Leiß, K (2009) The ER protein BEM46 appears to be essential for hyphal development upon ascospore germination in *Neurospora crassa*. Annual Conference of the German Genetics Society, **Köln**

Mercker, M, Kolláth-Leiß, K, Alves, S, Weiland, N und Kempken, F (2009) Funcional analysis of the conserved BEM46-like protein from *Neurospora crassa*. 25th Fungal Genetics Conference, **Asilomar, USA**

Kempken, F und Kolláth-Leiß, K (2010) The ER protein BEM46 influences hyphal development upon ascospore germination. 3rd European Neurospora Meeting, **Wien, Österreich**

Kolláth-Leiß, K, Quintanilla, J und Kempken, F (2011) BEM46 is essential for hyphal development upon ascospore germination in *Neurospora crassa*. 10th VAAM Symposium: Molecular Biology of Fungi, **Marburg**

Kumar, A, Kolláth-Leiß, K und Kempken, F (2011) Understanding the bud emergence 46 (BEM46) protein from functional and evolutionary perspectives. India Cell Biology Conference and Symposium on Membrane Dynamics, **Bhubaneswar, India**

Kumar, A, Kolláth-Leiß, K, Qiuntanilla, J und Kempken, F (2011) The evolutionary conserved BEM46-like protein is required for fungal ascospore germination. Annual Conference of the German Genetics Society, **Würzburg**

Kolláth-Leiß, K und Kempken, F (2011) The BEM46-like protein from *N. crassa* is required for ascospore germination. 26th Fungal Genetics Conference, **Asilomar, USA**

Kolláth-Leiß, K, Kumar, A und Kempken, F (2011) The *N. crassa* Bem46-like protein is involved in ascospore germination and interacts with the F domain of the anthranilate synthase component II. Neurospora Satellite Meeting, **Marburg**

Kumar, A, Kolláth-Leiß, K und Kempken, F (2012) Sequence, structure, function and evolution of BEM46 proteins. German Conference Bioinformatics, **Jena**

Kolláth-Leiß, K, Kumar, A, Sardar, P, Bönniger, C und Kempken, F (2013) Does BEM46 play a role in the regulation of auxin biosynthesis in *N. crassa*. Annual Conference of the German Genetics Society, **Braunschweig**

Bönniger, C, Kolláth-Leiß, K und Kempken, F (2013) Involvement of BEM46 on auxin biosynthesis in *Neurospora crassa*. XI International Fungal Biology Conference, **Karlsruhe**

Kumar, A, Kolláth-Leiß, K und Kempken, F (2013) Known unknown genes: evolution of eucaryotic BEM46. 27th Fungal Genetics Conference, **Asilomar, USA**

Kolláth-Leiß, K und Kempken, F (2013) The *N. crassa* Bem46 protein: alternative splicing and eisosomal association. 27th Fungal Genetics Conference, **Asilomar, USA**

Vortrag

Kolláth-Leiß, K und Kempken, F (2011). Funktion und Lokalisation des Bem46-Proteins in Neurospora crassa. 45. Wissenschaftliche Tagung der Deutschsprachigen Mykologischen Gesellschaft e.V., **Kiel**

Danksagung

An erster Stelle bedanke ich mich herzlich bei meinem akademischen Lehrer und Doktorvater Professor Dr. Frank Kempken für die Möglichkeit zur Promotion in seiner Arbeitsgruppe sowie für die Auswahl des Themas, das mir einerseits zeitliche Flexibilität, andererseits wissenschaftliche Kreativität bei der Bearbeitung ermöglicht hat. Ich möchte mich bei ihm für seine Unterstützung und sein Interesse bezüglich meiner Arbeit und ganz besonders für sein Verständnis für meine persönliche Situation bedanken. Auch bin ich ihm dafür dankbar, dass er es mir ermöglicht hat, wertvolle Erfahrungen bei zahlreichen Kongressen im In– und Ausland zu sammeln und schließlich dafür, dass ich meine Daten publizieren konnte.

Mein Dank gilt auch Frau Professorin Dr. Margret Sauter für die Bereitstellung der DR5::GUS *A. thaliana* Samen sowie für die konstruktive Diskussion hinsichtlich der Auxin-Bildung von *N. crassa*. Frau Dr. Christine Desel danke ich dafür, dass sie mir bei jeglichen Mikroskopie-Problemen zur Seite stand.

Ich danke herzlich allen gegenwärtigen und ehemaligen Mitarbeitern der Abteilung Botanische Genetik und Molekularbiologie für eine konstruktive und besonders familiäre Arbeitsatmosphäre, allen voran Frau Hanna Schmidt, die erste Ansprechpartnerin bei praktischen Problemen im Labor war und mir mit ihrer nordischen Art sehr ans Herz gewachsen ist. Ich danke Dr. Anika Bruhs, Dr. ElKbir Hihlal, Stefanie Grüttner, Linda Paun und Annika Regulin (meiner langjährigen Labor-WG-Mitbewohnerin) für die vielen wissenschaftlichen und nichtwissenschaftlichen Gespräche. Das Gleiche gilt für Dr. Abhishek Kumar, Hossein Emami, Pradeep Phule und Puspendu Sardar, die mit multikulturellem Flair meinen Alltag bereicherten.

Mein besonderer Dank gilt meiner ganzen Familie in Kiel und Ungarn, insbesondere meinem Sohn und meinem Mann, die alle Höhen und Tiefen meiner Promotionszeit hautnah miterleben mussten, meinen Großeltern und meiner Mama, die aus der Ferne mitgefiebert und mich unterstützt haben, sowie meiner Schwester und Anna für ihre lockere und liebevolle Art, mich aufzubauen.

Als Letztes danke ich allen meinen Freunden, die mir tagtäglich das Gefühl geben, in Deutschland zu Hause zu sein.

Lebenslauf

Krisztina Kolláth-Leiß

Persönliche Daten

Geburtsdatum:	16.02.1980
Geburtsort:	Salgótarján (Ungarn)
Staatsangehörigkeit:	ungarisch

Schulische Ausbildung

1986-1994	Jurijj Gagarin Általános Iskola (Grundschule)
1994-1998	ELTE Apáczai Csere János Gyakorlógimnázium (Gymnasium, Abschluss mit Abitur)

Studium

1998-2001	Biologiestudium an der ELTE Budapest
2001	Deutschkurs an der CAU zu Kiel (Abschluss mit PNDS)
2001	Chemiestudium an der CAU zu Kiel (1 Fachsemester)
2002-2008	Biologiestudium an der CAU zu Kiel (12 Fachsemester)
2008	Diplomarbeit in der Fachrichtung botanische Zellbiologie mit dem Titel „Untersuchungen zur Entstehung von Vesikeln in Blättern der Gerste (*Hordeum vulgare L.*)“
seit Oktober 2008	Lehrkraft für besondere Aufgaben am Botanischen Institut der CAU zu Kiel
seit 2010	Promotionsvorhaben an der CAU zu Kiel unter Betreuung von Professor Dr. Frank Kempken in der Abteilung Botanische Genetik und Molekularbiologie am Botanischen Institut

Erklärung

Hiermit erkläre ich, dass die vorliegende Dissertation nach Inhalt und Form meine eigene Arbeit ist. Abgesehen von der Beratung durch meine akademischen Lehrer wurden keine weiteren Hilfsmittel und Quellen verwendet als es angegeben ist. Textstellen, die inhaltlich oder wörtlich aus anderen Quellen entnommen wurden, sind als solche gekennzeichnet.

Die Arbeit wurde bisher weder ganz noch in Auszügen an anderer Stelle im Rahmen eines Prüfungsverfahrens vorgelegt. Des Weiteren erkläre ich hiermit, dass ich bisher keine Promotionsversuche unternommen habe.

Die Arbeit wurde unter Einhaltung der Regeln guter wissenschaftlicher Praxis der Deutschen Forschungsgemeinschaft verfasst.

Der Zulassung von Zuhörern bei der Disputation wird nicht widersprochen.

Kiel, ……

Krisztina Kolláth-Leiß

Anhang

Curr Genet (2009) 55:151–161
DOI 10.1007/s00294-009-0232-3

RESEARCH ARTICLE

The BEM46-like protein appears to be essential for hyphal development upon ascospore germination in *Neurospora crassa* and is targeted to the endoplasmic reticulum

Moritz Mercker · Krisztina Kollath-Leiß · Silke Allgaier · Nancy Weiland · Frank Kempken

Received: 19 January 2009 / Revised: 29 January 2009 / Accepted: 29 January 2009 / Published online: 24 February 2009

Abstract The bud emergence (BEM)46 proteins are evolutionarily conserved members of the α/β-hydrolase super family, but their exact role remains unknown. To better understand the cellular role of BEM46 and its homologs, we used the model organism *Neurospora crassa* in conjunction with *bem46* RNAi, over-expression vectors, and repeat induced point mutation analyzes. We clearly demonstrated that BEM46 is required for cell type-specific hyphal growth, which indicates a role for BEM46 in maintaining polarity. Vegetative hyphae, perithecia, and ascospores developed normally, but hyphae germinating from ascospores exhibited a loss-of-polarity phenotype. We also found that the BEM46 protein is targeted to the perinuclear endoplasmic reticulum (ER) and also localizes at or close to the plasma membrane. Our findings show that BEM46 can be used as a new ER marker for filamentous fungi, the first for *N. crassa*. Our data suggest that BEM46 plays a role in a signal transduction pathway involved in determining or maintaining cell type-specific polarity. This implies a higher degree of fungal hyphae differentiation than previously expected. This work also has implications for higher eukaryotic cells with polarized growth, such as pollen tubes or neuronal cells.

Keywords Cell type-specific growth · Ascospore germination · Polarity · ER localization · *Neurospora crassa* · Bud emergence 46-like (*bem46*)

Communicated by S. Hohmann.

Data deposition footnote: Accession number AM237804 *Ascobolus immersus bem46* fragment.

M. Mercker · K. Kollath-Leiß · S. Allgaier · N. Weiland · F. Kempken (✉)
Abteilung für Botanik mit Schwerpunkt Genetik und Molekularbiologie, Botanisches Institut, Christian-Albrechts-Universität zu Kiel, Olshausenstraße 40, 24098 Kiel, Germany
e-mail: fkempken@bot.uni-kiel.de

Present Address:
M. Mercker
Institut für Angewandte Mathematik, Universität Heidelberg, Im Neuenheimer Feld 294, 69120 Heidelberg, Germany

Present Address:
S. Allgaier
Neugenesis Corporation, 849 Mitten Road Suite 102, Burlingame, CA 94010, USA

Present Address:
N. Weiland
Institut für Allgemeine Mikrobiologie, Christian-Albrechts-Universität zu Kiel, Olshausenstraße 40, 24098 Kiel, Germany

Introduction

All eukaryotic organisms carry a homolog of the bud emergence (BEM)46 gene (Mochizuki et al. 2005), which was originally described by Valencik and Pringle (1995). The BEM46 protein and other homologous proteins possess conserved amino acid motifs of the α/β-hydrolase super family, which includes a variety of enzymes with diverse functions and a wide range of substrates (Ollis et al. 1992; Holmquist 2000). However, only a few members of the α/β-hydrolase super family have been assigned functions.

The BEM46 gene from *Schizosaccharomyces pombe* is a temperature-sensitive suppressor of a *bem1/bud5* double mutant from baker's yeast, *Saccharomyces cerevisiae* (Valencik and Pringle 1995). This double mutant exhibits

defects in cell polarity and bud emergence (Cabib et al. 1998; Madden and Synder 1998). The exact function of BEM46 is not yet known in yeast. However, a functional analysis of BEM1 has suggested that BEM1 is a scaffold protein which has two actin-binding domains (Chenevert et al. 1993). In addition to its interaction with actin, BEM1 has also been shown to interact with the G-protein BUD1, cell division cycle CDC42 (Park et al. 1997; Irazoqui et al. 2003), and with GDP–GTP exchange factors, such as BUD5 (Chant et al. 1991; Cabib et al. 1998), which are necessary for the positioning of a complex involved in bud formation. It is possible that the *S. pombe* BEM46 peptide combines the functions of BEM1 and BUD5. The *Aspergillus nidulans* homolog of BEM1, BemA, seems to play a role in polarisome formation (Leeder and Turner 2008). Potential targets of BUD5 include proteins involved in bud site selection and bud formation, BUD1 and CDC42, respectively (Chant et al. 1991). Taken together, these studies implicate a role of BEM46 in signal transduction and actin organization.

In *Drosophila melanogaster*, two-hybrid assays have suggested that a BEM46-homolog interacts with the Rapsynoid protein (Giot 2003), a putative GDP–GTP exchange factor for a Gα protein involved in the asymmetrical cell division of larval neuroblast cells (Parmentier et al. 2000). In the weed *Arabidopsis thaliana*, a BEM46 homolog called Wavy Growth 2 has been shown to negatively regulate stimulus-induced root bending through the inhibition of root tip rotation (Mochizuki et al. 2005). These studies also suggest that BEM46 homologs may play a role in signal transduction or cell polarity. It has also been suggested that BEM46 might influence cell morphogenesis at the cell surface (Mochizuki et al. 2005), though the exact functions remain unknown.

Functional analysis of the fungal BEM46 protein is of general interest because fungal hyphae serve as a model system for polarized growth, such as neuronal polarity (Arimura and Kaibuchi 2005). In a previous study concerning fungal transposable elements (Kempken 2001), a homolog of the evolutionarily conserved *bem46* was identified close to a retro-element in the genome of the filamentous fungus *Ascobolus immersus*. Shortly after that study, the *Neurospora crassa* genome sequence was published, which contains approximately 10,000 predicted protein-encoding genes (Galagan et al. 2003; Mannhaupt et al. 2003), including a *bem46* homolog. Because *N. crassa* has been used as a genetic model organism for a long time, we aimed to analyze the function of the evolutionarily conserved BEM46 protein in this species of fungus.

In this paper, we present evidence that BEM46 is required for hyphal growth upon ascospore germination. Most likely, BEM46 is necessary for maintaining cell type-specific polarity. We also describe evidence that BEM46 is targeted to the ER and localizes at or close to the plasma membrane. Our data suggest that BEM46 plays a role in a signal transduction pathway involved in determining or maintaining cell type-specific polarity.

Materials and methods

Strains

In a previous study of the filamentous fungus *Ascobolus immersus*, we identified a *bem46* homolog adjacent to the integration site of a retro-element (EMBL accession number AM237804). When the *N. crassa* genomic sequence became available (Galagan et al. 2003; Mannhaupt et al. 2003), we were able to identify an *N. crassa bem46* ortholog (NCU03276). Therefore, all further work was done using this well characterized model organism.

The following fungal strains were used in this study: *N. crassa* F10292-1 [*arg-1* K166, *his-3* K480, *cot-1* C102T, *rec-2*, A], FGSC #6103 [*his-3* (Y234M723) mat A], and FGSC #9716 [*his-3* (1-234-723) mat a] (Fungal Genetics Stock Center, Kansas City, USA). For the propagation of vector constructs under standard culture conditions, we used *E. coli* strain XL-Blue1 [*recA1, endA1, gyrA96, thi-1, hsdR17, supE44, relA1, lac F'proAB lacI^{q}ZΔM15 Tn10* (*Tet^r*), Stratagene, La Jolla]. For the propagation of RNAi constructs, we used *E. coli* strain SURE [*e14–*, (*McrA–*), *D*(*mcrCB-hsdSMR-mrr*)*171, endA1, supE44, thi-1, gyrA96, relA1, lac, recB, recJ, sbcC, umuC::Tn5,* (*Kan^r*), *uvrC, F' proAB lacI^{q}ZDM15 Tn10* (*Tet^r*), Stratagene, Heidelberg].

DNA and RNA isolation

The isolation of DNA was performed according to a previously described protocol (Borges et al. 1990). In brief, mycelium was ground under liquid nitrogen, transferred into lysis buffer (10 mM Tris–HCl, 1 mM EDTA, 100 mM NaCl, 2% SDS, pH 8.0), and phenol extraction performed. Subsequently, the aqueous phase was incubated with 100 µg RNAseA, followed by an additional phenol extraction and ethanol precipitation. Bacterial plasmid DNA was isolated using NucleoSpin reagent sets (Macherey–Nagel, Düren). For the isolation of RNA from macroconidia, ascospores, and perithecia, tissue was disrupted using a Brinkmann mixer mill from Retsch (Hilden). RNA was isolated from mycelium using published procedures (Kempken and Kück 1996).

Gel electrophoresis, blotting, and hybridization

Agarose gel electrophoresis, Southern and Northern blotting, and DNA–DNA and DNA–RNA hybridization were

performed according to previously described protocols (Sambrook et al. 1989). A decaprime kit (Ambion, Austin) was used to label 20–30 ng of template DNA with ^{32}P αdCTP. Markers for DNA from MBBL (Bielefeld) were used to determine size in DNA gel electrophoresis.

PCR and RT-PCR amplification

PCR and RT-PCR were carried out as previously described (Howad and Kempken 1997; Staudinger and Kempken 2003). For semi-quantitative RT-PCR, 5 µl aliquots were removed from PCR amplified samples after 34, 37, and 40 cycles. For the location of the *bem46*-specific oligonucleotides, see Fig. 1. Actin mRNA was amplified using oligonucleotides FK790 (5′-GGACGACATGGAGAAGATTTG G-3′) and FK791 (5′-GAGCGGACCTAGCCTATACTG C-3′) in the same reaction tube with *bem46* mRNA, which was amplified using oligonucleotides FK701 (5′-GGCA AGCATGTCATCTCCATC-3′) and FK702 (5′-ATGTTG AGCCCAGATTCGTC-3′) or FK701 and NW872 (5′-CT ATTTCTTTTCGGGGTCTCC-3′). For experiments using different tissues, the actin control could not be used because actin was differentially expressed. In these cases, the amount of RNA used for RT-PCR was determined using a NanoDrop ND-1,000 spectrophotometer (NanoDrop Technologies, Wilmington). The RNA concentration of six samples were: ascospores wild-type, 58.1 ng/µl; ascospores RNAi, 19.2 ng/µl; mycelium wild-type, 163.0 ng/µl; mycelium RNAi, 389.0 ng/µl; macro conidia wild-type, 278.9 ng/µl; macro conidia RNAi, 86.2 ng/µl. For RT-PCR

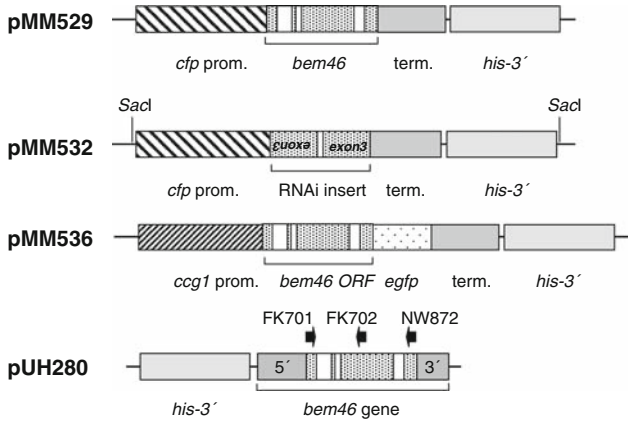

Fig. 1 Schematic representation of vectors pMM529, pMM532, pMM536, and pUH280. Vector components are indicated below the drawings. The positions of *bem46*-specific oligonucleotides used for RT-PCR of *bem46* mRNA are indicated for vector pUH280. For vector pUH280, 5′ and 3′ untranslated regions (UTRs) are indicated. The *bem46* exons (*dotted boxes*) and introns (*white boxes*) are indicated. The *his′-3* gene fragment was used for auxotrophic selection. Promoter, prom.; terminator, term. For vector pMM532 *Sac*I restriction sites are shown, as these are used for digestion of total DNA in the Southern blot shown in Fig. 3a

or quantitative RT-PCR, equal amounts of RNA were calculated based on NanoDrop readings.

All oligonucleotides were synthesized by MWG Biotech (Ebersberg). Quantitative RT-PCR assays were performed as described by (Veit et al. 2006) using a QuantiTect Probe RT-PCR Kit (Qiagen) and a 7,300 real-time PCR system (ABI, Foster City, USA). The primers used for the quantitative RT-PCR reactions are the same as listed above. The fold change in transcript abundance for each gene of interest in an RNA preparation was determined by comparison with the threshold cycle (Ct) of transcripts from the *N. crassa* actin gene. The fold change in the abundance of a transcript was calculated using the formula: fold change = 2 − DDCt, as previously described (Talaat et al. 2004).

Transformation, transformant analysis and microscopy

Cloning and *E. coli* transformation were performed according to standard procedures (Sambrook et al. 1989). Vector construction is described below. Spheroplasts were prepared from *N. crassa* and used for DNA-mediated transformation as previously described (Yuan and Marzluf 1992; Margolin et al. 1997). Primary transformants were obtained by site-specific recombination at the *his-3* locus (Bowring and Catcheside 1993) and selection for growth on Vogel's minimal medium (Vogel 1956). All cloning and transformation experiments were conducted in accordance with the requirements of the German gene technology law (GenTG).

Repeat induced point (RIP) assays were based on published procedures (Cambareri et al. 1991). The vector pUH280 was inserted into the *N. crassa* genome at the *his-3* locus, creating an additional copy of *bem46* in order to trigger the RIP mechanism. Ascospores were obtained from crosses with strain F10292-1.

For the germination assays, ejected ascospores were harvested and incubated in 500 µl sterile water at 60°C for 90 min to inactivate contaminating macroconidia. Ascospore numbers were adjusted to 4×10^3 spores/ml. All light microscopy was performed using a Zeiss Axiophot-Mikroskop equipped with a SONY 3CCD digital camera. Confocal fluorescence analysis was performed using a confocal laser scanning microscope (TCS SP1 or SP5 (used for ER Tracker™ Red, Leica). Fungi were cultivated for microscopy as previously described (Hickey et al. 2002). Membranes were stained with SynaptoRed (Sigma-Aldrich, Steinheim) directly applying a drop of 6.4 µM SynaptoRed solution to the mycelium or conidia. Nuclei were stained with DAPI (4′,6-diamidino-2-phenylindole, 1 µg/ml, Sigma-Aldrich, Steinheim); ER was stained using ER Tracker™ Red (BODIPY® FL glibenclamide, Molecular Probes, Eugene), 10 µM, incubation for 30 min at room temperature in the dark.

Vector construction

The vectors are depicted in Fig. 1. The vector pUH280 carries the entire BEM46 gene, which was amplified with oligonucleotides FK371 (5′-GGGAAGCTTGAACG GTTCAATTGACCG1GAAGTTGC-3′) and FK372 (5′-G GGAAGCTTTCAAGCCACCAAGGTCGTGGTTGTCG-3′) from *N. crassa* genomic DNA. The vector over-expressing *bem46,* pMM529, was generated by cloning the PCR amplified *bem46* open reading frame (ORF) (FK 832 5′-GG GCGCGCCATGTCATCTCCATCTGTCAC-3′ and FK833 5′-GATTTAAATCTATTTCTTTTCGGGGTCTC-3′) into an *N. crassa* expression vector (Allgaier et al. in preparation). The RNAi vector pMM532 is based on exon III of *bem46*. Using oligonucleotides FK815 (5′-GGGCGCGCC GATCAAGGTGTCGGTAGCC-3′) and FK816 (5′-GGG ATCCAGCCCTAATCTATCCCTCTCA-3′), a 596 bp fragment of exon III was amplified in the inverse orientation. The oligonucleotides FK813 (5′-GGGATCCGTATG TGGTCCCCAATCTGA-3′) and FK814 (5′-GATTTAAA TGATCAAGGTGTCGGTAGCC-3′) were used to amplify exon III and the adjacent intron II. Flanking restriction sites integrated into the oligonucleotides were used to ligate the amplicons into an expression vector. The *egfp*-fusion-vector pMM536 consists of the 1357 bp *bem46* ORF amplified with FK832 and FK430 (5′-GGGAAGCTTTTTCTTTTCG GGGTCTCCTGAG-3′). The 734 bp *egfp* ORF was amplified with FK431 (5′-GGGAAGCTTGTGAGCAAGGGC GAGGAGCTG-3′) and FK652 (5′-GATTTAAATTACTT GTACAGCTCGTCCAT-3′). Both ORFs were fused and ligated in an expression vector under the control of the *ccg1* promoter (Freitag et al. 2004). The promoter of the clock-controlled gene (*ccg*) 1 is regulated by development and light (Loros et al. 1989; Arpaia et al. 1995) and active in vegetative hyphae, developing asci, and ascospores (Freitag et al. 2004). The *cfp* (former name: cytoplasmic filament protein, record name: pyruvate decarboxylase) promoter drives carbon source-dependent expression of transgenes in *N. crassa*. The *cfp* gene encodes a polypeptide of 59-kDa constituent of pyruvate decarboxylase, a key postglycolytic enzyme catalyzing the branch-point step between fermentation and respiration (Temporini et al. 2004).

Sequence analysis

All sequence analysis was carried out by MWG Biotech (Ebersberg) and SEQlab (Göttingen).

Results

All known BEM46 peptide sequences from a variety of eukaryotes exhibit a high degree of similarity. In a FASTA comparison, approximately 50 orthologs with *e* values lower than −30 were identified. Figure 2a shows a partial alignment of selected BEM46 amino acid sequences with the main conserved part of these proteins. In Fig. 2b the structure of selected BEM46 peptides with putative signal peptides, transmembrane domains and the α/β hydrolase is shown.

Because the endogenous *bem46* transcript is not detectable by Northern blot hybridization (Fig. 3d), RT-PCR was used to analyze the level of *bem46* expression in mycelia, macroconidia, and ascospores. As shown in Fig. 3b, *bem46* was transcribed in ascospores, macroconidia, and mycelia.

To elucidate the function of the *N. crassa bem46* homolog, four vectors were constructed as described in "Materials and methods" (Fig. 1). Transformants of all four vectors were obtained. While numerous transformed colonies were obtained with vectors pUH280, pMM529, and pMM536 (data not shown), only a small number of transformants could be obtained with the RNAi vector pMM532 (Fig. 3a, lanes 4 and 8).

RT-PCR and real-time PCR were employed to monitor RNAi-mediated transcript degradation in four-day-old mycelia. As shown in Fig. 3b (Ri lanes), *bem46* transcripts were greatly reduced in RNAi transformants when the RNAi construct was expressed, whereas the internal actin amplification control, was properly amplified in both RNAi transformant and untransformed recipient types (Fig. 3b, lane nt). To quantify these data, real-time RT-PCR was employed (Fig. 3c) using actin RNA as an internal control. Silencing was confirmed in ascospores, mycelium, and macroconidia. The real-time data fit well with the previous RT-PCR results. Thus, we concluded that RNAi-mediated *bem46* RNA degradation was successfully achieved.

To investigate the effect of over-expressing the BEM46 protein, vector pMM529 (Fig. 1) was used. Four out of five pMM529 transformants strongly expressed the *bem46* transcript, at levels far above that seen in wild-type (Fig. 3d, lanes 1, 3, 4, and 5). The *bem46* RNAi and over-expressing transformants exhibited normal vegetative growth, conidiation, conidial germination (Fig. 4) and mating response compared to wild-type mycelia. They also entered the sexual cycle and generated fruiting bodies and asci (data not shown). However, early hyphal development upon ascospore germination was strongly impaired (Fig. 5). Hyphae from the germinating ascospores of these transformants usually developed a terminal bubble-like structure, indicating loss-of-polarity, and stopped growing. Interestingly, this phenotype was visible in both RNAi (Fig. 5a) and over-expressing ascospore progeny (Fig. 5b). Ascospores germinated with one or two short hyphae but stopped growing shortly afterwards. As a consequence, the mycelia did not develop from affected ascospores. Most interestingly, the loss-of-polarity phenotype occurred in a cell type-specific

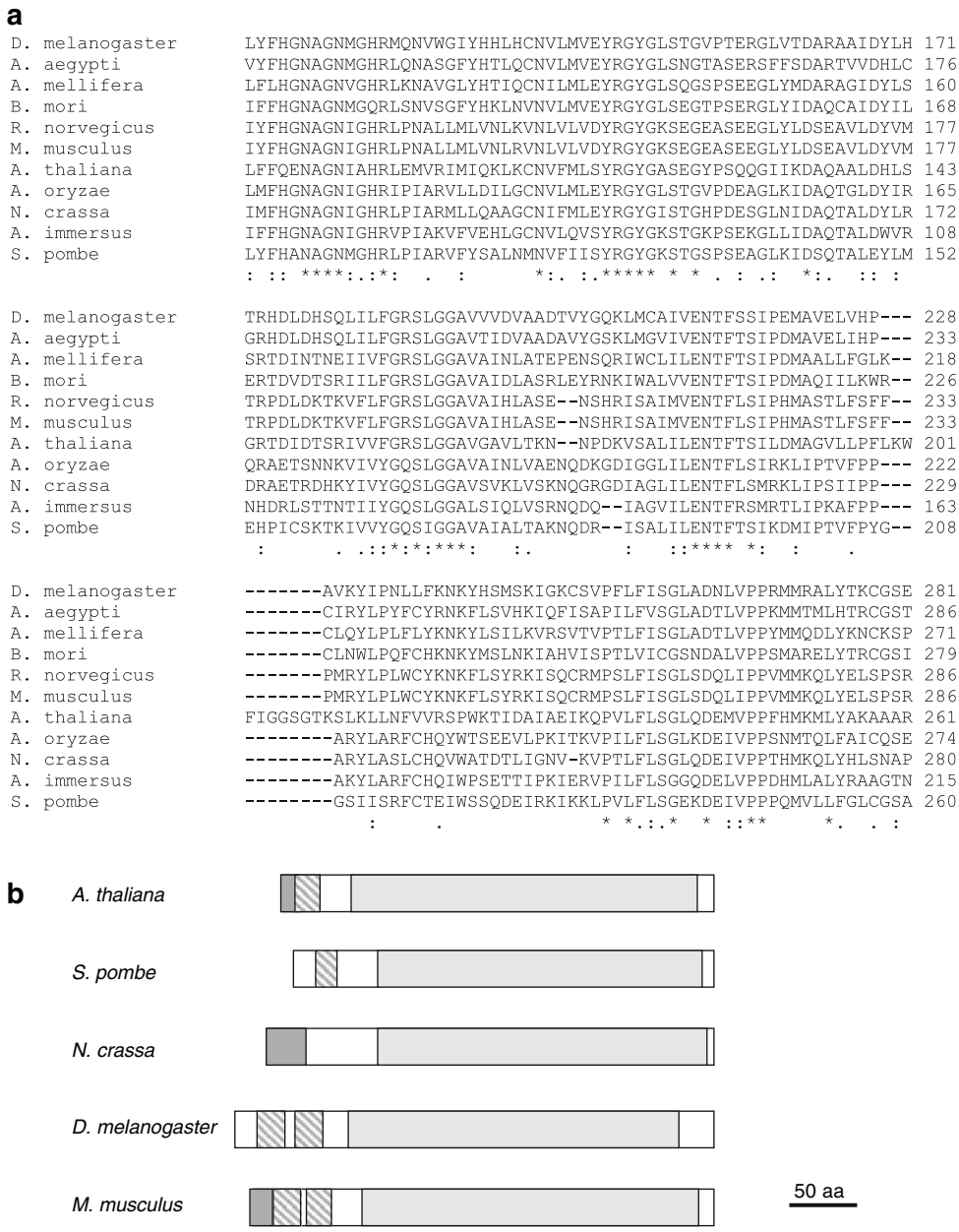

Fig. 2 **a** Partial alignment of BEM46 peptide sequences from *N. crassa* and ten other organisms, including fungi, plant and animal sequences. The sequences were aligned using ClustalW. Sequences were obtained from the EMBL database. **b** Localization of transmembrane (*hatched boxes*), signal peptide (*dark grey boxes*), and α/β hydrolase domains (*grey boxes*) in selected BEM46 proteins [modified from (Mochizuki et al. 2005)]

manner; it occurred only in hyphae germinating from ascospores. This is a particular, and new, feature of the *N. crassa* BEM46 homolog. A similar phenotype was not observed in hyphae germinating from conidia. The same phenotype was observed with the RIP mutation assay. Using vector pUH280, an additional copy of the *bem46* gene was introduced into *N. crassa* at the *his-3* site (not shown) and ascospores were isolated from a cross with the untransformed recipient of the opposite mating type. Many ascospores did not germinate properly and exhibited a phenotype as shown in Fig. 5d, which is very similar to that obtained from *bem46* RNAi or over-expressing transformants (Fig. 5a, b). Unfortunately, these mutants putatively caused by the RIP mechanism could not be analyzed further, as they did not form mycelia. However it is possible, that the phenotypes observed with over-expressing or RNAi lines are caused by a RIP event due to additional gene copies. To avoid this we isolated ascospore under mild-RIP conditions (Barbato et al. 1996). In order to confirm whether a RIP event took place or not, DNA was isolated from germinating ascospores resulting from crosses with the RNAi line. The *bem46* gene was PCR amplified and sequenced. We did not observe RIP-like mutations, indicating that the phenotype of the RNAi line was not caused by RIP (data not shown).

The significant effect on ascospore germination and hyphal development became even more obvious when ascospores were allowed to germinate on Vogel's minimal

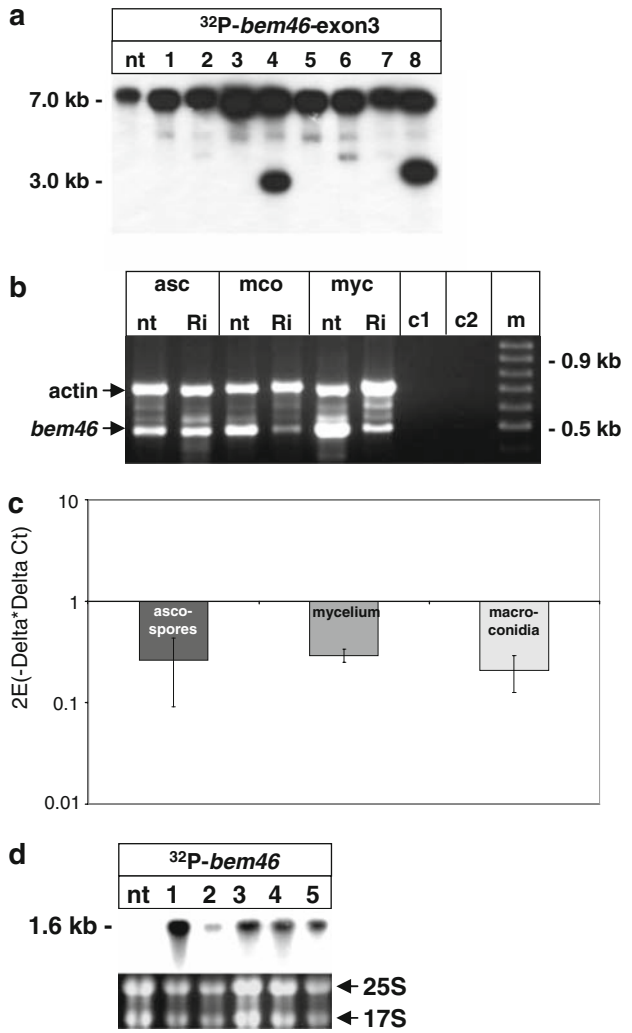

Fig. 3 RNAi and over-expressing lines. **a** Southern blot analysis of *N. crassa* mycelia transformed with the RNAi vector pMM532. DNA of non-transformed wild-type (*nt*) and transformants (*lanes 1–8*) were digested with *Sac*I and submitted to gel electrophoresis. In addition to the *bem46* wild-type hybridization signal (7 kb), two transformants (*lanes 4 and 8*) exhibit an additional band of approximately 3 kb representing the *Sac*I vector fragment carrying the RNAi construct (see vector pMM532, Fig. 1). **b** Example of RNAi-directed loss of *bem46* transcription. RT-PCR was performed using oligonucleotides FK701 and FK702 (see "Materials and methods"). As an internal control, actin mRNA was amplified using FK790 and FK791. *N. crassa* RNAi transformant no. NcT289 = Ri; not transformed (recipient) = nt; ascospores = asc; macroconidia = mco; mycelium = myc. c1 = DNA contamination control prior to RT-PCR; c2 = RT-PCR control without template RNA. **c** Quantitative real-time PCR using RNA from the same samples as (**b**). Mean values of three experiments are shown; value > 1: gene upregulated in comparison to wild-type; value < 1: gene downregulated in comparison to wild-type. **d** Northern blot analysis showing *bem46* over-expression in *N. crassa* mycelia transformed with vector pMM529 (*lanes 1–5*). 25S and 17S rRNA represent the loading controls; *nt* non-transformed wild-type

medium (Fig. 6a). We performed reverse crosses using non-transformed *his-3*$^{-}$ mycelia that require histidine for growth as maternal or paternal mating partners. In the

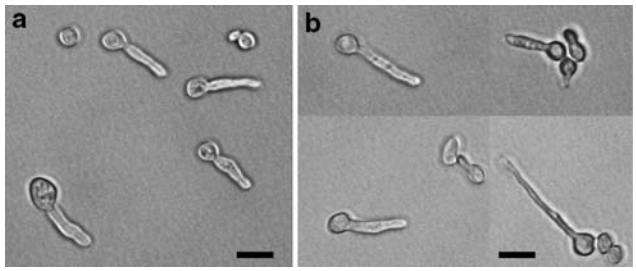

Fig. 4 Morphology of vegetative hyphae. **a** Germinating macroconidia from wild-type and **b** macroconidia from RNAi transformant NcT289. *Scale bars* 5 μm

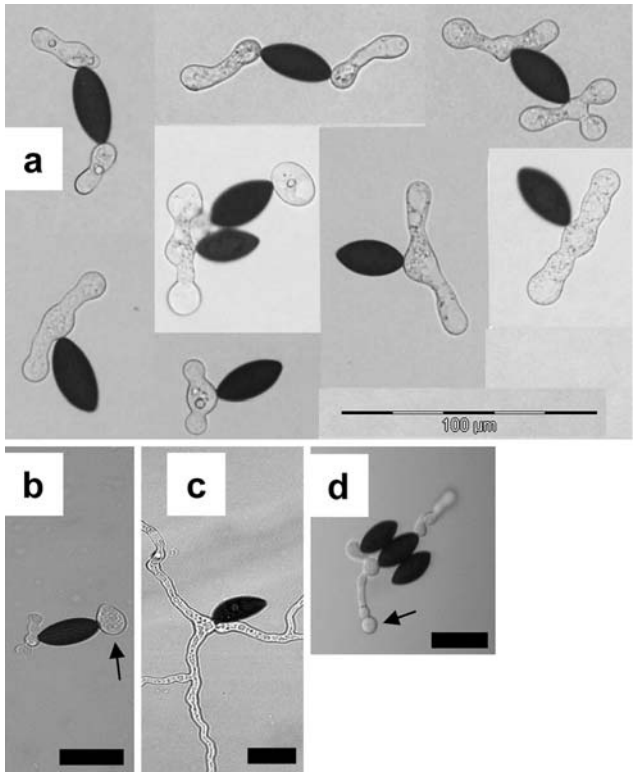

Fig. 5 Morphology of germinating ascospores. **a** Cross of RNAi transformant NcT289 with the untransformed recipient of the opposite mating type. Several germinating ascospores with terminal "bubbles" at the hyphae, which indicate loss-of-polarity and growth arrest are shown. *Scale bar* 100 μm. **b** Cross of *bem46* over-expressing transformant NcT285 with wild-type. **c** Wild-type crossed with NcT179 carrying the expression vector without *bem46*. **d** An ascospore from RIP. Ascospore germination was carried out on Vogel's minimal medium with glucose at 25°C in the light. *Arrows* in (**b**) and (**d**) highlight terminal "bubbles" at the hyphae. *Scale bars* in (**b**)–(**d**) represent 25 μm

transformants (NcT289 and NcT288 in Fig. 6), the restored *his-3* gene was tightly linked to the RNAi or over-expressing construct. The *his-3*$^{-}$ ascospores were not able to grow on minimal medium, and it is highly unlikely that a crossing-over event occurred between the *his-3* gene and the transgene in the transformants. A hundred ascospores were

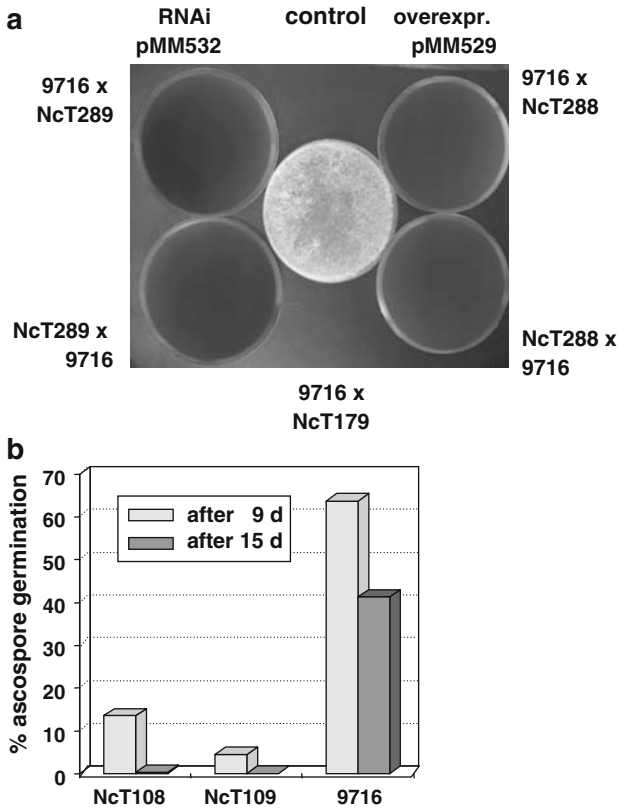

Fig. 6 Ascospore germination. **a** Ascospore germination from reciprocal crosses of transformants (NcT288 and NcT289) with non-transformed recipient his$^-$ strain (9716) of the opposite mating type. Spores carrying the his$^-$ allele cannot grow on minimal medium. *Left* transformant NcT289 with RNAi constructs pMM532, ascospore plated on minimal medium. *Center* cross of NcT179 (carries empty vector) on minimal medium for comparison. *Right* transformant NcT288 with over-expressing construct pMM529 on minimal medium. **b** Ascospore germination on minimal medium upon RIP assay (NcT108, NcT109 with additional copy of *bem46* triggering RIP) or from control cross. Spores were harvested 9 or 15 days after perithecia formation

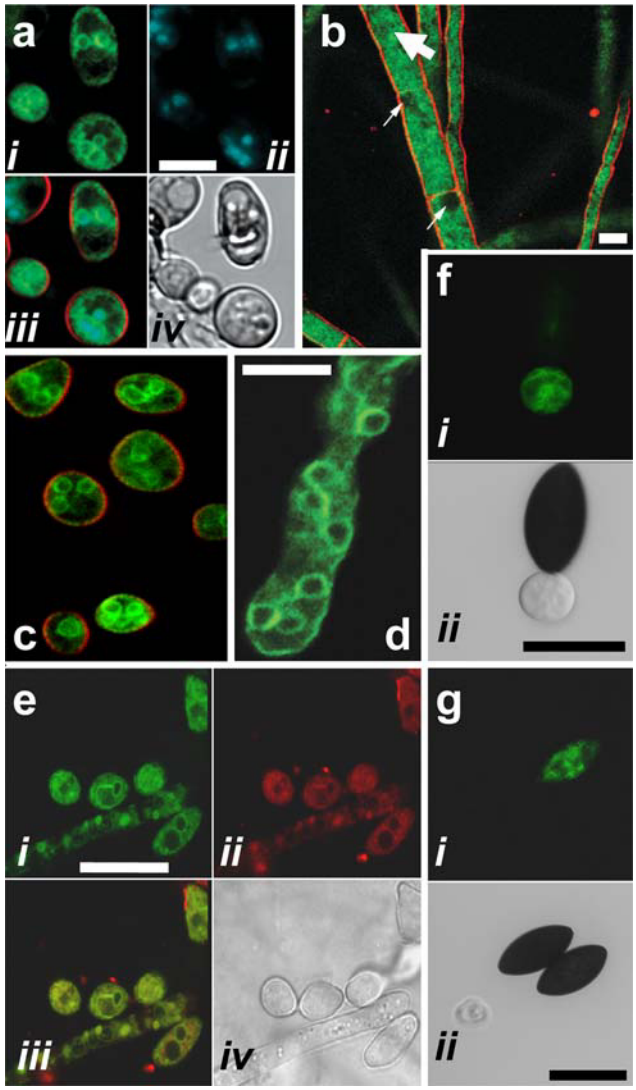

Fig. 7 Cellular localization of BEM46. Transformants carrying pMM536 express a BEM46:eGFP fusion protein. **a** Macro-conida exhibiting (*i*) eGFP fluorescence, (*ii*) DAPI staining, (*iii*) an overlay with additional staining of the plasma membrane using SynaptoRed and (*iv*) calculated bright field. **b** eGFP fluorescence in mature hyphae. *Small arrows* indicate vacuoles; the *large arrow* indicates round-shaped structures similar to (**a**); plasma membrane stained with SynaptoRed. **c** Macroconidia with BEM46:eGFP expression and plasma membrane stained with SynaptoRed. **d** BEM46:eGFP fluorescence in young hyphae germinating from macroconidia. **e** (*i*) BEM46:eGFP fluorescence in hyphae and conidia (*ii*) ER Tracker^{TM} Red; (*iii*) an overlay of both; (*iv*) calculated bright field **f** Germinating ascospores (*i*) BEM46:eGFP fluorescence, and (*ii*) calculated bright field. **g** Premature ascospore (*i*) BEM46:eGFP fluorescence, and (*ii*) calculated bright field. All pictures were obtained by confocal laser microscopy. *White scale bars* represent 10 µm, *black scale bars* represent 30 µm

plated for each and incubated for 48 h. While the wild-type ascospores germinated well and formed a visible mycelium (Fig. 6a), no mycelial growth from ascospores in any cross containing the RNAi or over-expressing construct was observed. This result was obtained consistently in repeated experiments. Using crosses employing an RNAi strain, 2,000 and 5,000 spores were plated in additional experiments. Only 6 and 12 spores, respectively, did germinate and form colonies. Rare germination may be due to the down-regulation of the RNAi construct or a rare recombination at the *his*-locus. Similarly, RIP assays led to reduced ascospore germination, which was significantly lower when testing ascospores from RIP mutation experiments compared to wild-type crosses (Fig. 6b).

The BEM46 peptide was predicted to possess a secretion signal (see Fig. 2b). Vectors expressing a *bem46:egfp* gene fusion under the control of the endogenous *bem46* promoter did not exhibit significant eGFP fluorescence. This result was not unexpected, as similar observations had been made previously (Freitag et al. 2004). Therefore, we used the *ccg1* promoter for eGFP expression, as it is known to work well in *N. crassa* (Freitag et al. 2004) (Fig. 7). Hyphae,

macroconidia, and young hyphae from macroconidia exhibited a similar level of eGFP distribution. Circular ring-like structures were clearly visible in varying numbers (Fig. 7a i, c, d), identical in shape to those observed in SNARE-eGFP fusions in *Aspergillus oryzae* (Kuratsu et al. 2007). Co-staining with DAPI (Fig. 7a ii, iii) led to the conclusion that the ring-like structures surround the nuclei, suggesting that they are perinuclear ER. Co-localization studies using the ER Tracker™ Red are shown in Fig. 7e (i–iv) and confirm ER localization of BEM46:eGFP.

This effect is less apparent in older hyphae (Fig. 7b) as they may contain hundreds of nuclei. However, on closer inspection, similar circular structures were present (Fig. 7b, big arrow). Moreover, in germinating hyphae from macroconidia, the BEM46:eGFP protein was often localized in the hyphal tip area (Fig. 7d i) or in linear structures near the plasma membrane. In macroconidia, the BEM46:eGFP protein was visible in small dots localized near to or directly associated with the plasma membrane (Fig. 7a, c). There was no co-localization of BEM46:eGFP with SynaptoRED indicating these structures are not surrounded by membranes, i.e. are neither vesicles nor small vacuoles. It should be noted that the transformants exhibiting BEM46:eGFP over-expression had the same phenotype as BEM46 over-expressing lines, indicating that the fusion protein was functional. Likewise, hyphae germinating from ascospores as shown in Fig. 7f exhibited the same phenotype as seen in Fig. 5a or b and showed BEM46:eGFP fluorescence as well. We observed BEM46:eGFP fluorescence in some ascospores as shown in Fig. 7g, indicating that the *bem46:egfp* gene was not affected by RIP or meiotic silencing. This was also demonstrated by BEM46:eGFP expression in hyphae germinating from ascospores (Fig. 7f).

Discussion

Previous studies on BEM46 homologs in various eukaryotes linked these proteins to developmental processes and cellular polarity; in *S. pombe*, it appears to be involved in cell polarity (Chant et al. 1991; Valencik and Pringle 1995; Madden and Synder 1998); in *Arabidopsis*, Wavy Growth 2, the BEM46 homolog is required for root growth (Mochizuki et al. 2005); and in *Drosophila,* a homolog plays a role in larval development (Parmentier et al. 2000; Giot 2003). Though, in *S. cerevisiae* and *Arabidopsis*, BEM46 homologs are not essential (Giaever et al. 2002; Mochizuki et al. 2005). Similarly, the *N. crassa* BEM46 protein is not essential for vegetative hyphal growth or sexual development. However, BEM46 is essential for hyphae development from germinating ascospores; BEM46 acts in a cell type-specific manner. This is a new and unexpected finding.

In wild-type *N. crassa*, *bem46* appears to be differentially expressed in different tissues. A significant increase and decrease in the level of *bem46* mRNA led to very similar phenotypes in the corresponding transformants. An alternative explanation would be the action of the *N. crassa* RIP mechanism, but this was excluded by sequencing DNA from germinating ascospores. Also, *bem46:egfp* fusions were functional in ascospores, indicating that the RIP process is not responsible for the observed phenotype. While meiotic silencing might have occurred (Shiu and Metzenberg 2002), it would not result in any phenotype, as it would only effect expression of the introduced constructs. Unlike the other vectors we utilized, only a small number of transformants could be obtained with the RNAi vector pMM532. This may indicate interference by the inverted repeat construct with the recombination process necessary for the genomic integration of vector DNA, or, alternatively, a deleterious effect of the RNAi construct on primary transformants. The RNAi vector was constructed because there is not yet a *bem46* knock-out available from BROAD center.

It has long been established that *N. crassa* is able to detect repeated DNA sequences and introduce point mutations, thus inactivating these sequences (Cambareri et al. 1989; Selker 1997). The RIP mutation occurs in the haploid nuclei of fertilized, premeiotic cells before fusion of the parental nuclei. Both copies of the duplications of gene-sized sequences are affected in the first generation at frequencies of approximately 50–100%. As a consequence, multiple GC-to-AT mutations occur (Cambareri et al. 1991). It is possible that the observed phenotype might have been caused by the action of the RIP process, as the RNAi construct might have triggered a RIP response. However, the exon sequence used in the RNAi vector was only 596 bp in size, and, thus, close to the lower size limit of RIP (Galagan and Selker 2004). To prevent a RIP event, crosses were also done under conditions which would lead to mild-RIP only (Barbato et al. 1996).

The similar observation, that over-expression and knockdown leads to the same phenotype, has been made in many other organisms; the over-expression and knockdown of the zebrafish gadd45beta gene has been shown to cause somite defects (Kawahara et al. 2005). In this, and other cases, the corresponding proteins were found to be involved in or associated with signal transduction pathways (Bedell et al. 2005; Hu et al. 2005; Kawahara et al. 2005). Thus, the BEM46 protein may be involved in the signal transduction required for a specific cell type; in this case, the development of hyphae from ascospores. To date, a number of mutations affecting ascospore germination or early hyphal development are known. Some mutated phenotypes exhibit a reduced germination rate (Murray and Srb 1961; Garnjobst and Tatum 1967; Chang and Nakashima 1998), whereas

other phenotypes exhibit delayed hyphal growth (Davis 1979; Perkins et al. 1997; Perkins et al. 2001) or a change in early mycelial morphology (Garnjobst and Tatum 1967). However, none of these mutants exhibit a loss-of-polarity phenotype.

Loss-of-polarity has been observed in some temperature-sensitive *N. crassa* mutants (Bruno et al. 1996; Seiler and Plamann 2003) that exhibit similar effects as observed in this study, but only in the vegetative hyphae. It should be noted that, in the articles cited, temperature-sensitive mutants were used that exhibit normal growth at the permissive temperature. Nevertheless, phenotypes of hyphae at restrictive temperatures (Bruno et al. 1996) are very similar to those observed in our study. Therefore, we conclude that BEM46 is an additional factor required to determine or maintain polarity and acts in a cell type-specific manner. This finding is rather unexpected and implies that fungal hyphae have at least two different ways of maintaining polarity, as hyphae germinating from vegetative macroconidia are not affected by *bem46* RNAi or over-expression. This finding also implies a higher degree of differentiation of fungal hyphae than previously expected. This work has implications for higher eukaryotic cells with polarized growth, such as pollen tubes or neuronal cells.

The subcellular localization of BEM46 was studied using eGFP fusion proteins. Such assays are preferably done using the endogenous promoter of the gene in question. However, this is not possible in *N. crassa*, as most endogenous promoters are unable to provide the required level of gene expression (Freitag et al. 2004). Therefore, we cannot fully exclude the possibility that artificial localization may be observed due to high expression levels, although our data confirm in silico predictions for the localization of BEM46 peptide. Nevertheless, because the transformants carrying the BEM46:eGFP fusion protein exhibit the same phenotype as the BEM46 over-expressing lines, the BEM46:eGFP fusion appears to be functional.

Our data clearly indicate that BEM46 is transported into the ER. Studies using ER-labeled yeast cells or filamentous fungi have also given comparable results to those reported here, i.e. ring-shaped structures surrounding the nucleus (Fernández-Ábalos et al. 1998; Wedlich-Söldner et al. 2002; Grimme et al. 2004; Estrada de Martin et al. 2005; Faulhammer et al. 2005). In fact our observation appears to be similar or identical to those observed in SNARE-eGFP fusions in *A. oryzae* (Kuratsu et al. 2007). Data regarding the S. pombe BEM46 protein also suggest localization in the membrane of the ER (Matsuyama et al. 2006). Finally, in silico analysis indicates the presence of a signal peptide in the BEM46 protein (Fig. 2b). There is, however, no detectable ER retention signal. This indicates that the BEM46 protein is not permanently localized in the ER. Indeed, as shown in Fig. 7, BEM46:eGFP is also visible close to the plasma membrane in macroconidia and at the tip area of growing vegetative hyphae. It is possible that at least some of these areas are part of the ER too, as they co-localize with ER Tracker^{TM} Red. Localization of BEM46 to the ER fits well with an assumed function in signal transduction; recent data indicate an important role of the ER in the activation and concentration of signal molecules. In *Drosophila* and *Xenopus*, specific ER retention mechanisms are important for the regulation of development-specific signal transduction pathways. For example, a protein termed Shisa inhibits both Wnt- and fibroblast growth factor (FGF)-signaling pathways during *Xenopus* gastrulation by mediating ER retention of the Wnt receptor Frizzled and the FGF receptor (Schlesinger and Shilo 2005; Yamamoto et al. 2005). A role of BEM46 in similar mechanisms may explain the absence of an ER retention signal.

To our knowledge, we identified, for the first time, an ER marker for living cells of *N. crassa*. Therefore, vector pMM536 will be a valuable tool for ER studies in this important model organism and related fungi, such as *Podospora anserina* or *Sordaria macrospora*.

Acknowledgments The authors thank Hanna Schmidt for excellent technical assistance. We thank the Zentrum für Molekularbiologie und Biochemie, Kiel for assistance with the Nanodrop apparatus and Ruth Schmitz-Streit for providing access to her 7,300 real-time PCR system. English language editing was performed by San Francisco Edit.

References

Arimura N, Kaibuchi K (2005) Key regulators in neuronal polarity. Neuron 48:881–884

Arpaia G, Loros JJ, Dunlap JC, Morelli G, Macino G (1995) Light induction of the clock-controlled gene *ccg–1* is not transduced through the circadian clock in *Neurospora crassa*. Mol Gen Genet 247:157–163

Barbato C, Calissano M, Pickford A, Romano N, Sandmann G, Macino G (1996) Mild RIP—an alternative method for in vivo mutagenesis of the *albino-3* gene in *Neurospora crassa*. Mol Gen Genet 252:353–361

Bedell VM et al (2005) Roundabout4 is essential for angiogenesis in vivo. Proc Natl Acad Sci USA 102:6373–6378

Borges MI, Azevedo MO, Bonatelli R, Felipe MSS, Astolfi-Filho S (1990) A practical method for preparation of total DNA from filamentous fungi. Fungal Genet Newsl 37:269–276

Bowring FJ, Catcheside DEA (1993) The effect of *rec-2* on repeat-induced point mutation (RIP) and recombination events that excise DNA sequence duplications at the *his-3* locus of *Neurospora crassa*. Curr Genet 23:496–500

Bruno KS, Aramayo R, Minke PF, Metzenberg RL, Plamann M (1996) Loss of growth polarity and mislocalization of septa in a *Neurospora* mutant altered in the regulatory subunit of cAMP-dependent protein kinase. Embo J 15:5772–5782

Cabib E, Drgonová J, Drgon T (1998) Role of small G proteins in yeast cell polarization and wall biosynthesis. Annu Rev Biochem 67:307–333

Cambareri EB, Jensen BC, Schabacht E, Selker EU (1989) Repeat-induced G–C to A–T mutations in *Neurospora*. Science 244:1571–1575

Cambareri EB, Singer MJ, Selker EU (1991) Recurrence of repeat-induced point mutation (RIP) in *Neurospora crassa*. Genetics 127:699–710

Chang B, Nakashima H (1998) Isolation of a temperature-sensitive rythm mutant in *Neurospora crassa*. Genes Genet Syst 73:71–73

Chant J, Corrado K, Pringle JR, Herskowitz I (1991) Yeast BUD5 encoding a putative GDP–GTP exchange factor, is necessary for bud site selection and interacts with bud formation gene BEM1. Cell 65:1213–1224

Chenevert J, Corrado K, Bender A, Pringle J, Herskowitz I (1993) A yeast (BEM1) necessary for cell polarization whose product contains two SH3 domains. Nature 356:77–79

Davis RH (1979) The genetics of arginine biosynthesis in *Neurospora crassa*. Genetics 93:557–575

Estrada de Martin P, Du Y, Novick P, Ferro-Novick S (2005) Ice2p is important for the distribution and structure of the cortical ER network in *Saccharomyces cerevisiae*. J Cell Sci 118:65–77

Faulhammer F, Konrad G, Brankatschk B, Tahirovic S, Knodler A, Mayinger P (2005) Cell growth-dependent coordination of lipid signaling and glycosylation is mediated by interactions between Sac1p and Dpm1p. J Cell Biol 168:185–191

Fernández-Ábalos JM, Fox H, Pitt C, Wells B, Doonan JH (1998) Plant-adapted green fluorescent protein is a versatile vital reporter for gene expression, protein localization and mitosis in the filamentous fungus, *Aspergillus nidulans*. Mol Microbiol 27:121–130

Freitag M, Hickey PC, Raju NB, Selker EU, Read ND (2004) GFP as a tool to analyze the organisation. dynamics and function of nuclei and microtubules in *Neurospora crassa*. Fungal Genet Biol 41:897–910

Galagan JE, Selker EU (2004) RIP: the evolutionary cost of genome defense. Trends Genet 20:417–423

Galagan JE et al (2003) The genome sequence of the filamentous fungus *Neurospora crassa*. Nature 422:859–868

Garnjobst L, Tatum EL (1967) A survey of new morphological mutants in *Neurospora crassa*. Genetics 57:579–604

Giaever G et al (2002) Functional profiling of the *Saccharomyces cerevisiae* genome. Nature 418:387–391

Giot L (2003) A protein interaction map of *Drosophila melanogaster*. Science 302:1727–1736

Grimme SJ et al (2004) Deficiencies in the endoplasmic reticulum (ER)-membrane protein Gab1p perturb transfer of glycosylphosphatidylinositol to proteins and cause perinuclear ER-associated actin bar formation. Mol Biol Cell 15:2758–2770

Hickey C, Jacobson DJ, Read ND, Glass NL (2002) Live-cell imaging of vegetative hyphal fusion in *Neurospora crassa*. Fungal Genet Biol 37:109–119

Holmquist M (2000) Alpha/Beta-Hydrolase fold enzymes: structures, functions and mechanisms. Curr Prot Peptid Sci 1:209–235

Howad W, Kempken F (1997) Cell-type specific loss of *atp6* RNA editing in cytoplasmic male sterile *Sorghum bicolor*. Proc Natl Acad Sci USA 94:11090–11095

Hu H et al (2005) Cross GTPase-activating protein (CrossGAP)/Vilse links the Roundabout receptor to Rac to regulate midline repulsion. Proc Natl Acad Sci USA 102:4613–4618

Irazoqui JE, Gladfelter AS, Lew DJ (2003) Scaffold-mediated symmetry breakting by Cdc24p. Nat Cell Biol 5:1062–1070

Kawahara A, Che Y-S RH, Takeda H, DI B (2005) Zebrafish GADD45-beta genes are involved in somite segmentation. Proc Natl Acad Sci USA 102:361–366

Kempken F (2001) *Hideaway*, a repeated element from *Ascobolus immersus* is rDNA associated and may resemble a class I transposon. Curr Genet 40:179–185

Kempken F, Kück U (1996) *Restless*, an active *Ac*-like transposon from the fungus *Tolypocladium inflatum*: structure, expression, and alternative RNA splicing. Mol Cell Biol 16:6563–6572

Kuratsu M, Taura A, Shoji JY, Kikuchi S, Arioka M, Kitamoto K (2007) Systematic analysis of SNARE localization in the filamentous fungus *Aspergillus oryzae*. Fungal Genet Biol. 44:1310–1323

Leeder AC, Turner G (2008) Characterisation of *Aspergillus nidulans* polarisome component BemA. Fungal Genet Biol 45:897–911 Epub 2007 Dec 2008

Loros JJ, Denome SA, Dunlap JC (1989) Molecular cloning of genes under control of the circadian clock in *Neurospora*. Science 243:385–388

Madden K, Synder M (1998) Cell polarity and morphogenesis in budding yeast. Annu Rev Microbiol 52:687–744

Mannhaupt G et al (2003) What's in the genome of a filamentous fungus? Analysis of the *Neurospora* genome sequence. Nucleic Acids Res 31:1944–1954

Margolin BS, Freitag M, Selker EU (1997) Improved plasmids for gene targeting at the *his-3* locus of *Neurospora crassa* by electroporation. Fungal Genet Newsl 44:34–36

Matsuyama A et al (2006) ORFeome cloning and global analysis of protein localization in the fission yeast *Schizosaccharomyces pombe*. Nat Biotech 24:841–847

Mochizuki S et al (2005) The Arabidopsis WAVY GROWTH 2 protein modulates root bending in response to environmental stimuli. Plant Cell 17:537–547

Murray JC, Srb AM (1961) A mutant locus determining abnormal morphology and ascospore lethality in *Neurospora*. J Hered 52:149–153

Ollis DL et al (1992) The α/β hydrolase fold. Protein Eng 5:197–211

Park HO, Pringle JR, Herskowitz I (1997) Two active states of the Ras-related Bud1/Rsr1 protein bind two different effectors to determine yeast cell polarity. Proc Natl Acad Sci USA 94:4463–4468

Parmentier ML et al (2000) Rapsinoid/partner of inscuteable controls asymmetric division of larval neuroblasts in *Drosophila*. J Neurosci 20:RC84

Perkins DD, Margolin BS, Selker EU, Haedo SD (1997) Occurence of repeat-induced point mutations in long segmental duplications of *Neurospora*. Genetics 141:125–136

Perkins DD, Radford A, Sachs MS (2001) The *Neurospora* compendium chromosomal loci. Academic Press, San Diego

Sambrook J, Fritsch EF, Maniatis T (1989) Molecular cloning. A laboratory manual. Cold Spring Harbor Lab Press, New York

Schlesinger A, Shilo BZ (2005) ER retention of signaling modules. Dev Cell 8:136–137

Seiler S, Plamann M (2003) The genetic basis of cellular morphogenesis in the filamentous fungus *Neurospora crassa*. Mol Biol Cell 14:4352–4364

Selker EU (1997) Epigenetic phenomena in filamentous fungi: useful paradigms or repeat-induced confusion? Trends Genet 13:296–301

Shiu P, Metzenberg R (2002) Meiotic silencing by unpaired DNA: properties, regulation and suppression. Genetics 161:1483–1495

Staudinger M, Kempken F (2003) Electroporation of isolated higher-plant mitochondria: transcripts of an introduced *cox2* gene, but not an *atp6* gene, are edited in organello. Mol Genet Genomics 269:553–561

Talaat AM, Lyons R, Howard ST, Johnston SA (2004) The temporal expression profile of *Mycobacterium tuberculosis* infection in mice. Proc Natl Acad Sci USA 101:4602–4607

Temporini ED, Alvarez ME, Mautino MR, Folco HD, Rosa AL (2004) The *Neurospora crassa cfp* promotor drives a carbon source-dependent expression of transgenes in filamentous fungi. J Appl Microbiol 96:1256–1264

Valencik ML, Pringle JR (1995) *Schizosaccharomyces pombe bem1/bud5* suppressor (*bem46*) mRNA. In. EMBL database, accession number U29892

Veit K et al (2006) Global transcriptional analysis of *Methanosarcina mazei* strain Gö1 under different nitrogen availabilities. Mol Genet Genomics 276:41–55

Vogel HJ (1956) A convenient growth medium for *Neurospora* (medium N). Microbiol Genet Bull 13:42–43

Wedlich-Söldner R, Schulz I, Straube A, Steinberg G (2002) Dynein supports motility of endoplasmic reticulum in the fungus *Ustilago maydis*. Mol Biol Cell 13:965–977

Yamamoto A, Nagano T, Takehara S, Hibi M, Aizawa S (2005) Shisa promotes head formation through the inhibition of receptor protein maturation for the caudalizing factors, Wnt and FGF. Cell 120:223–235

Yuan GF, Marzluf GA (1992) Molecular characterization of mutations of *nit4*, the pathway-specific regulatory gene which controls nitrate assimilation in *Neurospora crassa*. Mol Microbiol 6:67–73

Biochemical and Biophysical Research Communications 438 (2013) 526–532

Contents lists available at ScienceDirect

Biochemical and Biophysical Research Communications

journal homepage: www.elsevier.com/locate/ybbrc

Characterization of bud emergence 46 (BEM46) protein: Sequence, structural, phylogenetic and subcellular localization analyses

Abhishek Kumar, Krisztina Kollath-Leiß, Frank Kempken *

Abteilung für Botanik mit Schwerpunkt Genetik und Molekularbiologie, Botanisches Institut und Botanischer Garten, Christian-Albrechts-Universität zu Kiel, Kiel, Germany

ARTICLE INFO

Article history:
Received 17 July 2013
Available online 31 July 2013

Keywords:
Bud emergence 46 (*bem46*)
Evolution
Fungi
Indels
Endoplasmic retention signal
eGFP-fusion
α/β-hydrolase

ABSTRACT

The bud emergence 46 (BEM46) protein from *Neurospora crassa* belongs to the α/β-hydrolase superfamily. Recently, we have reported that the BEM46 protein is localized in the perinuclear ER and also forms spots close by the plasma membrane. The protein appears to be required for cell type-specific polarity formation in *N. crassa*. Furthermore, initial studies suggested that the BEM46 amino acid sequence is conserved in eukaryotes and is considered to be one of the widespread conserved "known unknown" eukaryotic genes. This warrants for a comprehensive phylogenetic analysis of this superfamily to unravel origin and molecular evolution of these genes in different eukaryotes. Herein, we observe that all eukaryotes have at least a single copy of a *bem46* ortholog. Upon scanning of these proteins in various genomes, we find that there are expansions leading into several paralogs in vertebrates. Usingcomparative genomic analyses, we identified insertion/deletions (indels) in the conserved domain of BEM46 protein, which allow to differentiate fungal classes such as ascomycetes from basidiomycetes. We also find that exonic indels are able to differentiate BEM46 homologs of different eukaryotic lineage. Furthermore, we unravel that BEM46 protein from *N. crassa* possess a novel endoplasmic-retention signal (PEKK) using GFP-fusion tagging experiments. We propose that three residues namely a serine 188S, a histidine 292H and an aspartic acid 262D are most critical residues, forming a catalytic triad in BEM46 protein from *N. crassa*. We carried out a comprehensive study on *bem46* genes from a molecular evolution perspective with combination of functional analyses. The evolutionary history of BEM46 proteins is characterized by exonic indels in lineage specific manner.

1. Introduction

Bud emergence 46 (*bem46*) genes encode proteins belonging to the BEM46 family within the α/β-hydrolase superfamily. This α/β-hydrolase superfamily possesses a typical α/β-hydrolase domain, which is characterized by a β-sheet core of five to eight strands connected by α-helices to form a α/β/α sandwich [1,2]. Several hydrolytic enzymes share the common α/β-hydrolase domain with a wide array of catalytic functions with different phylogenetic history [2,3]. In fact, there are over 30,000 manually annotated members of this domain in the ESTHER database [1]. However, the functional characterization of BEM46 family members remainslargely unknown with no information of their hydrolase activity and substrate binding. The *S. pombe bem46* gene was originally described as a temperature-sensitive suppressor of *S. cerevisiae bem1* and *bud5* double mutant [4]. Mutations in *bem1* and *bud5* show defects in cell polarization and establishment of non-random budding patterns [5,6]. BUD5 is a GTP–GDP exchange factor (GEF) for a BUD1 Ras-like small G protein and is necessary for bud site selection [7]. BEM1 is a scaffold protein binding to BUD1, the Cdc24p GEF for the Cdc42p Rho-like small G protein, GTP-CDC42p, and to actin [5,8,9]. The *bem46* homologous gene-YNL320W in *S. cerevisiae* is not an essential single-copy gene [10]. Likewise, a *bem46* homolog *WAV2* in *Arabidopsis thaliana* was identified and it has no essential function [11]. Global analysis of protein interactions in *D. melanogaster* indicate that there is a low-confidence interaction between *Drosophila* BEM46 and RAPSYNOID [12], which is a putative GEF for Gα protein and involved in the control of asymmetric cell divisions [13]. In *N. crassa*, BEM46 may play a role in a signal transduction pathway involved in determining or maintaining cell type-specific polarity [14]. Hence members of the BEM46 family may modulate the function of some morphogenic determinants, like GEF or actin, on the cell surface. However, *bem46* remains as one of the widespread conserved "known unknown" eukaryotic genes, whose function remains elusive [15,16]. Further studies are clearly required for a better understanding of the function(s) of members belonging to the BEM46 family.

In the current study, we analyzed the molecular evolution of BEM46 family and we compiled BEM46 repository from selected eukaryotic genomes. We demonstrate that BEM46 from different

* Corresponding author.
E-mail address: fkempken@bot.uni-kiel.de (F. Kempken).

0006-291X/$ - see front matter © 2013 Elsevier Inc. All rights reserved.
http://dx.doi.org/10.1016/j.bbrc.2013.07.103

eukaryotic lineages show lineage-specific indels that can be used as molecular marker for differentiating BEM46 in different lineages. Using GFP-fusion tagging, we provide evidence that the BEM46 protein (from *N. crassa*) has a novel and previously uncharacterized endoplasmic-retention signal (PEKK).

2. Materials and methods

We describ details of strains, DNA isolation, gel electrophoresis and PCR amplification in supplementary section S1. We also describ details of vector construction, transformation, transformant analysis and microscopic methods in supplementary section S2. We extracted sequences using full-length *N. crassa* BEM46 via NCBI, JGI and Ensembl [17] using BLAST suite [18]. We generated protein alignments of BEM46 sequences with MUSCLE [19] and visualized using GENEDOC [20]. We constructed Bayesian phylogenetic tree in the MrBayes 3.2.1 [21]. We performed divergence analysis for fungal BEM46 protein as described previously [22,23]. We created the homology model of BEM46 protein from *N. crassa* using the I-TASSER [24] and visualized it using YASARA [25]. We predicted active site residues of BEM46 from *N. crassa* using COFACTOR [26]. We provide details of data collection, sequence-structural and phylogenetic analyses in supplementary section S3.

3. Results and discussion

3.1. All eukaryotic organisms possess at least one copy of bem46 gene

We have compiled a comprehensive repository of BEM46 from representative eukaryotic organisms, as summarized by the Bayesian phylogenetic tree (Fig. 1). The majority of eukaryotic organisms have a single copy of BEM46 homolog, however, vertebrates have several paralogs of BEM46 (originated by duplication events), which separated in three different branches in this Bayesian phylogenetic tree (Fig. 1). Fungal BEM46 proteins are grouped into four sub-branches namely ascomycetes, basidiomycetes, *saccharomycetes* and methylotrophic yeasts. Interestingly, the parasitic fungus *Batrachochytrium dendrobatidis* (infecting frogs) has two copies of BEM46 and one copy is a close homolog of vertebrate BEM46 homologs (marked by arrow in Fig. 1). Possibly, this bem46 gene originated from horizontal gene transfer.

We have not detected *bem46* genes in bacterial genomes, however they possess other α/β-hydrolase superfamily members such as lysophospholipase in *Thioalkalivibrio* sp. ALJ9 (Genbank accession id: WP_018173930.1). The members of α/β-hydrolase superfamily are one of the largest and most diverse protein families known and these are comprised of proteases, lipases, esterases, dehalogenases, peroxidases, and epoxide hydrolases with different phylogenetic origin and catalytic function [2,3]. These members have been extensively studied in last two decades after the first report on α/β-hydrolases in 1992 [3]. Hence, we limited our study to the BEM46 protein family. To evaluate the sequence features of BEM46, we examined protein sequences in different eukaryotic lineages and were able to illustrate several insertions/deletions (indels) that might have played important roles in enhancing local diversities within overall conserved BEM46 core domain as described below. The existence of lineage-specific indels may also explain the differences between Bem46 homologs within different eukaryotic lineages.

3.2. Fungal BEM46 proteins have indels specific for fungal phyla

Using protein sequence analyses, we illustrate that there are distinct differences in terms of indels for ascomycetes and basidiomycetes (Fig. 2). A large indel is found in the region between 87P-128I amino acids (according to BEM46 protein numbering from *N. crassa*) as an insertion in basidomycetes but a deletion in ascomycetes. Another two amino acid indels, located between positions 205G-206D, are present in ascomycetes except yeast, but absent in basidiomycetes except rusts. These indels were mapped to BEM46 protein model structure to highlight their respective locations. The large indel is localized in between the β-sheet β2 to the helix α3, just before the α/β-hydrolase domain, while the two amino acid indel between positions 205G-206D is localized in the loop L10 in the α/β-hydrolase domain.

3.3. BEM46 protein from N. crassa possesses novel endoplasmic reticulum (ER)-retention signal

We considered BEM46 protein from *N. crassa* as a standard fungal BEM46, which is characterized by the presence of a signal peptide at the N-terminus with hydrophobic residues and an endoplasmic reticulum (ER)-retention signal PEKK at the C-terminal end (Fig. 3A). The ER-retention signal is designated by a prosite pattern as [KRHQSA]-[DENQ]-E-L. The ER-retention signal for *N. crassa* BEM46 does not fit into this typical pattern, however, it fits into recently reported 35 newly defined ER-retention signals [27] by using various permutation and combinations at these four positions. To examine if this putative motif serves as an authentic ER retention signal, we performed a localization study with (Fig. 3B, C) and without PEKK (Fig. 3D) at the C-terminal end using eGFP as a tag. The native protein carrying the putative ER retention signal coupled with eGFP showed the previously described localization to the perinuclear ER and in additional small spots near to the plasma membrane [14]. In contrast, the eGFP tagged protein without the PEKK sequence was not located to the ER any more, but forms several small cytoplasmic spots (Fig. 3C). Our experiment indicates that the PEKK motif is indeed an ER retention signal.

3.4. Structural analysis of BEM46 protein reveals catalytic triad

We modeled the BEM46 protein from *N. crassa* using I-TASSER [24]. It illustrates that BEM46 has a core α/β-hydrolase domain with eight β-sheets (Fig. 4A). In addition, BEM46 has an extra region with two β-sheets and two α-helices in the N-terminal region. To evaluate diversity within secondary structural elements, we carried out divergence analysis of individual secondary structural elements of different BEM46 proteins during fungal evolution. Fig. 4B illustrates the divergence pattern of these elements among different BEM46 proteins. We found that four loops L5, L11, L13 and L15 are particularly conserved. Normally, loops are conserved in a typical α/β-hydrolase and they harbor active site for ligand bindings. We computed putative binding site residues for three different ligands (Table 1) with C-score higher than −1.5, which reflects correct fold prediction whereas TM-score illustrates structural similarity between the template and the predicted model, [24]. We found that loop L2 possess an important residue, a glycine 117G, for two ligands namely acetic acid and glycerol. Furthermore, amino acid positions between 186G-189L spanning over β-sheet β6 and the loop L9 appear to be critical positions for putative binding sites of fungal BEM46 protein as summarized in Table 1. Among β-sheets, the β-sheet β7 is highly conserved and it harbors a putative binding site residue (isoleucine 211I). The loop L11 harbors an important residue, a phenyl alanine (216F). Among α-helices, the helix α6 appears to be a critical one, as it possesses an important residue, leucine 222L, while the next loop L12 possesses another critical position (proline 228P). Additionally, a potential binding site residue, valine 265 V, is also located near the loop L15, and also a histidine (292H) is located in loop L17. By combining these data, we propose that positions 117G, 188S,

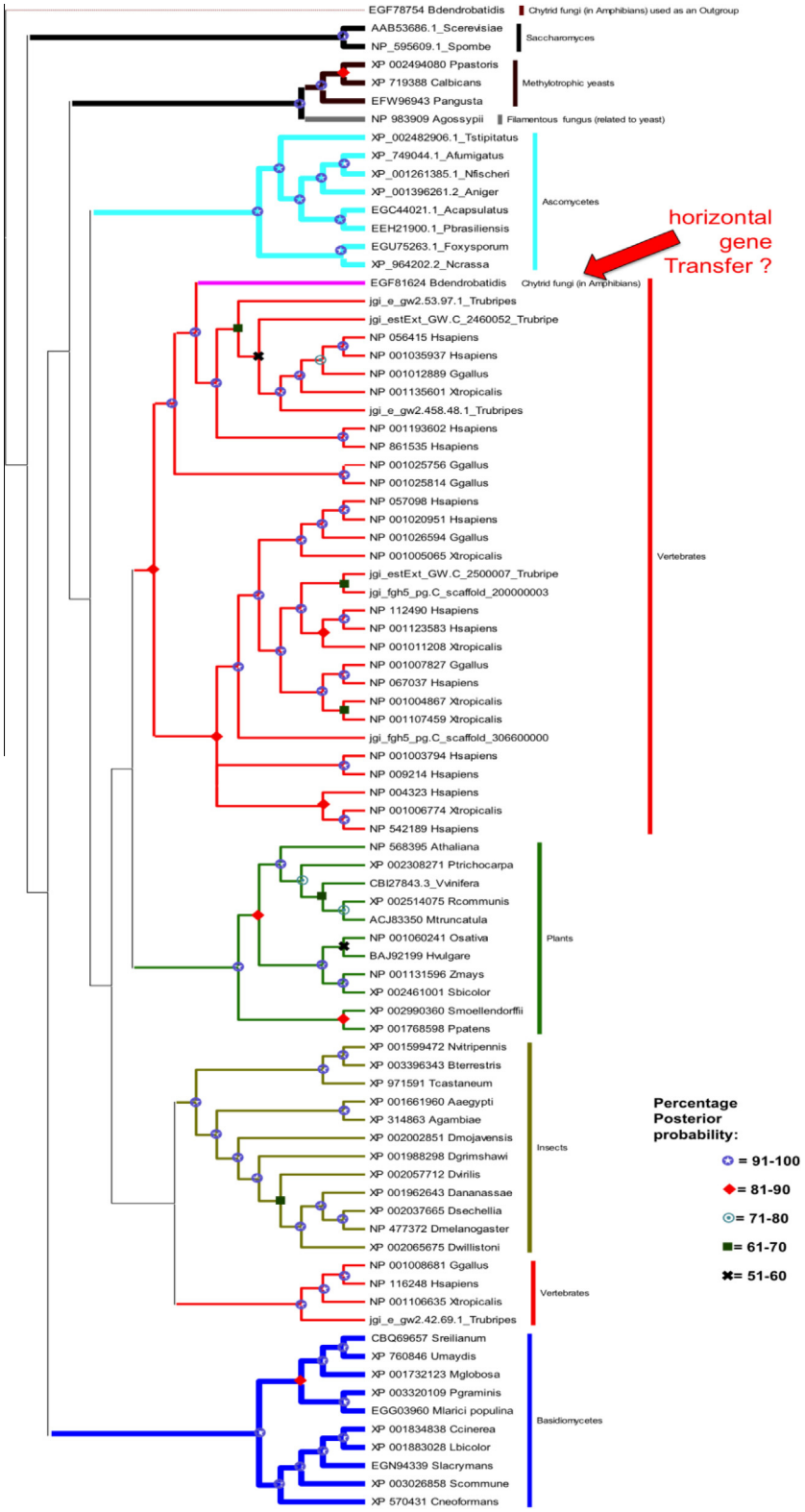

Fig. 1. Bayesian phylogenetic analysis depicts BEM46-like proteins are conserved across different lineages of eukaryotic organisms. Fungal branches are shown by thicker lines.

189L are very critical as more than two ligands are binding to these residues. On closer inspection, region 186G-189L harbors critical residues that are important for ligand binding (Table 1).

To further define the most essential residues, we predicted active site residues for BEM46 protein of *N. crassa,* and found that residues 188S, 262D and 292H are most influential residues for putative active site of BEM46 (marked by bold letters in Table 2). An E-score (higher than 1.0) indicate an excellent structural/functional prediction [24]. Serine 188S appears to be highly important residue in the BEM46 active site along with 262D and 292H. These two independent methods hint for four most critical residue for ligand binding and for activity of BEM46 protein as a serine 188S,

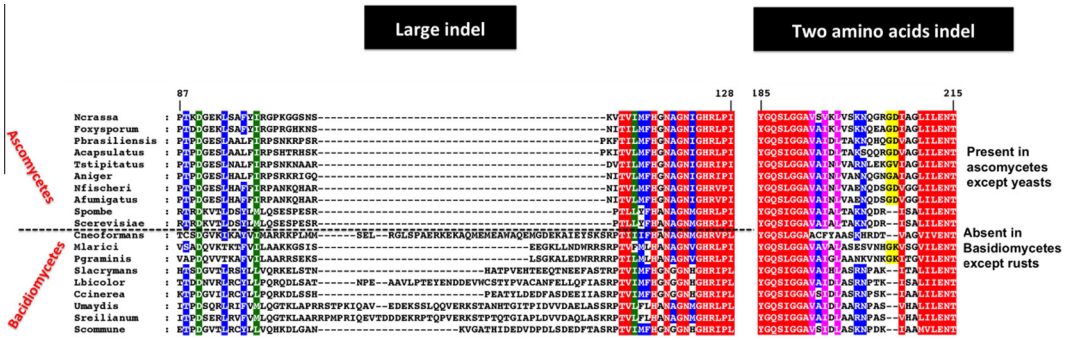

Fig. 2. Major insertions/deletions (indels) segments in BEM46-like proteins from different fungi. Numbering designates amino acid numbering of BEM46 from *N. crassa*. 100, 90 and 70% (with allowed substitutions) conserved residues is marked in red, green and blue, respectively. (For interpretation of the reference to color in this figure legend, the reader is referred to the web version of this article.)

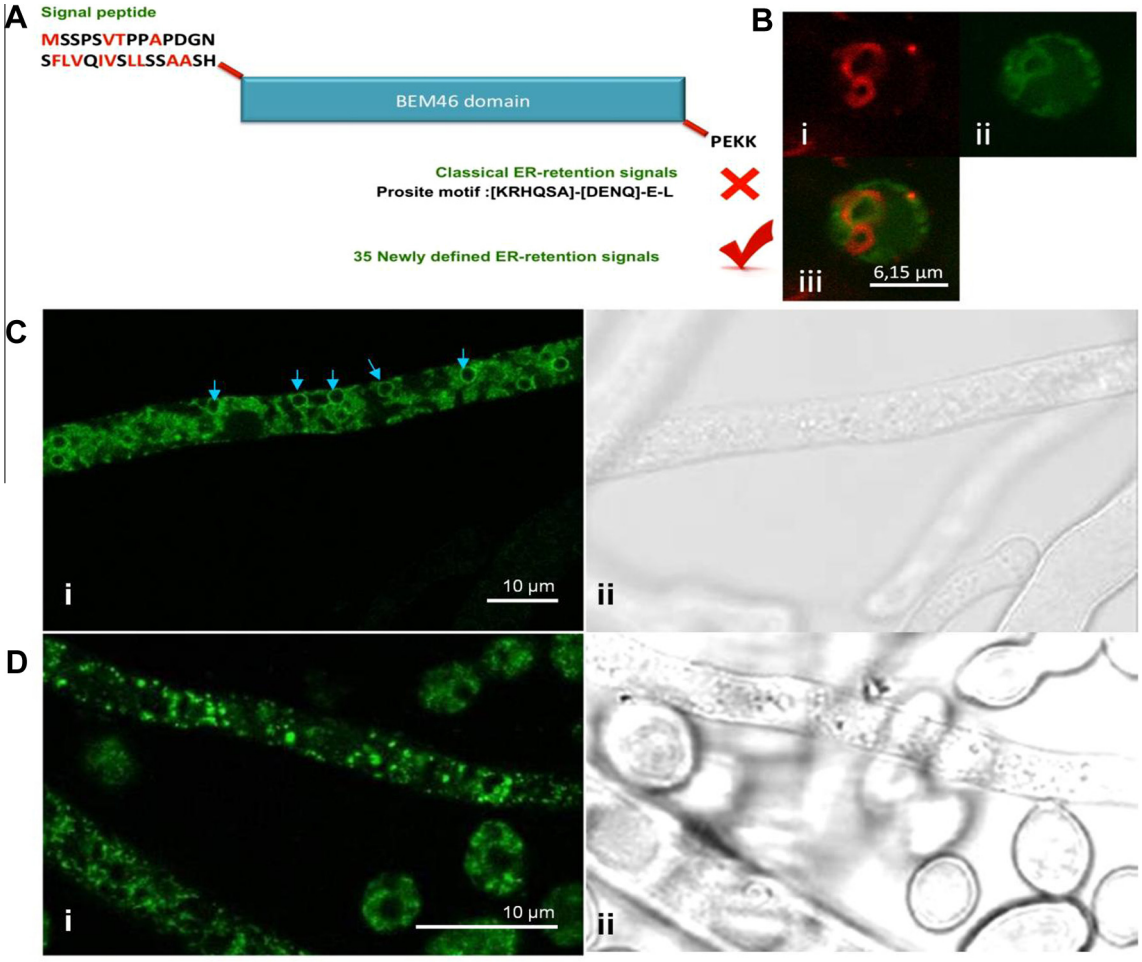

Fig. 3. Cellular localization analysis of BEM46 protein. The BEM46 protein of *N. crassa* carries a PEKK motif at the C-terminal end, which acts as an ER retention signal. (A) BEM46 protein from *N. crassa* is characterized by a signal peptide with patches of hydrophobic residues (red color) at N-terminus and an exceptional endoplasmic-reticulum (ER) retention signal at the C-terminal end. Raykhel et al. reported 35 newly defined ER-retention signals [27]. (B) Intracellular localization of Bem46::eGFP in a macroconidospore stained with the ER specific fluorescent marker ER Tracker™ Red. As previously reported [13] the Bem46::eGFP fusion construct colocalizes with the perinuclear ER stained with the fluorescent marker ER Tracker™ Red. Confocal laser scanning microscopical images of ER Tracker™ Red (i) Bem46::eGFP (ii) and overlay of both (iii). (C) Intracellular localization of the eGFP-tagged BEM46 protein with the PEKK motif. (D) Intracellular localization of the eGFP-tagged BEM46 protein without the PEKK motif. The perinuclear localization (green circles marked by blue arrows) of the BEM46:eGFP protein disappears, when the PEKK motif at the C-terminal end is missing. Confocal laser scanning microscopical images of young hyphae and macroconidia exhibiting (i) eGFP fluorescence, (ii) calculated bright field. (For interpretation of the reference to color in this figure legend, the reader is referred to the web version of this article.)

followed by a leucine 189L, a histidine 292H and an aspartic acid 262D. Upon comparing known canonical α/β-hydrolases, it is prominent that catalytic triads of these α/β-hydrolases are composed of a nucleophile (serine/cysteine/aspartic acid), an acid residue and a conserved histidine and they must be localized in the loops [2]. Three out of four proposed residues 188S, 262D and 292H fulfill these requirements for forming a catalytic triad of BEM46 protein. Furthermore, these residues are structurally con-

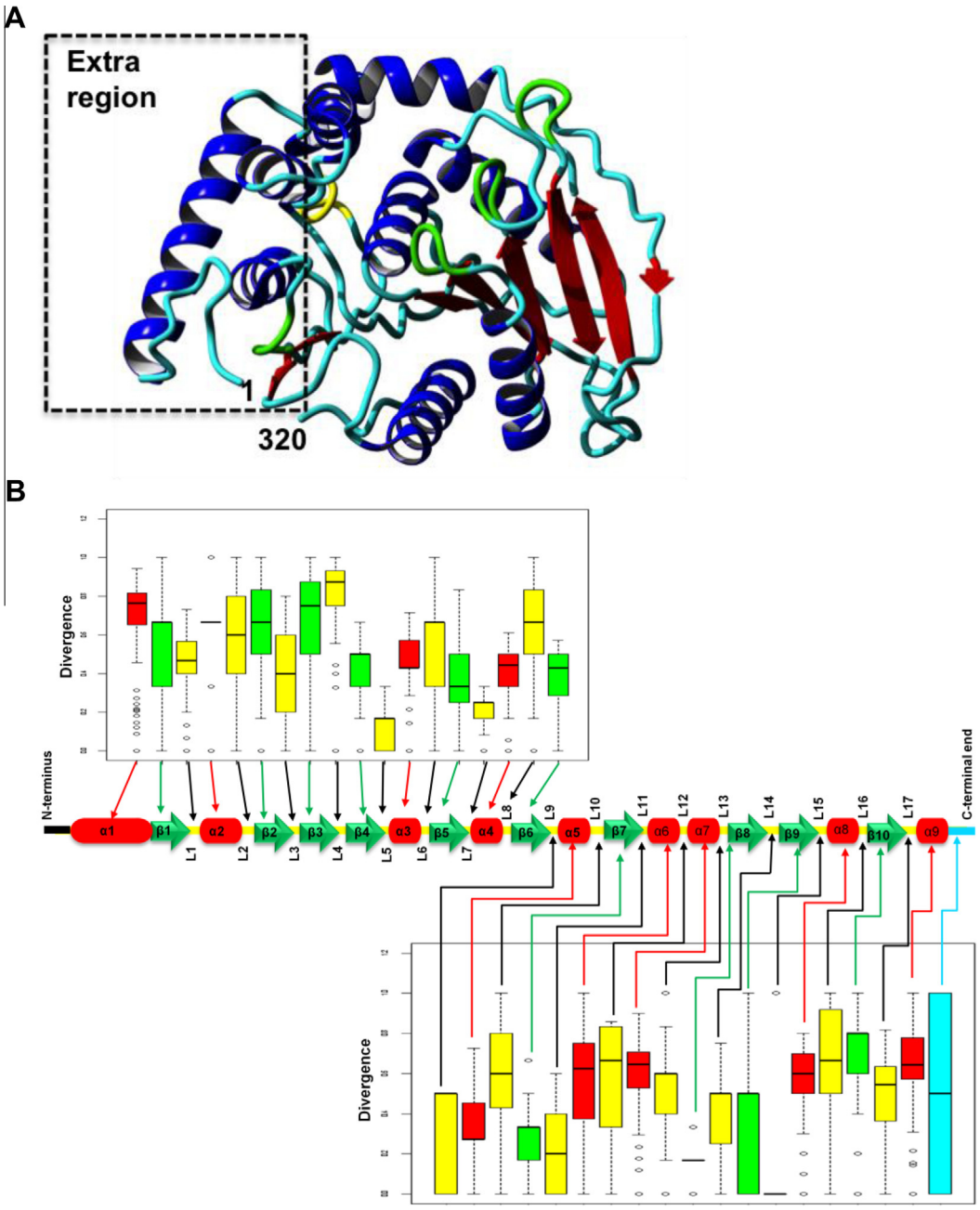

Fig. 4. Structural analysis of fungal BEM46. (A) Homology model of BEM46 from *N. crassa* suggests that BEM46 is composed of an extra region with two β-sheets and two α-helices in N-terminal region other than a typical α/β hydrolase with eight β-sheets. (B) Divergence analysis of different secondary structural elements in fungal BEM46 homologs. All values are significant ($P < 2.2e\text{-}16$, Kuskal–Wallis test).

Table 1
Prediction of putative binding sites of BEM46 from *N. crassa* based on known crystal structures as template with similar binding site. Predicted with I-TASSER software. Putative active site residues conserved in more than one ranking are marked in bold.

Rank	Cscore	PDB Hit	TM-score	RMSD	IDEN	Cov.	BS-score	Ligands	Predicted binding site residues in the model
1	0.45	3fyuC	0.786	2.34	0.181	0.866	1.30	Acetic acid (ACY)	**117G, 188S, 189L**, 216F, 292H
2	0.35	2z3wA	0.677	3.33	0.117	0.784	0.88	Glycerol (GOL)	**117G, 188S, 189L**, 222L, 228, 265 V
3	0.06	3dduA	0.692	3.49	0.130	0.819	0.85	Glycerol (GOL)	186G, 187Q, **189L**, 211I, 256F

Cscore is the confidence score of predicted binding site. Cscore values range in between [0–1]; where a higher score indicates a more reliable ligand-binding site prediction. BS-score is a measure of local similarity (sequence and structure) between template binding site and predicted binding site in the query structure. Based on large scale benchmarking analysis, we have observed that a BS-score > 1.1 reflects a very good local match between the predicted and template binding site.
TM-score is a measure of global structural similarity between query and template protein.
RMSD is the RMSD between residues that are structurally aligned by TM-align.
IDEN is the percentage sequence identity in the structurally aligned region.
Cov. represents the coverage of global structural alignment and is equal to the number of structurally aligned residues divided by length of the query protein.

Table 2
Prediction of putative active site residues of BEM46 from *N. crassa* in comparison of top 5 enzyme homologs in protein databank (PDB) using COFACTOR software [35]. Putative active site residues conserved in more than one ranking are marked in bold.

Ranking	EC-score	PDB Hit	TM-score	RMSD	IDEN	Cov.	EC Number	Predicted active site residues
1	1.365	2jbwD	0.597	2.34	0.141	0.750	3.7.1.-	**188S, 292H**
2	1.210	1yr2A	0.591	3.32	0.106	0.800	3.4.21.26	191G, **262D**
3	1.188	1thtA	0.539	3.08	0.143	0.722	2.3.1.-	**188S, 292H**
4	1.109	1l7aA	0.692	2.35	0.161	0.872	3.1.1.72 3.1.1.41	125R
5	1.087	3ga7A	0.550	3.21	0.111	0.734	3.1.1.-	**262D, 292H**

EC-score is a confidence score for the Enzyme Classification (EC) Number prediction and it is used for ranking purpose. E-score (higher than 1.0) is indicatively of excellent structural/functional prediction [33].
PDB Hit is known enzyme structure in Protein databank
TM-score is a measure of global structural similarity between query and template protein.
RMSD is the RMSD between models and the PDB structure in the structurally aligned regions by TM-align.
IDEN is percentage sequence identity in the structurally aligned region.
Cov. represents the coverage of the alignment and is equal to the number of structurally aligned residues divided by length of model.

served in same positions as of the residues in the catalytic triad among several canonical α/β-hydrolases. A catalytic triad is defined by residues which share surface in the three dimensional space. To illustrate that we mapped surface area of these three residues (188S, 262D and 292H) as illustrated in Fig. S1 and it reveals that their combined surface area is interacting as required for any other catalytic triad. This triad is conserved across all known alpha/beta-hydrolases, which is also true with BEM46 as illustrated for insect BEM46 proteins aligned with BEM46 from *N. crassa* (Fig. S2).

3.5. BEM46 homologs share indels in other eukaryotic lineages

BEM46-like proteins from insects have only one amino acid indel at the position 80 (Fig. S2). Furthermore, these BEM46 homologs have an extension at the C-terminal end.

BEM46-like proteins from plant genomes have five indels (Fig. S3) namely one amino acid indel at the position 80, two amino acids indel between positions 205–206, eight to twelve amino acids indel between positions 232–233, two to three amino acids indel between positions 282–283 and two amino acids indel between positions 300–301.

Vertebrates possess several paralogs of fungal BEM46 protein, which are evolved by gene duplication events. These proteins have been termed as abhydrolase domain containing (ABHD) proteins, due to vertebrate-specific duplication events. Most prominent and close members to these ABHD proteins to fungal BEM46 are ABHD12 and ABHD13. These proteins are characterized by indels in comparison to BEM46 from *N. crassa* as summarized in Fig. S4. It is noteworthy that loss of function mutations in ABHD12 cause polyneuropathy, hearing loss, ataxia, retinitis pigmentosa, and cataract (PHARC) [28]. The ABHD12 has unique insertions in its core domain that are marked by red bars in Fig. S4. Mammalian ABHD proteins have important roles in lipid metabolism, lipid signal transduction, and metabolic disease, characterized via global profiling of dynamic protein palmitoylation [29,30]. However, annotations and computational characterizations of ABHD proteins are urgently required [29]. Our analysis shed first light into this direction.

3.6. Evolutionary history of BEM46 proteins are characterized by exonic indels

The findings here reveal a clear phylogenetic history of bem46 genes. BEM46 homologs are conserved in all eukaryotic organisms from fungi to human (Fig. 1). We demonstrated that the conserved BEM46 proteins are characterized by indels that discriminate these homologs in different lineages. Indels are generally considered as rare genomic characters and they serve a phylogenetic marker during evolution [31]. The phylogeny of eukaryotes is always under state of flux [32]. An influx of mutations governs the evolution of genes/genomes and these mutations undergo a stochastic process of neutral fixation via application of multiple selective pressures that can control the neutral fixation dynamics [32,33]. Characterization of both the mutational and fixation events assists in understanding the evolutionary processes. Indels are structural genomic changes, which play instrumental roles in applications that try to reveal genomic loci that are evolving under selection by virtue of either slowly or rapidly evolving sequences. In these analyses, it is essential that the mutational input at the genomic regions under study is not abnormally high or low [33–36]. Otherwise, the artifacts of the mutational dynamics predominate over inferred selection and it will be not a true indication for a functional constraint on the sequence. Genetic changes are introduced into genomes through three methods such as point mutations, insertions and deletions. The dynamics of each of these mechanisms are influenced by the genomic fragments under consideration and also by the presence of various factors acting in *trans*.

Prior to availability of genome sequences, evolutionary studies were primarily focused on either replacements of entire genes or fragments of genomic regions or point mutations. Loss or gains of genetic contents have direct immediate functional implications and can be scanned over long evolutionary times. Small structural changes such as 1–50 bps indels are intermediate in scale and are less frequent than single base substitutions. However, they can account for comparable base pairs of change. For instance, previously it was reported that 3.2% and 0.8% of the base pair changes between the fly species and in the primate species, respectively, were affected by indels. In contrast, only 1.8% and 1.5% of the base pairs were affected by point mutations in flies and primates, respectively [37]. Therefore, short indels are as sensitive as primary sequences and serve as significant factor in the mutational input that feeds into the evolutionary process, a fact that underlines the importance of characterizing the mechanisms that induce or suppress their activity. Earlier works were focused on human indels at disease loci [38–41] or on indels detected between relatively distant species [42–44]. These led to the suggestion that such events are correlated with specific sequence contexts. More recent works characterized extensive collections of indels in the human-chimp lineages [45,46], or human-mice lineages [37] and vertebrate-specific contexts of gene superfamily evolution [44]. These data further motivate a comprehensive approach to the description of their sequence contexts. Likewise, indels were also described in various studies in basal organisms such as for phylogenetic position of trichomonads [47] and also fungal genome analyses such

as during P-type ATPase gene family evolution [48] and during understanding of the anamorphic fungus *Rhizoctonia* species complex [49].

Generally, exonic indels require more complex mutational mechanisms and are more constrained than single base substitutions. In this work, we illustrate how indels play important roles in bringing diversity in homologous protein coding regions of *bem46* genes in various eukaryotic lineages, which could be implicated on functional level. However, attention is needed for further functional characterization in different eukaryotic lineages, which is yet in its infancy.

To the best of our knowledge, this is the first comprehensive study on *bem46* genes demonstrating BEM46 proteins being conserved from fungi to human, and BEM46 homologues being characterized by exonic indels that differentiate lineage of a particular BEM46 homolog. We defined the active site of fungal BEM46 using sequence and structural comparisons.

Acknowledgements

We thank the central microscopy plat form in the Biozentrum of our university (http://www.uni-kiel.de/biologie/zm/) for use of their equipment. We also thank Chandan Goswami for editing final version of this manuscript.

Appendix A. Supplementary data

Supplementary data associated with this article can be found, in the online version, at http://dx.doi.org/10.1016/j.bbrc.2013.07.103.

References

[1] N. Lenfant, T. Hotelier, E. Velluet, et al., ESTHER, the database of the alpha/beta-hydrolase fold superfamily of proteins: tools to explore diversity of functions, Nucleic Acids Res. 41 (2013) D423–429.
[2] M. Nardini, B.W. Dijkstra, Alpha/beta hydrolase fold enzymes: the family keeps growing, Curr. Opin. Struct. Biol. 9 (1999) 732–737.
[3] D.L. Ollis, E. Cheah, M. Cygler, et al., The alpha/beta hydrolase fold, Protein Eng. 5 (1992) 197–211.
[4] M.L. Valencik, J.R. Pringle, *Schizosaccharomyces pombe* bem1/bud5 suppressor (bem46) mRNA, EMBL database, accession number U29892. Website: <http://www.ebi.ac.uk/Tools/dbfetch/dbfetch?db=embl&id=U29892&style=raw>), 1995 (Accessed on 20 October 2011).
[5] E. Cabib, J. Drgonova, T. Drgon, Role of small G proteins in yeast cell polarization and wall biosynthesis, Annu. Rev. Biochem. 67 (1998) 307–333.
[6] K. Madden, M. Snyder, Cell polarity and morphogenesis in budding yeast, Annu. Rev. Microbiol. 52 (1998) 687–744.
[7] J. Chant, K. Corrado, J.R. Pringle, et al., Yeast BUD5, encoding a putative GDP-GTP exchange factor, is necessary for bud site selection and interacts with bud formation gene BEM1, Cell 65 (1991) 1213–1224.
[8] H.O. Park, E. Bi, J.R. Pringle, et al., Two active states of the Ras-related Bud1/Rsr1 protein bind to different effectors to determine yeast cell polarity, Proc. Natl. Acad. Sci. USA. 94 (1997) 4463–4468.
[9] J.E. Irazoqui, A.S. Gladfelter, D.J. Lew, Scaffold-mediated symmetry breaking by Cdc42p, Nat. Cell. Biol. 5 (2003) 1062–1070.
[10] G. Giaever, A.M. Chu, L. Ni, et al., Functional profiling of the *Saccharomyces cerevisiae* genome, Nature 418 (2002) 387–391.
[11] S. Mochizuki, A. Harada, S. Inada, et al., The *Arabidopsis* WAVY GROWTH 2 protein modulates root bending in response to environmental stimuli, Plant Cell 17 (2005) 537–547.
[12] L. Giot, J.S. Bader, C. Brouwer, et al., A protein interaction map of *Drosophila melanogaster*, Science 302 (2003) 1727–1736.
[13] M.L. Parmentier, D. Woods, S. Greig, et al., Rapsynoid/partner of inscuteable controls asymmetric division of larval neuroblasts in *Drosophila*, J. Neurosci. 20 (2000) RC84.
[14] M. Mercker, K. Kollath-Leiss, S. Allgaier, et al., The BEM46-like protein appears to be essential for hyphal development upon ascospore germination in *Neurospora crassa* and is targeted to the endoplasmic reticulum, Curr. Genet. 55 (2009) 151–161.
[15] M.Y. Galperin, E.V. Koonin, From complete genome sequence to 'complete' understanding?, Trends Biotechnol 28 (2010) 398–406.
[16] M.Y. Galperin, E.V. Koonin, 'Conserved hypothetical' proteins: prioritization of targets for experimental study, Nucleic Acids Res. 32 (2004) 5452–5463.
[17] P. Flicek, I. Ahmed, M.R. Amode, et al., Ensembl, Nucleic Acids Res. 41 (2013) (2013) D48–55.
[18] S.F. Altschul, T.L. Madden, A.A. Schaffer, et al., Gapped BLAST and PSI-BLAST: a new generation of protein database search programs, Nucleic Acids Res. 25 (1997) 3389–3402.
[19] R.C. Edgar, MUSCLE: multiple sequence alignment with high accuracy and high throughput, Nucleic Acids Res. 32 (2004) 1792–1797.
[20] K.B. Nicholas, H.B. Nicholas Jr., D.W.I. Deerfield, GeneDoc: analysis and Visualization of Genetic Variation, EMBNEW NEWS 4 (1997) 14.
[21] F. Ronquist, J.P. Huelsenbeck, MrBayes 3: bayesian phylogenetic inference under mixed models, Bioinformatics 19 (2003) 1572–1574.
[22] P. Sardar, A. Kumar, A. Bhandari, et al., Conservation of Tubulin-binding sequences in TRPV1 throughout evolution, PLoS ONE 7 (2012) e31448.
[23] A. Kumar, A. Bhandari, R. Sinha, et al., Molecular phylogeny of OVOL genes illustrates a conserved C2H2 zinc finger domain coupled by hyper variable unstructured regions, PLoS ONE 7 (2012) e39399.
[24] A. Roy, A. Kucukural, Y. Zhang, I-TASSER: a unified platform for automated protein structure and function prediction, Nat. Protoc. 5 (2010) 725–738.
[25] E. Krieger, G. Koraimann, G. Vriend, Increasing the precision of comparative models with YASARA NOVA – a self-parameterizing force field, Proteins 47 (2002) 393–402.
[26] A. Roy, J. Yang, Y. Zhang, COFACTOR: an accurate comparative algorithm for structure-based protein function annotation, Nucleic Acids Res. 40 (2012) W471–W477.
[27] I. Raykhel, H. Alanen, K. Salo, et al., A molecular specificity code for the three mammalian KDEL receptors, J. Cell Biol. 179 (2007) 1193–1204.
[28] T. Fiskerstrand, D. H'Mida-Ben Brahim, S. Johansson, et al., Mutations in ABHD12 cause the neurodegenerative disease PHARC: an inborn error of endocannabinoid metabolism, Am. J. Hum. Genet. 87 (2010) 410–417.
[29] C.C. Lord, G. Thomas, J.M. Brown, Mammalian alpha beta hydrolase domain (ABHD) proteins: lipid metabolizing enzymes at the interface of cell signaling and energy metabolism, Biochim. Biophys. Acta. 1831 (2013) 792–802.
[30] B.R. Martin, C. Wang, A. Adibekian, et al., Global profiling of dynamic protein palmitoylation, Nat. Methods 9 (2012) 84–U205.
[31] A. Rokas, P.W. Holland, Rare genomic changes as a tool for phylogenetics, Trends Ecol. Evol. 15 (2000) 454–459.
[32] H. Philippe, P. Lopez, H. Brinkmann, et al., Early-branching or fast-evolving eukaryotes? an answer based on slowly evolving positions, Proc. Biol. Sci. 267 (2000) 1213–1221.
[33] G. Lunter, C.P. Ponting, J. Hein, Genome-wide identification of human functional DNA using a neutral indel model, PLoS Comput. Biol. 2 (2006) e5.
[34] A.G. Clark, The search for meaning in noncoding DNA, Genome Res. 11 (2001) 1319–1320.
[35] D.J. Gaffney, P.D. Keightley, The scale of mutational variation in the murid genome, Genome Res. 15 (2005) 1086–1094.
[36] G. Lunter, Probabilistic whole-genome alignments reveal high indel rates in the human and mouse genomes, Bioinformatics 23 (2007) i289–296.
[37] A. Tanay, E.D. Siggia, Sequence context affects the rate of short insertions and deletions in flies and primates, Genome Biol. 9 (2008) R37.
[38] N.A. Chuzhanova, E.J. Anassis, E.V. Ball, et al., Meta-analysis of indels causing human genetic disease: mechanisms of mutagenesis and the role of local DNA sequence complexity, Hum. Mutat. 21 (2003) 28–44.
[39] A.S. Kondrashov, I.B. Rogozin, Context of deletions and insertions in human coding sequences, Hum. Mutat. 23 (2004) 177–185.
[40] E.V. Ball, P.D. Stenson, S.S. Abeysinghe, et al., Microdeletions and microinsertions causing human genetic disease: common mechanisms of mutagenesis and the role of local DNA sequence complexity, Hum. Mutat. 26 (2005) 205–213.
[41] J.M. Chen, N. Chuzhanova, P.D. Stenson, et al., Complex gene rearrangements caused by serial replication slippage, Hum. Mutat. 26 (2005) 125–134.
[42] E.E. Thomas, N. Srebro, J. Sebat, et al., Distribution of short paired duplications in mammalian genomes, Proc. Natl. Acad. Sci. USA 101 (2004) 10349–10354.
[43] S. Sinha, E.D. Siggia, Sequence turnover and tandem repeats in cis-regulatory modules in *Drosophila*, Mol. Biol. Evol. 22 (2005) 874–885.
[44] A. Kumar, H. Ragg, Ancestry and evolution of a secretory pathway serpin, BMC Evol. Biol. 8 (2008) 250.
[45] F.C. Chen, C.J. Chen, W.H. Li, et al., Human-specific insertions and deletions inferred from mammalian genome sequences, Genome Res. 17 (2007) 16–22.
[46] P.W. Messer, P.F. Arndt, The majority of recent short DNA insertions in the human genome are tandem duplications, Mol. Biol. Evol. 24 (2007) 1190–1197.
[47] E. Bapteste, H. Philippe, The potential value of indels as phylogenetic markers: position of trichomonads as a case study, Mol. Biol. Evol. 19 (2002) 972–977.
[48] N. Corradi, I.R. Sanders, Evolution of the P-type II ATPase gene family in the fungi and presence of structural genomic changes among isolates of *Glomus intraradices*, BMC Evol. Biol. 6 (2006) 21.
[49] D. Gonzalez, M.A. Cubeta, R. Vilgalys, Phylogenetic utility of indels within ribosomal DNA and beta-tubulin sequences from fungi in the *Rhizoctonia solani* species complex, Mol. Phylogenet. Evol. 40 (2006) 459–470.

Eukaryotic Cell

BEM46 Shows Eisosomal Localization and Association with Tryptophan-Derived Auxin Pathway in Neurospora crassa

K. Kollath-Leiß, C. Bönniger, P. Sardar and F. Kempken
Eukaryotic Cell **2014, 13(8):1051. DOI: 10.1128/EC.00061-14.**
Published Ahead of Print 13 June 2014.

EC
Journals.ASM.org

BEM46 Shows Eisosomal Localization and Association with Tryptophan-Derived Auxin Pathway in *Neurospora crassa*

K. Kollath-Leiß, C. Bönniger, P. Sardar, F. Kempken

Abteilung Botanische Genetik und Molekularbiologie, Botanisches Institut und Botanischer Garten, Christian-Albrechts-Universität zu Kiel, Kiel, Germany

BEM46 proteins are evolutionarily conserved, but their functions remain elusive. We reported previously that the BEM46 protein in *Neurospora crassa* is targeted to the endoplasmic reticulum (ER) and is essential for ascospore germination. In the present study, we established a *bem46* knockout strain of *N. crassa*. This Δ*bem46* mutant exhibited a level of ascospore germination lower than that of the wild type but much higher than those of the previously characterized *bem46*-overexpressing and RNA interference (RNAi) lines. Reinvestigation of the RNAi transformants revealed two types of alternatively spliced *bem46* mRNA; expression of either type led to a loss of ascospore germination. Our results indicated that the phenotype was not due to *bem46* mRNA downregulation or loss but was caused by the alternatively spliced mRNAs and the peptides they encoded. Using the *N. crassa* ortholog of the eisosomal protein PILA from *Aspergillus nidulans*, we further demonstrated the colocalization of BEM46 with eisosomes. Employing the yeast two-hybrid system, we identified a single interaction partner: anthranilate synthase component II (encoded by *trp-1*). This interaction was confirmed *in vivo* by a split-YFP (yellow fluorescent protein) approach. The Δ*trp-1* mutant showed reduced ascospore germination and increased indole production, and we used bioinformatic tools to identify a putative auxin biosynthetic pathway. The genes involved exhibited various levels of transcriptional regulation in the different *bem46* transformant and mutant strains. We also investigated the indole production of the strains in different developmental stages. Our findings suggested that the regulation of indole biosynthesis genes was influenced by *bem46* overexpression. Furthermore, we uncovered evidence of colocalization of BEM46 with the neutral amino acid transporter MTR.

The bud emergence 46 (BEM46) protein is conserved across the eukaryotic kingdom, and the molecular evolution of members of the BEM46 family has been described in detail recently (1). Our group has demonstrated that while the majority of eukaryotic genomes include a single copy of *bem46*, vertebrates possess several paralogs, which originated through duplication events (1).

Studies with various model organisms have revealed limited data regarding the function of BEM46. The *bem46* gene of *Schizosaccharomyces pombe* (EMBL accession number U29892) is reportedly a suppressor of the *bem1 bud5* double mutant of *Saccharomyces cerevisiae* (1), which shows defects in cell polarization and budding (2, 3). BEM1 is a scaffold protein that interacts with BUD1 (4), actin (5), CDC42 (6), and BUD5 (2, 7), and it is reportedly required for the positioning of a protein complex involved in bud formation (2). BUD5 is a GDP-GTP exchange factor for BUD1 and is necessary for bud site selection (7). The *bem46* homolog of baker's yeast (YNL320W) is not essential (8). Two-hybrid approaches with *Drosophila melanogaster* have shown that the BEM46 homolog interacts with the Rapsynoid protein (9), which is a putative GDP-GTP exchange factor for a Gα protein and is involved in controlling asymmetrical cell division (10). Wavy growth 2 (WAV2; encoded by *wav2*) is the BEM46 homolog in *Arabidopsis thaliana*, and a knockout mutant shows short-pitch waves related to root development (11). WAV2 is a common regulator involved in suppressing root bending caused by cell file rotation enhancement in response to touch stimuli, light, and gravity (12). The protein is expressed mainly in young seedlings and in the roots of adult plants, with subcellular localization in the plasma membrane and in compartment membranes (12).

All BEM46 proteins belong to an α/β hydrolase superfamily, characterized by the α/β hydrolase domain (13), comprising a β-sheet core of five to eight strands connected by α-helices. The α/β hydrolase domain is also found in several enzymes with diverse phylogenetic backgrounds, catalytic functions, and substrate specificities (14). The ESTHER database includes more than 30,000 members of this superfamily (15, 16).

Despite these hints, the exact function of BEM46 remains elusive. Therefore, *bem46* is considered one of the top 10 known genes encoding a protein with unknown function (17, 18). Previous results suggest that BEM46 may play a role in signal transduction or in the maintenance of cell polarity. Fungal hyphae serve as a model system for polarized growth (19); therefore, we have investigated the BEM46 protein of the ascomycete *Neurospora crassa*. We reported previously that BEM46 in *N. crassa* is localized to the perinuclear endoplasmic reticulum (ER), and in patches near the plasma membrane (20), as detected on the basis of an unusual ER retention signal at the C-terminal end of the protein (1). Either transcript overexpression or downregulation leads to a loss of ascospore germination. Using bioinformatic tools, we also previously predicted the native protein structure, which included an essential catalytic triad (1).

In the present study, we show that BEM46 in *N. crassa* is part of

Received 13 March 2014 Accepted 6 June 2014
Published ahead of print 13 June 2014
Address correspondence to F. Kempken, fkempken@bot.uni-kiel.de.
This publication is dedicated to Karl Esser on the occasion of his 90th birthday for his lifetime contributions to fungal genetics.
Supplemental material for this article may be found at http://dx.doi.org/10.1128/EC.00061-14.

doi:10.1128/EC.00061-14

the fungal eisosome and is an interaction partner of anthranilate synthase. We also demonstrate the colocalization of BEM46 with the putative tryptophan transporter MTR. Our present data indicate an influence of BEM46 on the auxin biosynthesis pathway of the fungus, and we use bioinformatic tools to predict a putative auxin biosynthesis pathway in *N. crassa*. Furthermore, we demonstrate that alternative splicing of the *bem46* transcript is responsible for the loss of ascospore germination in the *bem46* RNA interference (RNAi) lines.

MATERIALS AND METHODS

Strains. The present study used the following *Neurospora crassa* strains from the Fungal Genetics Stock Center (FGSC; Kansas City, MO, USA): FGSC 9718 (Δ*mus-51*::*bar mat a*), FGSC 9719 (Δ*mus-52*::*bar mat a*), FGSC 6103 [*his-3* (Y234M723) *mat A*], FGSC 9716 [*his-3* (Y234M723) *mat a*], FGSC 20870 [Δ*trp-1* (NCU00200.2) *mat a*], and FGSC 20871 [Δ*trp-1* (NCU00200.2) *mat A*]. Fungi were cultivated on Vogel's minimal medium (21). All expression vectors carrying fusion constructs used in the present study were transformed into the histidine auxotrophic strains FGSC 6103 and FGSC 9716; therefore, these strains served as the "wild type" in control experiments. Strains carrying auxotrophic markers were grown on media supplemented with the required amino acids. For crosses, fungi were plated on Westergaard's medium (22). In the colocalization studies, heterokaryons were formed as described previously (23).

For the propagation of vector constructs under standard culture conditions, we used *Escherichia coli* strain XL1-Blue {*recA1 endA1 gyrA96 thi-1 hsdR17 supE44 relA1 lac* [F′ *proAB lacI*^{q}*Z*ΔM15 Tn*10* (Tet^{r})]} (Stratagene, La Jolla, CA). For the propagation of RNAi constructs, we used *E. coli* strain SURE {e14^{-} (McrA^{-}) Δ(*mcrCB-hsdSMR-mrr*)*171 endA1 supE44 thi-1 gyrA96 relA1 lac recB recJ sbcC umuC*::Tn*5* (Kan^{r}) *uvrC* [F′ *proAB lacI*^{q}*Z*ΔM15 Tn*10* (Tet^{r})]} (Stratagene, Heidelberg, Germany).

DNA and RNA isolation. DNA was isolated as described previously (24). Briefly, mycelia were ground under liquid nitrogen and were transferred to lysis buffer (10 mM Tris-HCl, 1 mM EDTA, 100 mM NaCl, and 2% SDS [pH 8.0]), followed by phenol extraction. Subsequently, the aqueous phase was incubated with 100 μg RNase A, followed by an additional phenol extraction and ethanol precipitation. Bacterial plasmid DNA was isolated using NucleoSpin reagent kits (Macherey-Nagel, Düren, Germany). Plasmids were isolated from yeast according to standard procedures (25).

RNA was isolated from mycelia as published previously (26). Vegetative mycelia of *Neurospora crassa* strains were grown for 3 days in liquid Vogel's minimal medium with 5.8 mM saccharose. For strain FGSC 6103, 1 mM L-histidine was added to the medium. The mycelia were ground and were cooled with liquid nitrogen.

Gel electrophoresis, blotting, and hybridization. Agarose gel electrophoresis, Southern and Northern blotting, and DNA-DNA and DNA-RNA hybridizations were performed as described previously (27). A DECAprime kit (Ambion, Austin, TX) was used to label 20 to 30 ng of template DNA with [α-^{32}P]dCTP. MBBL (Bielefeld, Germany) DNA markers were used to determine size in DNA gel electrophoresis.

PCR and RT-PCR amplification. PCR was performed as described previously (20). For quantitative reverse transcription-PCR (qRT-PCR), isolated nucleic acids were treated with DNase (Roche Diagnostics, Mannheim, Germany) according to the manufacturer's recommendations. As a control for the success of DNase treatment, PCR was also performed using primers CB2480 (TACTTCACCGCCAGAAGTC) and CB2481 (TGCGGAGGGTGAAAGAAGAG) for the housekeeping gene L6_rRNA.

The oligonucleotides used for quantitative real-time PCR were synthesized by Eurofins MWG Operon (Ebersberg, Germany). Isolated and DNase-treated RNA (100 ng) was used as the template and was mixed with the contents of the QuantiTect SYBR green RT-PCR kit (Qiagen, Hilden, Germany). The recommended program from Qiagen was modified to use an annealing temperature of 58°C. Quantitative real-time PCR was performed in a 7300 Real-Time PCR system (Life Technologies, Darmstadt, Germany). For each gene of interest, we calculated the level of expression by the fold difference from the expression level of the housekeeping gene *tub2* and by using the $2^{-\Delta\Delta CT}$ method (28). Statistical analysis was performed using SigmaPlot, version 12.

Transformation and transformant analysis. Previously described methods were used for cloning and *E. coli* transformation (27) and for *N. crassa* transformation (29). All cloning and transformation experiments were conducted in accordance with the requirements of the German gene technology law (GenTG).

Microscopy. For the germination assays, ejected ascospores were harvested and were incubated for 90 min in 500 μl sterile water at 60°C to inactivate contaminating macroconidia. Ascospore concentrations were adjusted to 4×10^3 spores/ml. All light microscopy was performed using a Zeiss Axiophot microscope equipped with a SONY 3CCD digital camera. Confocal fluorescence analysis was performed using a confocal laser scanning microscope (CLSM) (TCS SP5; Leica). Fusion constructs containing enhanced green fluorescent protein (eGFP), enhanced yellow fluorescent protein (eYFP), or tag red fluorescent protein (tRFP) were excited at 488 nm, 514 nm, or 543 nm, respectively, and emission was detected at 500 to 550 nm, 520 to 550 nm, or 570 to 620 nm, respectively. Images were analyzed using Leica LAS AF Lite software. Fungi were cultivated for microscopy as described previously (30).

Vector construction. The construction of the pMM529 (*bem46*-overexpressing), pMM532 (*bem46* RNAi), pMM536 (*bem46*::*egfp* fusion), and pUH280 (used for the *bem46* repeat induced point mutation [RIP] mutation assay) vectors has been described previously (20). In the supplemental material, Fig. S1 presents a schematic representation of all other vectors used, and Table S1 lists the sequences of the oligonucleotides used in the present work. The vectors used for the yeast two-hybrid approach are described below.

The pKK790 and pKK791 vectors were used in the bimolecular fluorescence complementation assay. pKK790 consists of the *bem46* open reading frame (ORF) and the portion of *eyfp* encoding the C-terminal sequence (31), amplified in two steps by overlapping extension PCR. In the first step, the *bem46* ORF was created by using oligonucleotides KK2212 and KK2332. In parallel, the portion of *eyfp* encoding the C-terminal sequence was amplified using oligonucleotides KK2331 and KK2215. In the second step, the two fragments were united in a PCR using oligonucleotides KK2212 and KK2215. The fusion construct was ligated in an expression vector under the control of the *ccg1* promoter.

The pKK791 vector contains the *trp-1* ORF (amplified by KK2333 and KK2334) cloned into the portion of *eyfp* encoding the N-terminal sequence (amplified by KK2335 and KK2336) (31). The frame was corrected in an *in vitro* deletion step using oligonucleotides KK2388 and KK2389. For eisosomal localization studies, we created vector pJQ771, comprising the sequence encoding the *N. crassa* PILA homolog (NCU07495) amplified by KK2347 and KK2348 and fused to *trfp* amplified by KK2350 and KK2349 (32). The expression of this fusion construct was controlled by the *ccg1* promoter. The final frame was corrected by *in vitro* deletion using JQ2413 and JQ2414.

Three additional expression vectors with *egfp* fusion constructs under the control of the *ccg1* promoter were also created. Vector pCB779 contains the 0.5-kb alternative splicing product of *bem46*, amplified using oligonucleotides KK2433 and KK2434. The gene sequence encoding the MTR homolog in *N. crassa* (NCU006619.5) was generated by PCR with oligonucleotides CB2562 and CB2563, using *N. crassa* genomic DNA as the template. The restriction sites required for directed ligation into the final vector, pCB794, were added in a subsequent PCR with oligonucleotides CB2508 and CB2514.

Construction of the *N. crassa* Δ*bem46* mutant. A Δ*bem46* mutant strain was generated according to previously described procedures (33). The construction of the vector is described in Fig. S1 in the supplemental material. The final vector carries the full-length *hph* ORF under the con-

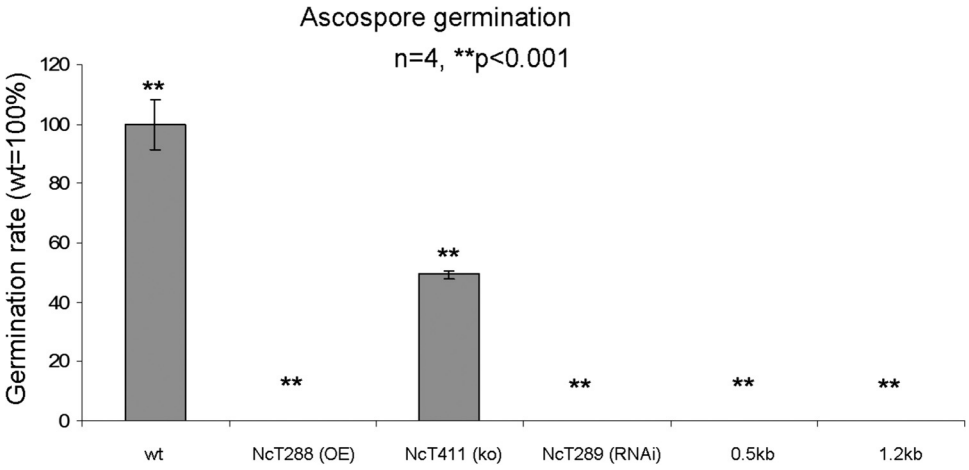

FIG 1 Ascospore germination in different *N. crassa* strains. Germination rates are expressed in relation to that of the wild-type (wt) strain (100%). wt, FGSC 6013 × FGSC 9016; OE, overexpression transformant strain; ko, knockout mutant strain; RNAi, RNAi-directed knockdown transformant strain; 0.5 kb, transformant strain containing the 0.5-kb alternative splicing product of *bem46*; 1.2 kb, transformant strain containing the 1.2-kb alternative splicing product of *bem46*. Strains were crossed with histidine auxotrophic strains FGSC 6103 and FGSC 9716. Statistical analysis was accomplished with SigmaPlot, version 12. Two asterisks indicate a *P* value of <0.01.

trol of the *Aspergillus nidulans trpC* promoter (amplified by FK547/FK548) and the *Neurospora crassa arg2* terminator (amplified by FK541/FK542), flanked by 1.0- to 1.3-kb fragments downstream and upstream of the *bem46* genomic DNA sequence (amplified by AS944/AS945 and AS946/AS947, respectively). The resulting vector, pHS606, was transformed into *Neurospora crassa* strains FGSC 9718 and FGSC 9719 by electroporation according to standard protocols (29). Transformants were selected on Vogel's minimal medium with 5.8 mM saccharose, supplemented with 200 μg/ml hygromycin B. Homokaryotic Δ*bem46* strains were obtained by isolation of single microconidia and were tested for homologous single-copy integration of the transformation cassette by Southern blot hybridization. Homokaryotic transformants free of the *mus* mutation were generated by crossing with the histidine auxotrophic strains FGSC 6103 and FGSC 9716.

Sequence analysis. All sequence analyses were performed by Eurofins MWG Operon (Ebersberg, Germany) and GATC Biotech (Constance, Germany).

Yeast two-hybrid assay. To identify proteins putatively interacting with BEM46, we applied the yeast two-hybrid approach (34, 35) by using Matchmaker GAL4 Two-Hybrid System 3 (Clontech, Mountain View, CA) according to standard protocols. The following yeast strains were utilized: *Saccharomyces cerevisiae* AH109 (*MAT***a** *trp1-901 leu2-3,112 ura3-52 his3-200 gal4*Δ *gal80*Δ *LYS2*::*GAL1*$_{UAS}$-*GAL1*$_{TATA}$-*HIS3 GAL2*$_{UAS}$-*GAL2*$_{TATA}$-*ADE2 URA3*::*MEL1*$_{UAS}$-*MEL1*$_{TATA}$-*lacZ*) and *Saccharomyces*

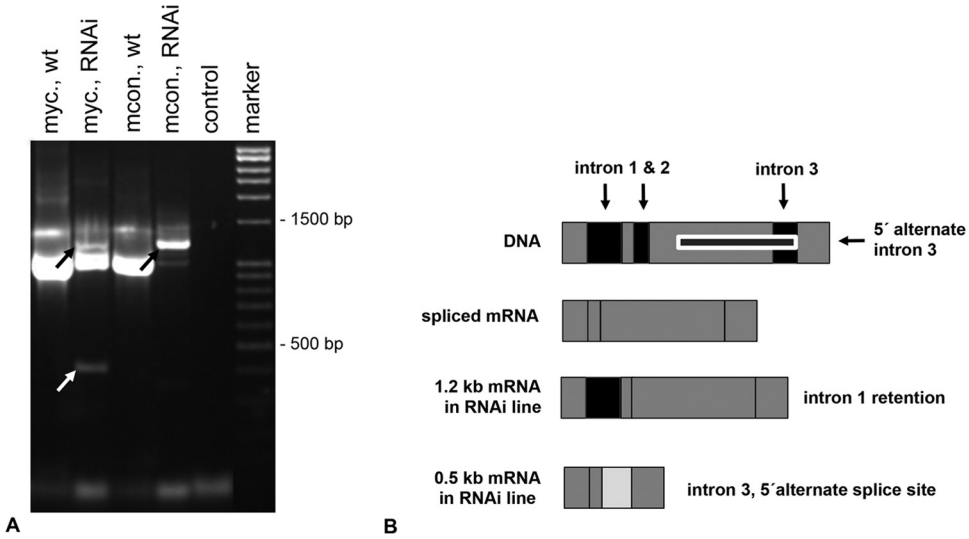

FIG 2 Alternative splicing of *bem46* in *N. crassa*. (A) RT-PCR amplification of different alternatively spliced *bem46* fragments. cDNAs from different strains and tissues were used as the templates. In addition to the full-length (0.9-kb) cDNA sequence, two alternative fragments (1.2 kb and 0.5 kb [indicated by black and white arrows, respectively]) were amplified using *bem46*-specific oligonucleotides. myc., mycelium; mcon., macroconidia; wt, wild-type strain; RNAi, *bem46* knockdown strain. (B) Schematic presentation of different spliced products of *bem46*. The *bem46* genomic DNA sequence consists of four exons divided by three introns (DNA). In most cases, splicing resulted in a 0.9-kb mRNA fragment (spliced mRNA). Two other *bem46* mRNA variants were generated by alternative splicing, i.e., 1.2-kb mRNA (which retains intron 1) and 0.5-kb mRNA (using the 5′ alternate splice site of intron 3), in the RNAi line. Gray rectangles, exons; black rectangles, introns. The alternate intron 3 resulting from the use of an alternate 5′ site is represented by a black rectangle with a white border.

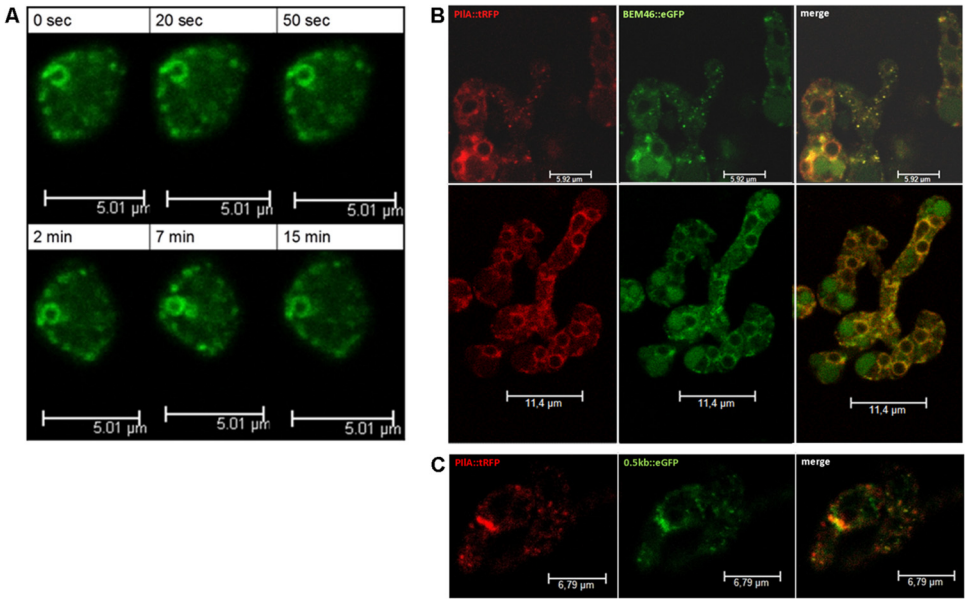

FIG 3 Subcellular localization of BEM46 and its derivatives. (A) CLSM images of a swollen macroconidiospore from a strain overexpressing the BEM46::eGFP fusion protein, observed over 15 min. The time point of each shot is presented; 0 s indicates the start of the investigation. (B) CLSM images of germinating macroconidiospores of a heterokaryon overexpressing both the BEM46::eGFP and PILA::tRFP fusion proteins. Rightmost panels (merge) show overlays of eGFP and tRFP fluorescence. (C) CLSM images of germinating macroconidiospores of a heterokaryon overexpressing both the 0.5-kb::eGFP and PILA::tRFP fusion proteins.

cerevisiae Y187 (MATα *ura3-52 his3-200 ade2-101 trp1-901 leu2-3,112 gal4*Δ *met*$^{-}$ *gal80*Δ *URA3*::*GAL1*$_{UAS}$-*GAL1*$_{TATA}$-*lacZ*) (both from Clontech, Mountain View, CA). Figure S1 in the supplemental material depicts the vectors. The bait vector (pEH646) was generated by cloning the *bem46* cDNA (which was amplified by oligonucleotides EH1132 and EH1133) into the pGBKT7 vector (Clontech, Mountain View, CA) in frame with the GAL4 DNA-binding domain. The prey vector carried an *N. crassa* cDNA bank (provided by S. Seiler, Göttingen, Germany) cloned into the pGADT7 vector (Clontech, Mountain View, CA), containing the GAL4 transcription activation domain.

Yeast transformation was performed by electroporation. First, 50 µl of an electrocompetent *Saccharomyces* cell suspension was mixed with 100 ng DNA, and the mixture was kept on ice for 5 min. Subsequently, the cells were transferred to a cold electroporation cuvette (Gene Pulser cuvette; Bio-Rad, Munich, Germany), and transformation was performed in a Gene Pulser system (Bio-Rad, Munich, Germany) at 200 Ω and 25 µF with 1.5 kV. Directly after transformation, 1 ml of 1 M sorbitol at 4°C was added, and the mixture was incubated at room temperature for 5 min. Finally, 100 µl of the sample was plated on a solid medium, and the plates were incubated at 30°C until colony development.

Putative positive colonies were identified on selective minimal medium (SD/-Ade/-His/-Leu/-Trp), and the putative interaction was confirmed using the α-galactosidase assay. Colonies were plated on selective minimal medium supplemented with 80 mg/liter 5-bromo-4-chloro-3-indolyl-α-D-galactopyranoside (X-α-Gal). After incubation at 30°C for 8 days, blue colonies were further tested for their β-galactosidase activity in a colony lift filter assay (36).

Plant material, growth conditions, and GUS assay. The β-glucuronidase (GUS) assay was performed with transgenic 5-day-old *Arabidopsis thaliana* (ecotype Col-0) seedlings carrying the synthetic auxin response element DR5 (37) coupled to the GUS reporter gene. In these plants, the glucuronidase activity is auxin dependent. Seeds were sterilized with 96% ethanol according to the standard procedure (38). Plants were grown on solidified half-strength MS nutrient medium (39) containing 1% sucrose

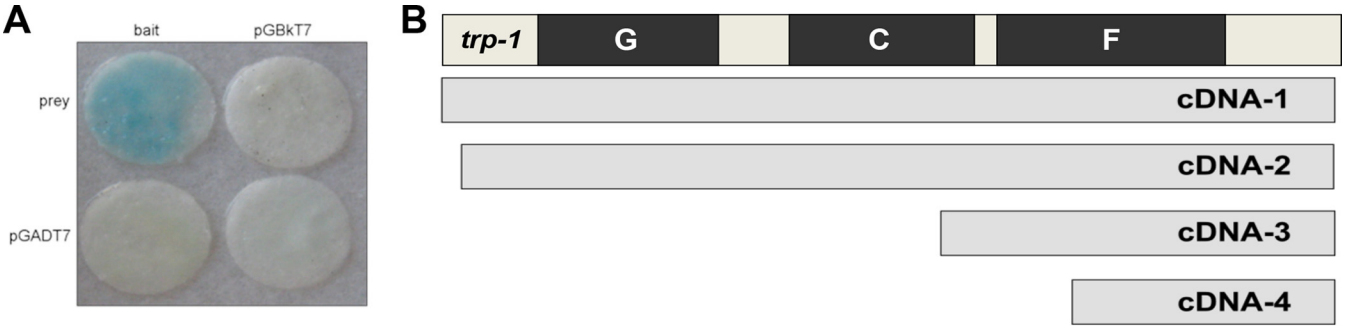

FIG 4 Yeast two-hybrid system. (A) Control experiment confirming the interaction between BEM46 (bait) and anthranilate synthase (prey) in a colony expressing cDNA-1 (diagramed in panel B). pGBKT7 and pGADT7 are empty expression vectors used in the yeast two-hybrid system. (B) Schematic presentation of the four cDNA fragments (cDNA-1 to cDNA-4) that encode putative interacting partners of BEM46, as identified by the yeast two-hybrid approach. All fragments belong to the same gene, *trp-1*, encoding the β subunit of anthranilate synthase complex II. G, C, and F are subdomains of anthranilate synthase.

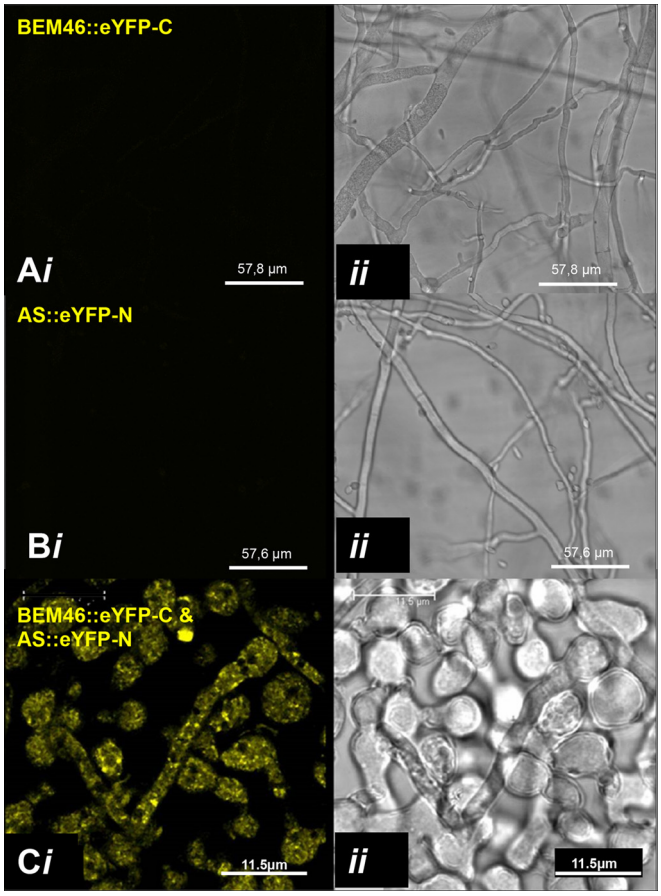

FIG 5 Bimolecular fluorescence complementation assay. (A) *N. crassa* transformant strain overexpressing the BEM46 protein coupled with the C-terminal portion of eYFP. (B) *N. crassa* transformant strain overexpressing the putative interaction partner (anthranilate synthase [AS]; identified by the yeast two-hybrid approach) fused to the N-terminal portion of eYFP. (C) Macroconidia of *N. crassa* strains overexpressing both the BEM46::eYFP-C and AS::eYFP-N vectors. (i) CLSM images; (ii) calculated bright field images.

at 25°C for 7 days under long-day conditions. Subsequently, 5 to 10 seedlings were incubated with either H_2O, 100 μM indole acetic acid (IAA), or germinated ascospores of *N. crassa*. A histochemical GUS assay was performed as described previously (38).

Indole extraction and qualitative and quantitative analysis. To determine indole production, fungi were cultivated in Vogel's minimal liquid medium supplemented with 0.5 mM tryptophan (incubation at 25°C and 180 rpm in darkness). Samples were collected at various time points and were either centrifuged at 7,000 × *g* for 15 min or filtered through one layer of Whatman paper to remove fungal residue. The supernatant was collected, and the pH was adjusted to 2.8 with 10% HCl.

The total indole content was determined quantitatively by using the Salkowski method (40, 41). In a light-protected tube, 500 μl Salkowski reagent was mixed with an equal volume of the collected supernatant. The probes were incubated at 30°C for 15 min, and the absorbance at 540 nm was then determined. Standard curves were prepared from serial dilutions of a 100 mM IAA stock solution.

Indoles were qualitatively analyzed by thin-layer chromatography (TLC). After pH adjustment, aliquots of the supernatant were extracted by the addition of a double volume of ethyl acetate, followed by vigorous shaking for 10 min. After phase separation, the ethyl acetate fraction was collected in light-protected tubes, the solvent was evaporated, and the solid indole-containing residue was dissolved in 30 μl methanol. Samples were spotted onto silica gel plates (TLC Silica gel 60 F_{254}; Merck, Darmstadt, Germany) and were developed with an ethyl acetate-isopropanol-ammonia solution (45:35:20). Subsequently, the plates were dried, stained with Ehmann's reagent (42), and heated to 90°C until spots were clearly visible. We applied 1 mM (each) IAA and tryptophan solutions as standards.

RESULTS

***bem46* knockout mutant.** We previously demonstrated the localization of *Neurospora crassa* BEM46 protein in the ER and in areas near the plasma membrane, as well as the loss of ascospore germination in *bem46* RNAi and *bem46*-overexpressing transformants (20). Here, to confirm the *bem46* mutant phenotype, we established a *bem46* knockout strain by replacing the *bem46* gene with the *hph* gene, carrying hygromycin B resistance, using *mus-51* and *mus-52* mutants provided by the Fungal Genetic Stock Center. Figure S2 in the supplemental material shows that we successfully generated several *bem46* knockout strains. These knockouts exhibited normal vegetative growth and produced micro- and macroconidia. The rate of ascospore germination was somewhat lower than that in the wild type (Fig. 1); however, the phenotype was much weaker than that of the RNAi or overexpressing transformant, neither of which exhibits ascospore germination.

Alternative splicing of the *bem46* transcript. This unexpected discrepancy between the knockout mutant and the RNAi and overexpression transformants could have been caused by nonspecific downregulation of some other RNA, but there was no evidence of any such occurrence (20). It was also possible that alternate RNAs had accumulated in the RNAi transformant, since alternative splicing has been reported for a number of *N. crassa* transcripts (43). To investigate this possibility, we performed RT-PCR with oligonucleotides located at the beginning and end of the *bem46* open reading frame in order to generate full-length cDNA. RT-PCR amplification from the wild-type and RNAi strains was performed using RNA isolated from mycelium and macroconidia. The amount of the full-length *bem46* amplicon was somewhat reduced in the RNA from mycelium, and strongly reduced in the RNA from macroconidia, for the RNAi transformant (Fig. 2A). More importantly, both RNA samples from the RNAi transformant produced additional amplicons, including a 1.2-kb amplicon, slightly larger than that from the wild type, and, in one sample, a smaller amplicon of about 0.5 kb.

These amplicons were eluted from the gel and were sequenced. Figure 2B presents a schematic view of the sequencing data, which provided direct evidence of alternative splicing. The small (0.5-kb) amplicon resembled an alternatively spliced form that was missing exon 3. The larger (1.2-kb) transcript still contained the first intron, suggesting a case of intron retention, a frequent alternative splicing event in fungi (43). Neither transcript would encode the full-length *bem46* protein. Assuming that translation was initiated at the same AUG start codon used for translation in the wild-type sequence, the 1.2-kb mRNA could encode a 40-amino-acid truncated BEM46 protein, and the 0.5-kb mRNA could encode a 123-amino-acid truncated BEM46 protein. Both truncated proteins would include the same N terminus as that in the 320-amino-acid full-length BEM46 protein. The alternatively spliced RNAs were cloned into a suitable vector under the control of the *cfp* promoter (44), and the products were transformed into *N. crassa* using homologous recombination at the *his-3* locus (45). The ascospore germination of transformants was compared to

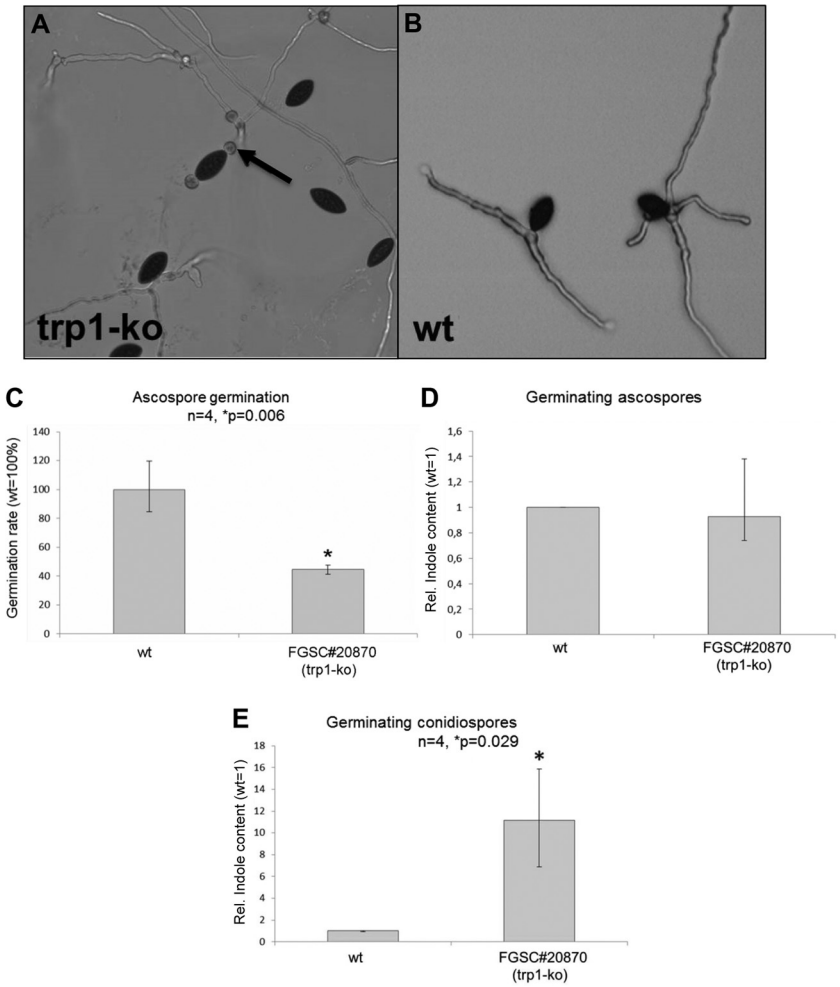

FIG 6 Analysis of the Δ*trp-1* strain (FGSC 20870 or FGSC 20871). (A) Bright-field images of single germinating ascospores of the *trp-1* knockout strain. The arrow indicates an ascospore developing the typical loss-of-polarity phenotype that has been reported previously for *bem46* transformants (20). (B) Wild-type germination. (C) Ascospore germination rate of the Δ*trp-1* mutant compared to that of the wild type. (D and E) Levels of indole production by germinating ascospores and conidiospores, respectively, compared to those of the wild type.

those of the wild-type, *bem46* RNAi, *bem46*-overexpressing, and *bem46* knockout strains. Expression of each type of truncated BEM46 caused complete loss of ascospore germination (Fig. 1), suggesting a possible inhibitory effect of truncated BEM46, which could be due to incorrect cellular localization (see below) or to a wrong or incomplete structure.

BEM46 colocalizes with the eisosomal PILA homolog protein. BEM46 localizes to the perinuclear ER and to spots near the plasma membrane (20), which are not actin patches (46). Microscopic analyses showed that these spots did not re-form within 15 min of investigation (Fig. 3A). Fungal eisosomes are reportedly stable protein complexes connected to the plasma membrane (47). Thus, we investigated the potential colocalization of BEM46 with the *Neurospora crassa* homolog of PILA (NCU07495), which has been described as an eisosomal core protein in *Aspergillus nidulans* (48). After identification using a bioinformatics approach, the full-length coding sequence of the PILA homolog was coupled to the reporter gene *trfp* under the control of the *ccg1* promoter. We subsequently performed transformation in *N. crassa* and selected homokaryotic lines expressing the *pilA*::*trfp* reporter gene construct. A heterokaryon comprising a transformant expressing BEM46 coupled to eGFP was investigated by confocal laser scanning microscopy. The BEM46::eGFP protein showed colocalization with the PILA::tRFP protein in germinating macroconidia of *N. crassa* (Fig. 3B).

Subcellular localization of the truncated BEM46 protein encoded by the 0.5-kb alternatively spliced fragment. We also analyzed the subcellular localization of the truncated protein encoded by the small (0.5-kb) alternative splicing product of *bem46*. To this end, the cDNA fragment was joined to the *egfp* reporter gene under the control of the *ccg1* promoter. The full-length BEM46 protein contains an unusual ER retention signal (1), which leads to the localization of the full-length protein to the perinuclear ER. The alternative splicing event results in a 123-amino-acid protein lacking the amino acids for the retention signal. The confocal microscopic image in Fig. 3C shows the subcellular localizations of the 0.5-kb::eGFP and PILA::tRFP proteins. As expected, the small peptide did not localize to the perinuclear ER but was found in several small spots close to the plasma membrane, similar to the spots observed for the full-length BEM46.

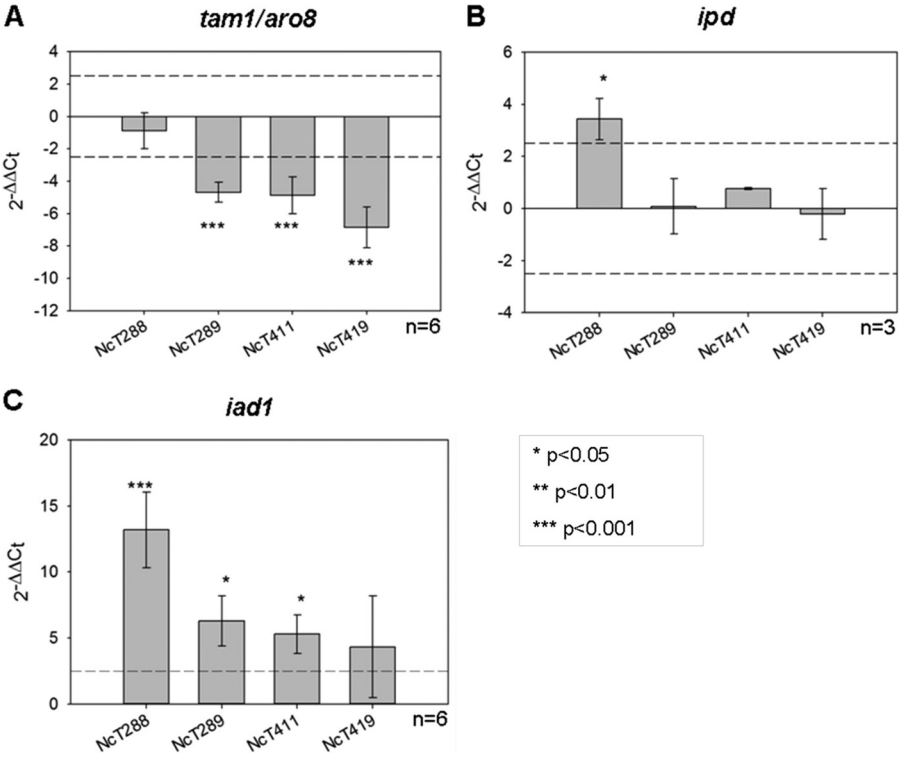

FIG 7 qRT-PCR results showing the relative levels of expression of the three genes involved in a putative auxin biosynthesis pathway of *N. crassa*, evaluated in different *bem46* transformant and mutant strains. The transcript quantities were calculated relative to that of the housekeeping gene *tub2*. NcT288, *bem46*-overexpressing strain; NcT289, *bem46* RNAi strain; NcT411, *bem46* knockout strain; NcT419, strain overexpressing the 0.5-kb alternatively spliced *bem46* fragment.

However, most of these patches showed no colocalization with the eisosomal PILA protein.

Anthranilate synthase component II is an interaction partner of BEM46. Using yeast two-hybrid analysis, we identified about 100 proteins specifically interacting with BEM46 (Fig. 4). Plasmid isolation and sequencing revealed that all plasmids analyzed contained one of four cDNA fragments from the same *trp-1* gene sequence, encoding anthranilate synthase component II (49). Among these four cDNAs (Fig. 4B), the two smaller ones encoded only the F domain, which resembles an *N*-(5′-phosphoribosyl)anthranilate isomerase. Since these cDNAs enabled a specific two-hybrid interaction with the BEM46 protein, it is likely that the F domain is sufficient for protein-protein interaction with BEM46. A bimolecular fluorescence complementation assay (31) was used to confirm the *in vivo* interaction of BEM46 and anthranilate synthase (Fig. 5).

The Δ*trp-1* mutant. Our results described above indicated a link between BEM46 and the tryptophan biosynthesis pathway. Tryptophan reportedly may act as a signal molecule and inhibit conidial anastomosis tube fusion in *N. crassa* (50). It is also an important precursor for secondary metabolites and plant hormones, such as auxin (51, 52), which is produced both in plants and in fungi (53).

Further investigation revealed that the Δ*trp-1* strains (FGSC 20870 and FGSC 20871) showed single ascospores developing no directed hyphae but rather growing bubble-like structures, similar to those observed in the *bem46* RNAi line (20), at the point of germination (Fig. 6A, arrow). The rate of germination in the Δ*trp-1* strains was reduced to about 50% of that in the wild-type ascospore (Fig. 6C), with conidia germinating earlier and building longer young hyphae. Since indole acetic acid reportedly promotes conidial germination and the elongation of young hyphae (54–57), we tested whether the observed phenotypic effect might be caused by auxin. In the medium, we determined the indole content released by germinating conidiospores. Indeed, the Δ*trp-1* mutants produced 10-fold-larger amounts of indoles than the wild-type strain when the medium was supplemented with 0.5 mM tryptophan (Fig. 6E). Determination of the indole content produced by ascospores revealed no differences between the Δ*trp-1* and wild-type strains (Fig. 6D).

A pathway for indole production in *N. crassa*. Auxin production has long been known to occur in filamentous fungi (58, 59) and has also been reported recently in symbiotic and phytopathogenic fungi (see, e.g., reference 60). Several pathways have been suggested for auxin production in plants, but not all are confirmed (52). The most studied such pathway is the indole-3-pyruvic acid (IPA) pathway (61), in which the main enzymes are tryptophan aminotransferase (TAM), indole-3-pyruvate decarboxylase (IPD), and indole-3-acetaldehyde dehydrogenase (IAD). Previous studies (58, 62) have shown the presence of TAM1 and IAD1 in *Ustilago maydis*. Here we used bioinformatic tools to identify the entire set of ortholog genes for the IPA pathway in *N. crassa*: NCU09166.7 (*tam1*), NCU02397.7 (*ipd*), and NCU03415 (*iad1*) (see Fig. S3 in the supplemental material).

Regulation of transcription of the auxin biosynthetic pathway in the *bem46* transformant and mutant strains of *N. crassa*.

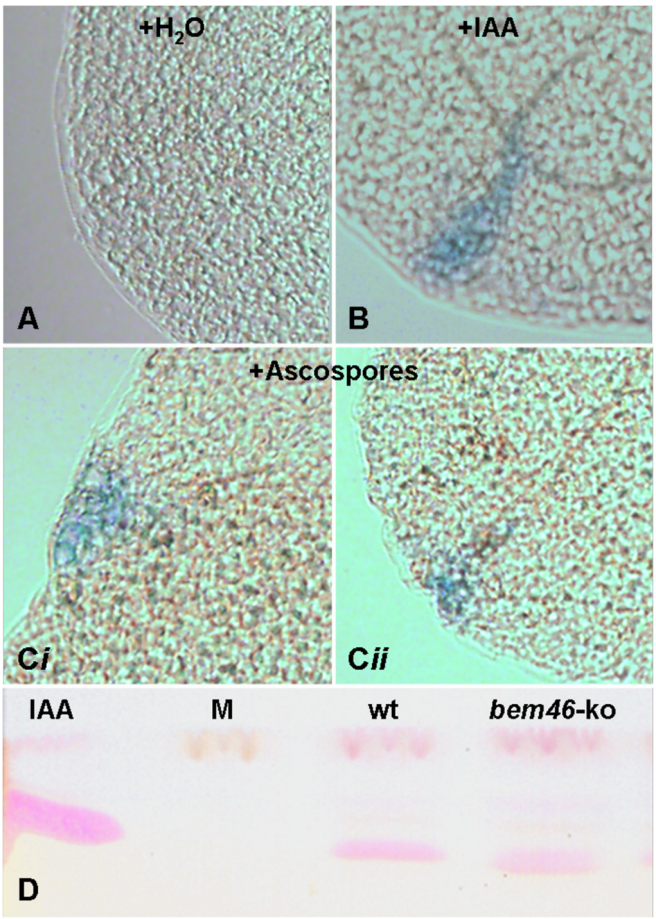

FIG 8 (A to C) Bright-field images of *Arabidopsis thaliana* seedlings expressing the auxin-responsive DR5::GUS fusion construct, incubated with water as a negative control (A), with indole acetic acid (IAA) as a positive control (B), or with germinating ascospores of wild-type *N. crassa* (Ci and Cii). (D) Thin-layer chromatographic separation of indole acetic acid from the culture medium on a silica plate. M, medium incubated without fungus; wt, medium incubated with wild-type *N. crassa*; *bem46*-ko, medium incubated with the *N. crassa bem46* knockout mutant.

We investigated the expression of *tam1*, *ipd*, and *iad1* in the wild-type, *bem46* mutant, and different transformant strains. Figure 7 shows the quantitative RT-PCR results for the mRNAs of these genes. The first gene of the pathway (*tam1*) was significantly downregulated in the *bem46* knockout (NcT411) and knockdown (NcT289) strains. Interestingly, overexpression of the 0.5-kb alternatively spliced fragment (NcT419) had the same effect. The *bem46*-overexpressing line (NcT288) showed no altered regulation of the *tam1* gene but was the only strain to show altered regulation of the *ipd* gene (3-fold upregulation). The last gene of the pathway, *iad1*, was upregulated in all strains investigated, except for the line expressing the 0.5-kb fragment. Expression of *iad1* was more than 10-fold higher in the *bem46*-overexpressing strain.

Indole production by the *bem46* transformant and mutant strains compared to that by the wild type. Figure 8 shows data indicating auxin production in *N. crassa*, which had been observed previously as well (63). Transgenic *Arabidopsis thaliana* plants expressing the DR5::GUS fusion protein (37, 64) were incubated either with water (Fig. 8A), with 100 μM IAA (Fig. 8B), or with germinating wild-type ascospores (Fig. 8Ci and ii). Seedlings incubated with either IAA or germinating ascospores showed positive staining for β-glucuronidase in cotyledon tips. Because the expression of the fusion protein is auxin dependent, our data provide indirect evidence for auxin production by germinating ascospores. Next, auxin was detected directly by thin-layer chromatography (Fig. 8D). Figure 9 shows the concentrations of auxin from germinating macroconidia and germinating ascospores in growth medium. Auxin concentrations did not differ significantly in 4-day-old mycelium, but we observed significant differences between auxin concentrations in the germinating macroconidia of different strains. Overexpression of the full-length *bem46* gene under the control of the *ccg1* promoter did not increase the auxin concentration over that in the wild type; however, the *bem46* knockout and RNAi lines showed significantly increased auxin concentrations. Auxin production during ascospore germination was also investigated (Fig. 9B). No significant differences from production by the wild type were observed for the *bem46* knockout and RNAi strains, but the overexpression line showed reduced indole production by germinating ascospores.

Investigation of indole production by germinating macroconidia also revealed differences in the time flow of macroconidial germination and in the rate of hyphal elongation. The micrographs in Fig. 9C show that most wild-type macroconidia germinated after 5 h, while the macroconidia of the *bem46*-overexpressing line germinated later. Macroconidia from the *bem46* knockout strain germinated within 5 h and produced longer germ tubes than the wild type. Determination of the growth rate of young hyphae within the first 4 days after germination (Fig. 9D) clearly showed strongly inhibited hyphal elongation in the *bem46* overexpression strain. In contrast, the knockout and RNAi strains showed growth rates somewhat higher than that of the wild type.

The MTR protein of *N. crassa*: a specific tryptophan transporter. The H^+-driven tryptophan and tyrosine permease TAT2 (YOL020W) of *Saccharomyces cerevisiae* is reportedly localized in eisosomes (65). MTR (NCU06619) is a neutral amino acid transport protein (66, 67) that we identified as the TAT2 homolog in *N. crassa*. We used qRT-PCR to analyze MTR expression in the different *bem46* transformant and mutant strains. Figure 10A shows 4-fold upregulation of the gene in the *bem46* overexpression strain (NcT288) relative to the wild type. The subcellular localization of MTR was studied using a *trfp* reporter gene construct. Figure 10B shows the localization of the protein in the perinuclear ER and in several additional small spots. The tRFP-coupled MTR protein colocalized with the BEM46::eGFP protein in swollen and germinating macroconidiospores and in mature hyphae.

DISCUSSION

BEM46 interacts with anthranilate synthase. Here we identified the anthranilate synthase encoded by the *trp-1* gene (49, 68) as an interaction partner of BEM46 in *N. crassa*. This result was unexpected, because in other model organisms, BEM46 interacts with proteins involved in developing/maintaining polar growth (9, 12, 69). Phenotypic analyses of the *N. crassa trp-1* mutant showed reduced ascospore germination, with spores developing the same loss-of-polarity phenotype as that described for the Δ*bem46* mutant (20). These results suggested a situation similar to that in the

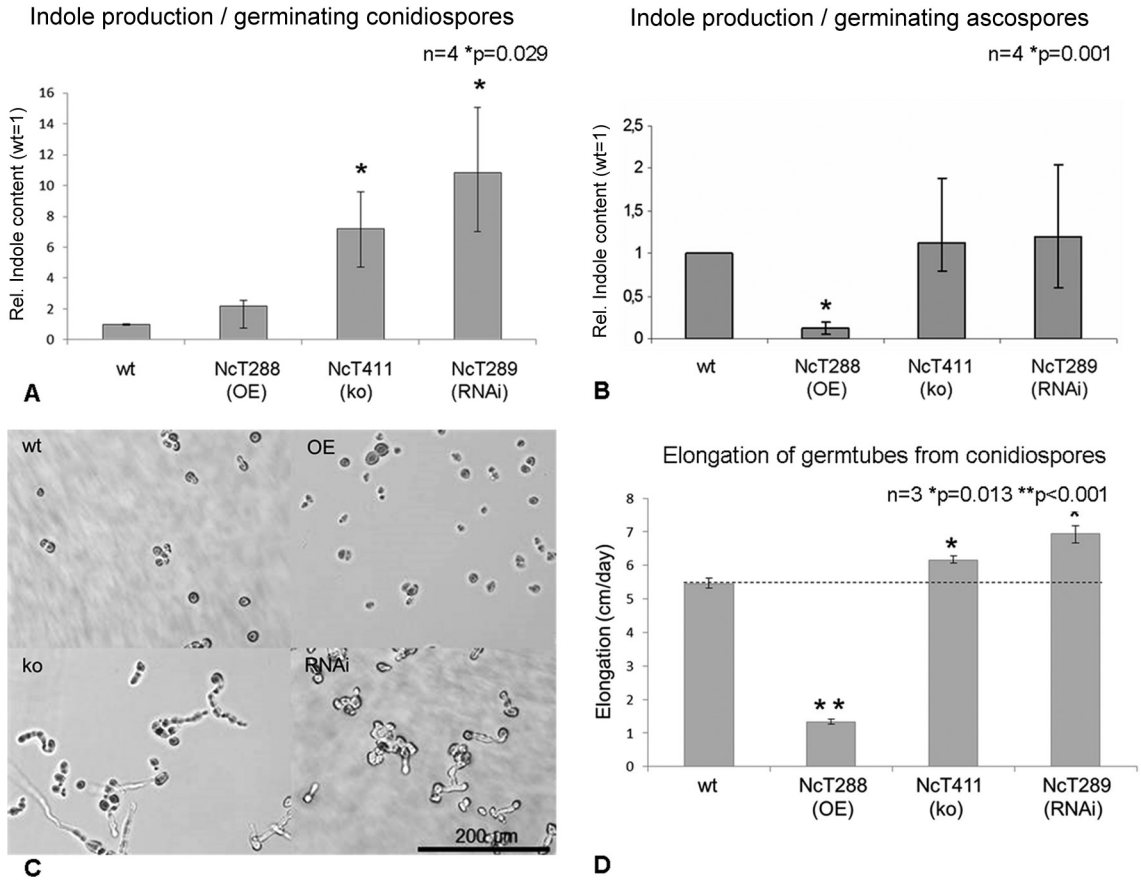

FIG 9 Indole production of *bem46* mutant and transformant strains. (A and B) Total indole production by germinating conidiospores (A) and ascospores (B). The total indole content of the medium is expressed relative to that of the medium for the wild type (taken as 1). (C) Bright-field images of germinating conidiospores that had been incubated for 4 h at 30°C on agar plates with Vogel's minimal medium. Macroconidia of the wild-type (wt), knockout (ko), knockdown (RNAi), and overexpressing (OE) strains are shown. (D) Hyphal elongation of the *bem46* transformant and mutant strains. The elongation rate is defined as the growth distance (cm) in 1 day.

model organism *A. thaliana*, where mutations in the *asa1* gene encoding anthranilate synthase result in a wavy root growth phenotype (70). The same phenotype was observed in the *bem46* homolog (*wavy growth 2*) knockout mutant (12). However, IAA was unable to rescue the wavy root phenotype in *A. thaliana* (70); thus, we considered that BEM46 might influence polar growth through an effect on IAA biosynthesis in the fungus. We observed that conidiospores of the Δ*trp-1* mutant germinated earlier and developed longer young hyphae than those of the wild type. The same effects were reported previously for *N. crassa* following external addition of IAA (54, 57). Therefore, we investigated the auxin biosynthesis and indole production of the different *N. crassa bem46* mutant and transformant strains.

Auxin biosynthesis in *Neurospora crassa* and its connection to BEM46. Although it is not widely known, auxin biosynthesis in fungi was reported many decades ago (59). These fungi include *N. crassa* (53, 63), and studies investigated the effects of externally applied auxins (56, 57). However, we discovered this information only after our present analyses of indole production in *N. crassa* wild-type and *bem46* knockout, RNAi, and overexpression lines. Recent research has focused mainly on auxin production by phytopathogenic fungi, e.g., *Ustilago maydis*, *Fusarium* species, and *Colletotrichum gloeosporioides* (58, 60, 71–73). In these phytopathogenic fungi, auxin is believed to affect host plant growth. In *N. crassa*, IAA at a concentration of 10^{-6} M enhanced the conidial germination rate after 2 h of incubation (54). At higher concentrations, an inhibitory effect was shown. It has been reported previously (55) that IAA removes the "conidial density effect" (74), and 10^{-6} M auxin reportedly induces the elongation of young hyphae germinating from conidia, while higher concentrations are inhibitory (57).

Here, using bioinformatic tools, we have presented evidence for a tryptophan-dependent IAA biosynthesis pathway in *N. crassa*. We showed that the expression of the three genes involved in this pathway (*tam1*, *ipd*, and *iad*) was altered in the different *bem46* transformants and mutant strains, indicating a connection between *bem46* and auxin biosynthesis in the fungus. However, the effects of auxin and its connection to *bem46* appear to differ in the different developmental stages of *N. crassa*. In germinating conidiospores, *bem46* downregulation led to *iad1* overexpression and higher indole production, resulting in earlier conidial germination and increased hyphal elongation. Interestingly, *bem46* overexpression also led to very high *iad1* expression. While indole content did not differ from that of the wild type, conidial germination was delayed and hyphal elongation strongly reduced,

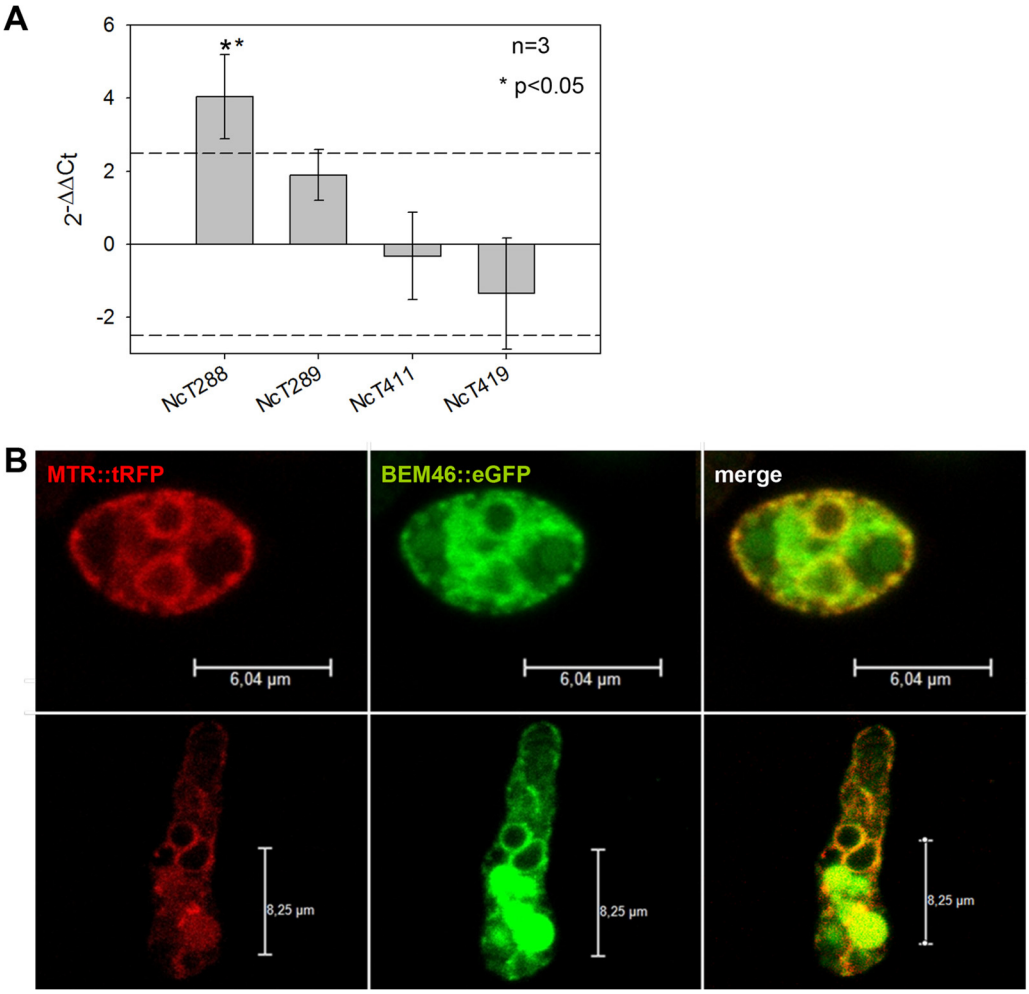

FIG 10 MTR is a putative tryptophan transporter. (A) qRT-PCR results showing the relative expression levels of the *mtr* gene in different *bem46* transformant and mutant strains of *N. crassa*. The transcript quantities were calculated relative to that for the housekeeping gene *tub2*. NcT288, *bem46*-overexpressing strain; NcT289, *bem46* RNAi strain; NcT411, *bem46* knockout strain; NcT419, strain overexpressing the alternatively spliced 0.5-kb *bem46* fragment. (B) Colocalization of MTR and BEM46 fusion proteins. Shown are CLSM images of macroconidiospores and germinating macroconidiospores of heterokaryons overexpressing both MTR::tRFP and BEM46::eGFP.

which may result from negative regulation, since high levels of IAA are inhibitory.

We further detected colocalization of BEM46 with the neutral amino acid transporter MTR. BEM46 may act at the crossing point between tryptophan synthesis and uptake. Indeed, *mtr* expression was significantly higher in the *bem46*-overexpressing strain, which may lead to high internal levels of indole, resulting in the inhibitory effects described above. The indole production of vegetative mycelia of *bem46* transformant and mutant strains did not differ significantly from that for the wild type; however, the expression of genes involved in the putative auxin biosynthesis pathway was affected. It is possible that indole content is additionally regulated by inactivation of the end product, as described for *A. thaliana* (75).

Alternative splicing of *bem46*. In multicellular organisms, alternative splicing is a mechanism by which gene expression is regulated on the mRNA level (76). Alternative splicing can affect the transcriptome both quantitatively and qualitatively, e.g., by degradation of alternatively spliced forms over the nonsense-mediated mRNA decay (NMD) pathway (77, 78). Such changes on the transcript level can potentially affect almost all areas of protein function (76). The transcript isoforms can be translated into various proteins with different sequences and/or domain arrangements (79). The resulting truncated proteins can act as dominant negative regulators of the authentic protein (80). Alternative splicing itself can be regulated by riboswitches or by different environmental cues (81, 82), thus making alternative splicing a flexible tool that allows adaptation to the environment (83). Alternative splicing also occurs in ascomycetes, though at a rate significantly lower than that in mammals (43). In *N. crassa*, 162 of 9,733 protein-coding genes exhibit evidence of alternative splicing. The most common form of alternative splicing in fungi is intron retention (43).

In the present study, we identified 0.5- and 1.2-kb alternatively spliced *bem46* fragments that encoded truncated proteins of 123 and 40 amino acids, respectively. There are two main reasons to assume that these are alternative splicing products rather than splicing intermediates. First, if they were splicing intermediates,

the fragments would have been detected in the wild-type strains; this was not the case in our investigations. Second, the fragment sequences were not simple combinations of exons; the 1.2-kb product resulted from intron retention (the most common method of alternative splicing in fungi), while the 0.5-kb product showed a very unusual splicing pattern that did not match any splicing intermediate. The alternatively spliced fragments accumulated in the *bem46* RNAi lines (20), which exhibited no ascospore germination. Since overexpression of either full-length or truncated BEM46 protein led to a loss of ascospore germination, it is possible that the alternatively spliced fragments (or rather, the translated truncated proteins) act as dominant competitors of the full-length protein. This would explain how overexpression of the small fragments leads to the same effect as overexpression of the full-length protein, i.e., the inhibition of ascospore germination.

It remains unknown how BEM46 may influence the mechanism of ascospore germination. Indole production was reduced in ascospores from strains overexpressing either the full-length or the truncated BEM46 protein. Hence, it is possible that BEM46 directly affects indole production, which negatively influences ascospore germination. However, indole production by the RNAi and knockout strains did not differ significantly from that by the wild type. With the knockout strain, a considerable number of ascospores will normally germinate, and even in the RNAi strain, one out of a few thousand ascospores may germinate (20). It is possible that indole production by these germinated spores could falsify the measurement of indole content. This may also explain the relatively high standard deviation found for indole production by these strains. Alternatively, the effect of the truncated BEM46 protein may be due to its apparently different cellular localization.

The qRT-PCR studies described here were focused on the *ipd* pathway, which was identified using a bioinformatics approach. However, additional biosynthetic pathways for indole production may also be relevant. Ongoing bioinformatic analyses indicate the potential presence of several possible auxin biosynthetic pathways in *N. crassa* (P. Sardar, unpublished data), some of which may share the last aldehyde dehydrogenase, encoded by *iad*. The coexistence of different pathways resulting in the same final product may enable precise regulation of the internal auxin level, which is advantageous considering the fact that the effect of auxin is concentration dependent. Phytosphingosine treatment— which induces programmed cell death in *N. crassa*—strongly upregulates *iad1* expression and slightly upregulates *bem46* expression (84). This could suggest the involvement of the two gene products in general stress response reactions.

Germination and hyphal elongation are critical points in the life of an ascomycete and are strongly dependent on the variable environment of the fungus. Therefore, flexible and effective regulation of these processes is required. It appears possible that one aspect of this mechanism may include regulation of the internal indole level of the fungus, which results from uptake as well as intracellular production. Our present results indicate that BEM46 may act at the crossing point of this regulation.

ACKNOWLEDGMENTS

We thank H. Schmidt and J. Quintanilla (Kiel, Germany) for technical assistance. We thank S. Seiler (Freiburg, Germany) for providing an *N. crassa* cDNA library, A. Lichius (Vienna, Austria) for the Lifeact-RFP vector, and U. Kück (Bochum, Germany) for providing split-YFP vectors and also for critical discussions. We are grateful to the Fungal Genetics Stock Center for providing *Neurospora* strains, as well as to the "Labor für Molekulare Biowissenschaften" and the "Zentralen Mikroskopie" of Christian-Albrechts-University for the use of equipment.

REFERENCES

1. **Kumar A, Kollath-Leiß K, Kempken F.** 2013. Characterization of bud emergence 46 (BEM46) protein: sequence, structural, phylogenetic and subcellular localization analyses. Biochem. Biophys. Res. Commun. **438:** 526–532. http://dx.doi.org/10.1016/j.bbrc.2013.07.103.
2. **Cabib E, Drgonova J, Drgon T.** 1998. Role of small G proteins in yeast cell polarization and wall biosynthesis. Annu. Rev. Biochem. **67:**307–333. http://dx.doi.org/10.1146/annurev.biochem.67.1.307.
3. **Madden K, Snyder M.** 1998. Cell polarity and morphogenesis in budding yeast. Annu. Rev. Microbiol. **52:**687–744. http://dx.doi.org/10.1146/annurev.micro.52.1.687.
4. **Park HO, Bi E, Pringle JR, Herskowitz I.** 1997. Two active states of the Ras-related Bud1/Rsr1 protein bind to different effectors to determine yeast cell polarity. Proc. Natl. Acad. Sci. U. S. A. **94:**4463–4468. http://dx.doi.org/10.1073/pnas.94.9.4463.
5. **Chenevert J, Corrado K, Bender A, Pringle J, Herskowitz I.** 1992. A yeast gene (*BEM1*) necessary for cell polarization whose product contains two SH3 domains. Nature **356:**77–79. http://dx.doi.org/10.1038/356077a0.
6. **Irazoqui JE, Gladfelter AS, Lew DJ.** 2003. Scaffold-mediated symmetry breaking by Cdc42p. Nat. Cell Biol. **5:**1062–1070. http://dx.doi.org/10.1038/ncb1068.
7. **Chant J, Corrado K, Pringle JR, Herskowitz I.** 1991. Yeast *BUD5*, encoding a putative GDP-GTP exchange factor, is necessary for bud site selection and interacts with bud formation gene *BEM1*. Cell **65:**1213–1224. http://dx.doi.org/10.1016/0092-8674(91)90016-R.
8. **Giaever G, Chu AM, Ni L, Connelly C, Riles L, Véronneau S, Dow S, Lucau-Danila A, Anderson K, André B, Arkin AP, Astromoff A, El-Bakkoury M, Bangham R, Benito R, Brachat S, Campanaro S, Curtiss M, Davis K, Deutschbauer A, Entian K-D, Flaherty P, Foury F, Garfinkel DJ, Gerstein M, Gotte D, Güldener U, Hegemann JH, Hempel S, Herman Z, Jaramillo DF, Kelly DE, Kelly SL, Kötter P, LaBonte D, Lamb DC, Lan N, Liang H, Liao H, Liu L, Luo C, Lussier M, Mao R, Menard P, Ooi SL, Revuelta JL, Roberts CJ, Rose M, Ross-Macdonald P, Scherens B, Schimmack G, Shafer B, Shoemaker DD, Sookhai-Mahadeo S, Storms RK, Strathern JN, Valle G, Voet M, Volckaert G, Wang C, Ward TR, Wilhelmy J, Winzeler EA, Yang Y, Yen G, Youngman E, Yu K, Bussey H, Boeke JD, Snyder M, Philippsen P, Davis RW, Johnston M.** 2002. Functional profiling of the *Saccharomyces cerevisiae* genome. Nature **418:**387–391. http://dx.doi.org/10.1038/nature00935.
9. **Giot L, Bader JS, Brouwer C, Chaudhuri A, Kuang B, Li Y, Hao YL, Ooi CE, Godwin B, Vitols E, Vijayadamodar G, Pochart P, Machineni H, Welsh M, Kong Y, Zerhusen B, Malcolm R, Varrone Z, Collis A, Minto M, Burgess S, McDaniel L, Stimpson E, Spriggs F, Williams J, Neurath K, Ioime N, Agee M, Voss E, Furtak K, Renzulli R, Aanensen N, Carrolla S, Bickelhaupt E, Lazovatsky Y, DaSilva A, Zhong J, Stanyon CA, Finley RL, White KP, Braverman M, Jarvie T, Gold S, Leach M, Knight J, Shimkets RA, McKenna MP, Chant J, Rothberg JM.** 2003. A protein interaction map of *Drosophila melanogaster*. Science **302:**1727–1736. http://dx.doi.org/10.1126/science.1090289.
10. **Parmentier ML, Woods D, Greig S, Phan PG, Radovic A, Bryant P, O'Kane CJ.** 2000. Rapsynoid/partner of inscuteable controls asymmetric division of larval neuroblasts in *Drosophila*. J. Neurosci. **20:**RC84.
11. **Okada K, Shimura Y.** 1990. Reversible root tip rotation in *Arabidopsis* seedlings induced by obstacle-touching stimulus. Science **250:**274–276. http://dx.doi.org/10.1126/science.250.4978.274.
12. **Mochizuki S, Harada A, Inada S, Sugimoto-Shirasu K, Stacey N.** 2005. The *Arabidopsis* WAVY GROWTH 2 protein modulates root bending in response to environmental stimuli. Plant Cell **17:**537–547. http://dx.doi.org/10.1105/tpc.104.028530.
13. **Ollis DL, Cheah E, Cyglerl M, Dijkstra B, Frolow F, Franken SM, Harel M, Remington SJ, Silman I, Schragl J, Sussman JL, Goldmans A.** 1992. The α/β hydrolase fold. Protein Eng. **5:**197–211. http://dx.doi.org/10.1093/protein/5.3.197.
14. **Nardini M, Dijkstra BW.** 1999. α/β Hydrolase fold enzymes: the family keeps growing. Curr. Opin. Struct. Biol. **9:**732–737. http://dx.doi.org/10.1016/S0959-440X(99)00037-8.

15. **Lenfant N, Hotelier T, Velluet E, Bourne Y, Marchot P, Chatonnet A.** 2013. ESTHER, the database of the α/β-hydrolase fold superfamily of proteins: tools to explore diversity of functions. Nucleic Acids Res. **41:** D423–D429. http://dx.doi.org/10.1093/nar/gks1154.
16. **Hotelier T, Renault L, Cousin X, Negre V, Marchot P, Chatonnet A.** 2004. ESTHER, the database of the α/β-hydrolase fold superfamily of proteins. Nucleic Acids Res. **32:**D145–D147. http://dx.doi.org/10.1093/nar/gkh141.
17. **Galperin MY, Koonin EV.** 2004. "Conserved hypothetical" proteins: prioritization of targets for experimental study. Nucleic Acids Res. **32:** 5452–5463. http://dx.doi.org/10.1093/nar/gkh885.
18. **Galperin MY, Koonin EV.** 2010. From complete genome sequence to "complete" understanding? Trends Biotechnol. **28:**398–406. http://dx.doi.org/10.1016/j.tibtech.2010.05.006.
19. **Fischer R, Zekert N, Takeshita N.** 2008. Polarized growth in fungi—interplay between the cytoskeleton, positional markers and membrane domains. Mol. Microbiol. **68:**813–826. http://dx.doi.org/10.1111/j.1365-2958.2008.06193.x.
20. **Mercker M, Kollath-Leiß K, Allgaier S, Weiland N, Kempken F.** 2009. The BEM46-like protein appears to be essential for hyphal development upon ascospore germination in *Neurospora crassa* and is targeted to the endoplasmic reticulum. Curr. Genet. **55:**151–161. http://dx.doi.org/10.1007/s00294-009-0232-3.
21. **Vogel HJ.** 1956. A convenient growth medium for *Neurospora* (Medium N). Microbiol. Genet. Bull. **13:**42–43.
22. **Westergaard M, Mitchell HK.** 1947. Neurospora V. A synthetic medium favoring sexual reproduction. Am. J. Bot. **34:**573–577.
23. **Fleissner A, Diamond S, Glass NL.** 2009. The *Saccharomyces cerevisiae* PRM1 homolog in *Neurospora crassa* is involved in vegetative and sexual cell fusion events but also has postfertilization functions. Genetics **181:** 497–510. http://dx.doi.org/10.1534/genetics.108.096149.
24. **Borges MI, Azevedo MO, Bonatelli R, Felipe MSS, Astolfi-Filho S.** 1990. A practical method for preparation of total DNA from filamentous fungi. Fungal Genet. Newsl. **37:**10.
25. **Hoffman CS, Winston F.** 1987. A ten-minute DNA preparation from yeast efficiently releases autonomous plasmids for transformation of *Escherichia coli*. Gene **57:**267–272. http://dx.doi.org/10.1016/0378-1119(87)90131-4.
26. **Kempken F, Kück U.** 1996. *Restless*, an active *Ac*-like transposon from the fungus *Tolypocladium inflatum*: structure, expression, and alternative RNA splicing. Mol. Cell. Biol. **16:**6563–6572.
27. **Sambrook J, Fritsch EF, Maniatis T.** 1989. Molecular cloning: a laboratory manual, 2nd ed. Cold Spring Harbor Laboratory Press, Cold Spring Harbor, NY.
28. **Livak KJ, Schmittgen TD.** 2001. Analysis of relative gene expression data using real-time quantitative PCR and the $2^{-\Delta\Delta CT}$ method. Methods **25:** 402–408. http://dx.doi.org/10.1006/meth.2001.1262.
29. **Margolin B, Freitag M, Selker EU.** 1997. Improved plasmids for gene targeting at the *his-3* locus of *Neurospora crassa* by electroporation. Fungal Genet. Newsl. **44:**34–36. (Author Correction, 47:112, 2000.)
30. **Hickey PC, Swift SR, Roca MG, Read ND.** 2004. Live-cell imaging of filamentous fungi using vital fluorescent dyes. Methods Microbiol. **34:**63–87. http://dx.doi.org/10.1016/S0580-9517(04)34003-1.
31. **Hoff B, Kück U.** 2005. Use of bimolecular fluorescence complementation to demonstrate transcription factor interaction in nuclei of living cells from the filamentous fungus *Acremonium chrysogenum*. Curr. Genet. **47:** 132–138. http://dx.doi.org/10.1007/s00294-004-0546-0.
32. **Berepiki A, Lichius A, Shoji J-Y, Tilsner J, Read ND.** 2010. F-actin dynamics in *Neurospora crassa*. Eukaryot. Cell **9:**547–557. http://dx.doi.org/10.1128/EC.00253-09.
33. **Colot HV, Gyungsoon P, Turner GE, Ringelberg C, Crew CM, Litvinkova L, Weiss RL, Borkovich KA, Dunlap JC.** 2006. A high-throughput gene knockout procedure for *Neurospora* reveals functions for multiple transcription factors. Proc. Natl. Acad. Sci. U. S. A. **103:**10352–10357. http://dx.doi.org/10.1073/pnas.0601456103.
34. **Chien CT, Bartel PL, Sternglanz R, Fields S.** 1991. The two-hybrid system: a method to identify and clone genes for proteins that interact with a protein of interest. Proc. Natl. Acad. Sci. U. S. A. **88:**9578–9582. http://dx.doi.org/10.1073/pnas.88.21.9578.
35. **Fields S, Song O.** 1989. A novel genetic system to detect protein-protein interactions. Nature **340:**245–246. http://dx.doi.org/10.1038/340245a0.
36. **Breeden L, Nasmyth K.** 1985. Regulation of the yeast HO gene. Cold Spring Harb. Symp. Quant. Biol. **50:**643–650. http://dx.doi.org/10.1101/SQB.1985.050.01.078.
37. **Ulmasov T, Murfett J, Hagen G, Guilfoyle TJ.** 1997. Aux/IAA proteins repress expression of reporter genes containing natural and highly active synthetic auxin response elements. Plant Cell **9:**1963–1971. http://dx.doi.org/10.1105/tpc.9.11.1963.
38. **Weigel D, Glazebrook J.** 2002. *Arabidopsis*: a laboratory manual. Cold Spring Harbor Laboratory Press, Cold Spring Harbor, NY.
39. **Murashige T, Skoog F.** 1962. A revised medium for rapid growth and bio assays with tobacco tissue cultures. Physiol. Plant. **15:**473–497. http://dx.doi.org/10.1111/j.1399-3054.1962.tb08052.x.
40. **Glickmann E, Dessaux Y.** 1995. A critical examination of the specificity of the Salkowski reagent for indolic compounds produced by phytopathogenic bacteria. Appl. Environ. Microbiol. **61:**793–796.
41. **Gordon SA, Weber RP.** 1951. Colorimetric estimation of indole acetic acid. Plant Physiol. **26:**192–195. http://dx.doi.org/10.1104/pp.26.1.192.
42. **Ehmann A.** 1977. The Van Urk-Salkowski reagent—a sensitive and specific chromogenic reagent for silica gel thin-layer chromatographic detection and identification of indole derivatives. J. Chromatogr. **132:**267–276. http://dx.doi.org/10.1016/S0021-9673(00)89300-0.
43. **Kempken F.** 2013. Alternative splicing in ascomycetes. Appl. Microbiol. Biotechnol. **97:**4235–4241. http://dx.doi.org/10.1007/s00253-013-4841-x.
44. **Temporini ED, Alvarez ME, Mautino MR, Folco HD, Rosa AL.** 2004. The *Neurospora crassa cfp* promoter drives a carbon source-dependent expression of transgenes in filamentous fungi. J. Appl. Microbiol. **96:** 1256–1264. http://dx.doi.org/10.1111/j.1365-2672.2004.02249.x.
45. **Aramayo R, Metzenberg RL.** 1996. Gene replacements at the *his-3* locus of *Neurospora crassa*. Fungal Genet. Newsl. **43:**9–13.
46. **Kolláth-Leiß K, Kempken F.** 2012. Bem46-Homologe: bekannte Proteine mit unbekannter Funktion. Biospektrum **18:**251–253. http://dx.doi.org/10.1007/s12268-012-0170-3.
47. **Walther TC, Brickner JH, Aguilar PS, Bernales S, Pantoja C, Walter P.** 2006. Eisosomes mark static sites of endocytosis. Nature **439:**998–1003. http://dx.doi.org/10.1038/nature04472.
48. **Vangelatos I, Roumelioti K, Gournas C, Suarez T, Scazzocchio C, Sophianopoulou V.** 2010. Eisosome organization in the filamentous ascomycete *Aspergillus nidulans*. Eukaryot. Cell **9:**1441–1454. http://dx.doi.org/10.1128/EC.00087-10.
49. **Walker MS, DeMoss JA.** 1986. Organization of the functional domains of anthranilate synthase from *Neurospora crassa*. Limited proteolysis studies. J. Biol. Chem. **261:**16073–16077.
50. **Fischer-Harman V, Jackson KJ, Muñoz A, Shoji J, Read ND.** 2012. Evidence for tryptophan being a signal molecule that inhibits conidial anastomosis tube fusion during colony initiation in *Neurospora crassa*. Fungal Genet. Biol. **49:**896–902. http://dx.doi.org/10.1016/j.fgb.2012.08.004.
51. **Radwanski ER, Last RL.** 1995. Tryptophan biosynthesis and metabolism: biochemical and molecular genetics. Plant Cell **7:**921–934. http://dx.doi.org/10.1105/tpc.7.7.921.
52. **Mano Y, Nemoto K.** 2012. The pathway of auxin biosynthesis in plants. J. Exp. Bot. **63:**2853–2872. http://dx.doi.org/10.1093/jxb/ers091.
53. **Gruen HE.** 1959. Auxins and fungi. Annu. Rev. Plant Physiol. **10:**405–440. http://dx.doi.org/10.1146/annurev.pp.10.060159.002201.
54. **Nakamura T, Kawanabe Y, Takiyama E, Takahashi N, Murayama T.** 1978. Effects of auxin and gibberellin on conidial germination in *Neurospora crassa*. Plant Cell Physiol. **19:**705–709.
55. **Nakamura T, Tomita K, Kawanabe Y, Murayama T.** 1982. Effect of auxin and gibberellin on conidial germination in *Neurospora crassa*. II. "Conidial density effect" and auxin. Plant Cell Physiol. **23:**1363–1369.
56. **Nakamura T, Mukai C, Ozaki Y, Saotome M, Murayama T.** 1988. Effects of auxin and gibberellin on conidial germination and elongation of young hyphae in a cyclic 3′:5′ adenosine monophosphate-dependent protein kinase mutant of *Neurospora crassa*. Plant Growth Regul. **7:**201–207.
57. **Tomita K, Murayama T, Nakamura T.** 1984. Effects of auxin and gibberellin on elongation of young hyphae in *Neurospora crassa*. Plant Cell Physiol. **25:**355–358.
58. **Basse CW, Lottspeich F, Steglich W, Kahmann R.** 1996. Two potential indole-3-acetaldehyde dehydrogenases in the phytopathogenic fungus *Ustilago maydis*. Eur. J. Biochem. **242:**648–656. http://dx.doi.org/10.1111/j.1432-1033.1996.0648r.x.
59. **Grün EH.** 1959. Auxin and fungi. Annu. Rev. Plant Physiol. **10:**405–440. http://dx.doi.org/10.1146/annurev.pp.10.060159.002201.
60. **Tsavkelova E, Oeser B, Oren-Young L, Israeli M, Sasson Y, Tudzynski**

B, Sharon A. 2012. Identification and functional characterization of indole-3-acetamide-mediated IAA biosynthesis in plant-associated *Fusarium* species. Fungal Genet. Biol. **49:**48–57. http://dx.doi.org/10.1016/j.fgb.2011.10.005.

61. **Mashiguchi K, Tanaka K, Sakai T, Sugawara S, Kawaide H, Natsume M.** 2011. The main auxin biosynthesis pathway in *Arabidopsis*. Proc. Natl. Acad. Sci. U. S. A. **108:**18512–18517. http://dx.doi.org/10.1073/pnas.1108434108.
62. **Zuther K, Mayser P, Hettwer U, Wu W, Spiteller P, Kindler BLJ, Karlovsky P, Basse CW, Schirawski J.** 2008. The tryptophan aminotransferase Tam1 catalyses the single biosynthetic step for tryptophan-dependent pigment synthesis in *Ustilago maydis*. Mol. Microbiol. **68:**152–172. http://dx.doi.org/10.1111/j.1365-2958.2008.06144.x.
63. **Tomita K, Kitsuwa T, Murayama T, Nakamura T.** 1987. Identification of indol-3-acetic acid in *Neurospora crassa*. Agric. Biol. Chem. **51:**2633–2634. http://dx.doi.org/10.1271/bbb1961.51.2633.
64. **Pozhvanov GA, Shavarda AL, Medvedev SS.** 2013. Quantitative analysis of IAA in DR5::GUS transgenic *Arabidopsis* plants. Russ. J. Plant Physiol. **60:**431–436. http://dx.doi.org/10.1134/S1021443713020179.
65. **Grossmann G, Malinsky J, Stahlschmidt W, Loibl M, Weig-Meckl I, Frommer WB, Opekarová M, Tanner W.** 2008. Plasma membrane microdomains regulate turnover of transport proteins in yeast. J. Cell Biol. **183:**1075–1088. http://dx.doi.org/10.1083/jcb.200806035.
66. **Stadler DR.** 1966. Genetic control of the uptake of amino acids in *Neurospora*. Genetics **54:**677–685.
67. **Stadler DR.** 1967. Suppressors of amino acid uptake mutants of *Neurospora*. Genetics **57:**935–942.
68. **Walker MS, DeMoss JA.** 1983. Purification and characterization of the trifunctional beta-subunit of anthranilate synthase from *Neurospora crassa*. J. Biol. Chem. **258:**3571–3575.
69. **Mercker M, Kollath-Leiss K, Allgaier S, Weiland N, Kempken F.** 2009. The BEM46-like protein appears to be essential for hyphal development upon ascospore germination in *Neurospora crassa* and is targeted to the endoplasmic reticulum. Curr. Genet. **55:**151–161. http://dx.doi.org/10.1007/s00294-009-0232-3.
70. **Rutherford R, Gallois P, Masson PH.** 1998. Mutations in *Arabidopsis thaliana* genes involved in the tryptophan biosynthesis pathway affect root waving on tilted agar surfaces. Plant J. **16:**145–154. http://dx.doi.org/10.1046/j.1365-313x.1998.00279.x.
71. **Reineke G, Heinze B, Schirawski J, Buettner H, Kahmann R, Basse CW.** 2008. Indole-3-acetic acid (IAA) biosynthesis in the smut fungus *Ustilago maydis* and its relevance for increased IAA levels in infected tissue. Mol. Plant Pathol. **9:**339–355. http://dx.doi.org/10.1111/j.1364-3703.2008.00470.x.
72. **Robinson M, Riov J, Sharon A.** 1998. Indole-3-acetic acid biosynthesis in *Colletotrichum gloeosporioides* f. sp. *aeschynomene*. Appl. Environ. Microbiol. **64:**5030–5032.
73. **Kulkarni GB, Sanjeevkumar S, Kirankumar B, Santoshkumar M, Karegoudar TB.** 2013. Indole-3-acetic acid biosynthesis in *Fusarium delphinoides* strain GPK, a causal agent of wilt in chickpea. Appl. Biochem. Biotechnol. **169:**1292–1305. http://dx.doi.org/10.1007/s12010-012-0037-6.
74. **Schmit JC, Brody S.** 1976. Biochemical genetics of *Neurospora crassa* conidial germination. Bacteriol. Rev. **40:**1–41.
75. **Woodward AW, Bartel B.** 2005. Auxin: regulation, action, and interaction. Ann. Bot. **95:**707–735. http://dx.doi.org/10.1093/aob/mci083.
76. **Roy B, Haupt LM, Griffiths LR.** 2013. Alternative splicing (AS) of genes as an approach for generating protein complexity. Curr. Genomics **14:**182–194. http://dx.doi.org/10.2174/1389202911314030004.
77. **McGlincy NJ, Smith CWJ.** 2008. Alternative splicing resulting in nonsense-mediated mRNA decay: what is the meaning of nonsense? Trends Biochem. Sci. **33:**385–393. http://dx.doi.org/10.1016/j.tibs.2008.06.001.
78. **Nicholson P, Mühlemann O.** 2010. Cutting the nonsense: the degradation of PTC-containing mRNAs. Biochem. Soc. Trans. **38:**1615–1620. http://dx.doi.org/10.1042/BST0381615.
79. **Syed NH, Kalyna M, Marquez Y, Barta A, Brown JWS.** 2012. Alternative splicing in plants—coming of age. Trends Plant Sci. **17:**616–623. http://dx.doi.org/10.1016/j.tplants.2012.06.001.
80. **Seo PJ, Kim MJ, Ryu J-Y, Jeong E-Y, Park C-M.** 2011. Two splice variants of the IDD14 transcription factor competitively form nonfunctional heterodimers which may regulate starch metabolism. Nat. Commun. **2:**303. http://dx.doi.org/10.1038/ncomms1303.
81. **Leal J, Squina FM, Freitas JS, Silva EM, Ono CJ, Martinez-Rossi NM, Rossi A.** 2009. A splice variant of the *Neurospora crassa hex-1* transcript, which encodes the major protein of the Woronin body, is modulated by extracellular phosphate and pH changes. FEBS Lett. **583:**180–184. http://dx.doi.org/10.1016/j.febslet.2008.11.050.
82. **Brunner M, Diernfellner A.** 2006. How temperature affects the circadian clock of *Neurospora crassa*. Chronobiol. Int. **23:**81–90. http://dx.doi.org/10.1080/07420520500545805.
83. **Kazan K.** 2003. Alternative splicing and proteome diversity in plants: the tip of the iceberg has just emerged. Trends Plant Sci. **8:**468–471. http://dx.doi.org/10.1016/j.tplants.2003.09.001.
84. **Videira A, Kasuga T, Tian C, Lemos C, Castro A, Glass NL.** 2009. Transcriptional analysis of the response of *Neurospora crassa* to phytosphingosine reveals links to mitochondrial function. Microbiology **155:**3134–3141. http://dx.doi.org/10.1099/mic.0.029710-0.

known unknown genes

Bem46-Homologe: bekannte Proteine mit unbekannter Funktion

KRISZTINA KOLLÁTH-LEIß, FRANK KEMPKEN
ABTEILUNG BOTANISCHE GENETIK UND MOLEKULARBIOLOGIE, UNIVERSITÄT KIEL

The bud emergence (BEM) 46 proteins are evolutionarily conserved members of the α/β-hydrolase super family. The exact function(s) of these proteins remains unknown. Vegetative hyphae, perithecia and ascospores of *Neurospora crassa* RNAi and over-expressing transformants develop normally, but hyphal germination from ascospores is impaired. The protein is localized in the perinuclear endoplasmatic reticulum and also forms spots near to the plasma membrane. One human paralog appears to be responsible for a genetic disorder.

DOI: 10.1007/s12268-012-0170-3

■ Viele Gene, die im Rahmen von Genomsequenzierprojekten beschrieben wurden, codieren für sogenannte hypothetische Proteine, denen bisher keine Funktion zugeordnet werden konnte [1]. Besonders interessant erscheinen unter diesen Genen diejenigen, die phylogenetisch weit verbreitet sind, da dies ein Hinweis auf eine wichtige Funktion sein kann. Unsere Arbeiten konzentrieren sich auf das Gen *bem46* (*bud emergence)*, das kürzlich unter die Top 10 bekannter Gene mit unbekannter Funktion (*known unknown*) aufgenommen wurde. Die Gruppe der *known unknown* enthält Gene, deren Produkte unbekannte biochemische Funktionen haben, aber zumindest teilweise bekannte zelluläre Funktionen [2]. Das *bem46*-Gen ist im eukaryotischen Reich universell verbreitet. Im Genom der Vertebraten ist eine Zunahme von paralogen Sequenzen zu beobachten (A. Kumar *et al.*, in Vorbereitung). Eines der humanen Paraloge (*abhd12*) wurde in Zusammenhang mit einer vererbbaren neurodegenerativen Krankheit (PHARC) beschrieben [3].

Die Bem46-Proteine gehören zu der α/β-Hydrolase-Superfamilie, deren Mitglieder alle das α/β-Hydrolasemotiv aufweisen [4, 5]. Die Gruppe umfasst zahlreiche Enzyme, die diverse Substratspezifitäten und Funktionen aufweisen, wie z. B. Lipidhydrolasen, Haloperoxidasen oder Dehalogenasen [6]. In der Vergangenheit wurden indirekte Hinweise auf die Rolle der Bem46-Homologe in einigen wenigen Modellorganismen gewonnen. Diese deuten auf seine Beteiligung am polaren Wachstum und/oder an der Signaltransduktion hin [6].

Unsere Arbeitsgruppe untersucht das Bem46-Protein aus *Neurospora crassa*, einem Hyphenpilz aus der Klasse der Ascomycota. *N. crassa* ist ein heterothallischer Haplo-Diplont mit einem sexuellen Hauptzyklus. Für die sexuelle Fortpflanzung sind zwei Kreuzungstypen – a und A – notwendig. Dabei reifen in Fruchtkörpern, den Perithecien, schlauchförmige Meiosporangien heran, die jeweils acht Ascosporen enthalten. Außer-

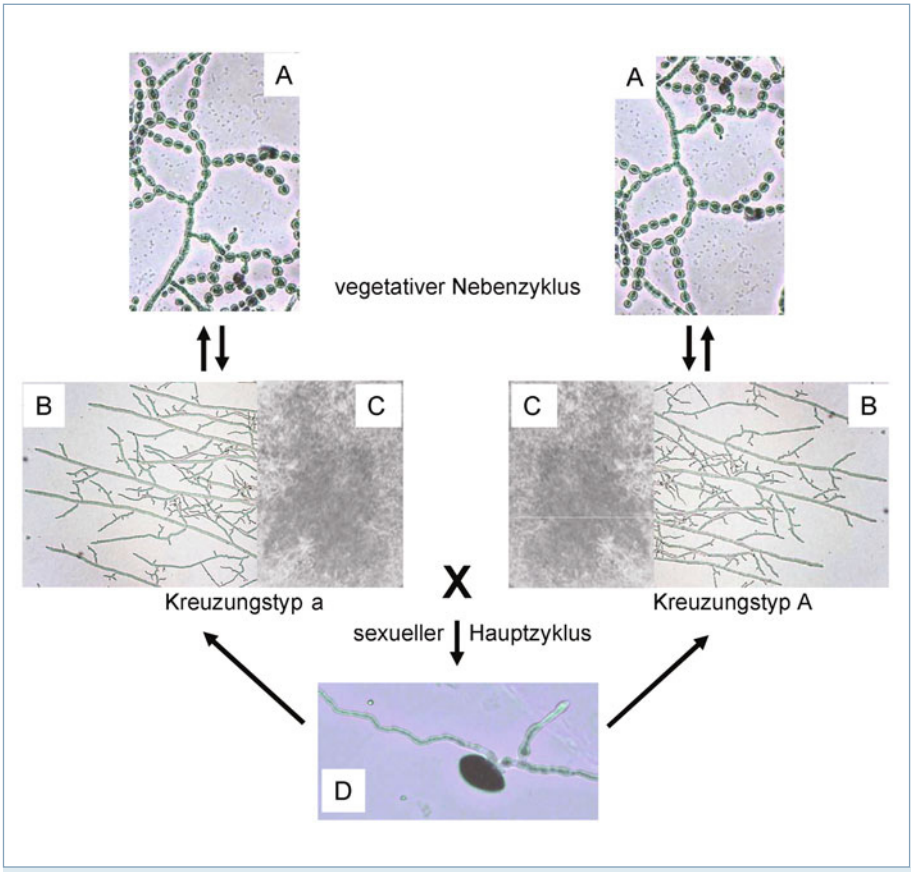

▲ **Abb. 1:** Lebenszyklus von *Neurospora crassa*. **A**, kettenförmig angeordnete (Makro-)Konidiosporen. **B**, vegetative Hyphen. **C**, Mycel. **D**, auskeimende Ascospore. Sowohl aus Ascosporen als auch aus Konidiosporen entwickelt sich ein septiertes Mycel. X = Kreuzung.

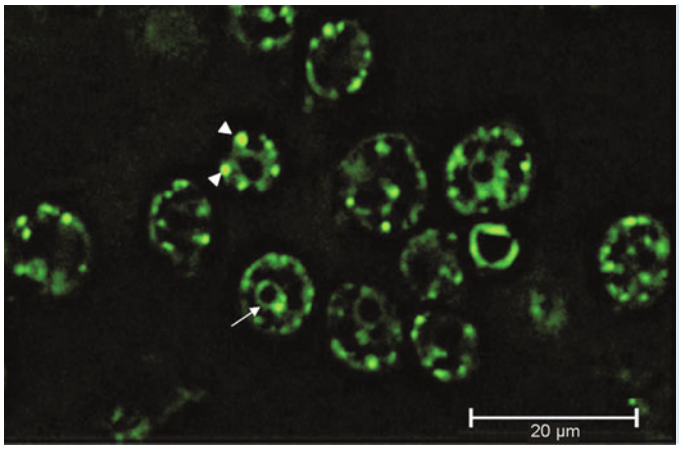

◀ **Abb. 2:** Interzelluläre Lokalisation des Bem46:eGFP-Proteins in Makrokonidien von *Neurospora crassa*. Die konfokale Laserrastermikroskopische Aufnahme zeigt eine Akkumulation des Proteins im perinukleären endoplasmatischen Retikulum (Pfeil) sowie in plasmamembrannahen Punkten (Dreiecke).

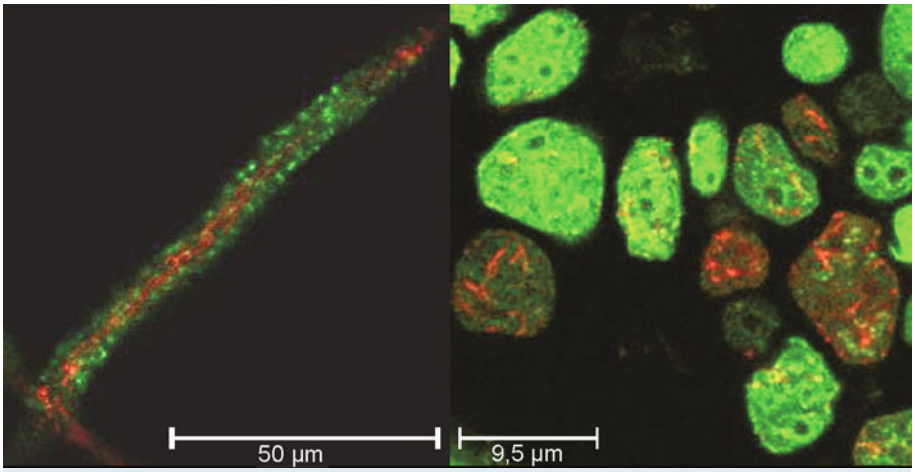

▲ **Abb. 3:** Konfokale Laserrastermikroskopische Aufnahmen von Hyphen (links) und Makrokonidien (rechts) eines Heterokaryons aus Bem46:eGFP- und lifeact:RFP-Transformanten. Heterokaryen zeigen keine Ko-Lokalisation des Bem46-Proteins mit dem Aktinzytoskelett.

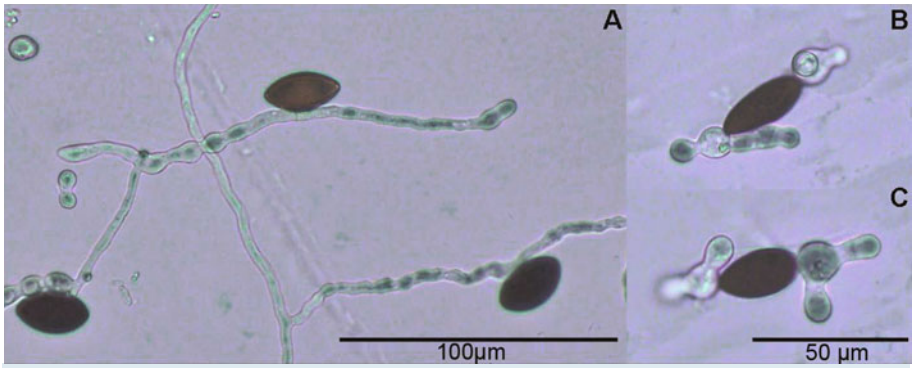

▲ **Abb. 4:** Lichtmikroskopische Aufnahmen keimender Ascosporen. **A**, Die aus den Ascosporen des Wildtyps keimenden Hyphen zeigen polares Spitzenwachstum. **B**, **C**, Dagegen wird die Entwicklung der Keimungshyphen der RNAi- (B) und Überexpressionstransformanten (C) kurz nach Auskeimung gestoppt. Die Hyphen enden zumeist in terminalen blasenartigen Strukturen, die auf eine verlorene Fähigkeit zum gerichteten Wachstum hindeuten.

dem besitzt der Pilz einen vegetativen Nebenzyklus, bei dem ein- oder mehrkernige Konidiosporen gebildet werden (**Abb. 1**). Sowohl aus den Konidien als auch aus den Ascosporen entwickelt sich ein septiertes Mycel, bei dem die Querwände einen zentralen Porus aufweisen, der den Durchtritt von Zellorganellen und Zellkernen erlaubt. Pilzhyphen weisen – wie z. B. auch pflanzliche Pollenschläuche oder tierische Neuronen – ein ausgeprägtes apikales Spitzenwachstum auf. Die subzelluläre Lokalisation des Bem46-Proteins in *N. crassa* wurde mithilfe von eGFP(*enhanced green fluorescent protein*)-Reporterkonstrukten untersucht. Das Bem46:eGFP-Protein zeigt einerseits eine Akkumulation im perinukleären endoplasmatischen Reticulum (ER) und andererseits nahe der Plasmamembran in punktförmigen Strukturen (**Abb. 2**). Färbungen der GFP-Transformanten mittels ER-TrackerRed haben die Lokalisation des Bem46:eGFP-Proteins im perinukleären ER bestätigt [7]. Eine zunächst vermutete Ko-Lokalisation mit sogenannten *actin patches*, den Anknüpfungspunkten des Aktinzytoskeletts an der Plasmamembran, bestätigte sich jedoch nicht. Die mikroskopischen Untersuchungen der aus den Bem46:eGFP- und lifeact:RFP-Transformanten [8] gebildeten Heterokaryen zeigten keine Überlagerung der beiden Fluoreszenzsignale, was eine Interaktion zwischen dem Aktinzytoskelett und Bem46 ausschließt (**Abb. 3**).

Um Hinweise auf die Funktion des Bem46-Proteins in *N. crassa* zu erhalten, wurden RNAi- und Überexpressionstransformanten phänotypisch analysiert. Beide Transformanten zeigten normale Konidienbildung und Konidienkeimung mit der Bildung von Mycelien. Dagegen führte sowohl die Herunter- als auch die Hochregulierung des Bem46-Transkripts zu einer abnormalen Ascosporenkeimung (**Abb. 4**). Die Keimungsrate der RNAi- und Überexpressionstransformanten war gegenüber dem Wildtyp drastisch reduziert, und nur sehr vereinzelt wurde die Keimung von Ascosporen beobachtet. Die lichtmikroskopischen Untersuchungen zeigten kurze Keimungsschläuche mit terminalen blasenartigen Strukturen, die auf eine verlorene Fähigkeit zum polaren Wachstum hindeuten. Daher ist von einer Rolle des Bem46-Proteins in *N. crassa* beim polaren Wachstum der aus den Ascosporen keimenden Hyphen auszugehen.

Unsere laufenden Experimente konzentrieren sich auf die Identifizierung von Interaktionspartnern des Bem46-Homologs in *N. crassa*. Die Bestimmung solcher interagierenden Proteine könnte wichtige Hinweise darüber liefern, auf welchem Wege Bem46 das polare Wachstum beeinflusst. Da Bem46-Homologe im eukaryotischen Reich universell vorkommen, sind diese Ergebnisse auch für Arbeiten an anderen Modellsystemen von Bedeutung. ■

Literatur

[1] Bork P (2000) Powers and pitfalls in sequence analysis: the 70 % hurdle. Genome Res 10:398–400
[2] Galperin YM, Koonin VE (2010) From complete genome sequence to 'complete' understanding? Trends Biotechnol 28:398–406

[3] Fiskerstrand T, H'mida-Ben Brahim D, Johansson S et al. (2010) Mutations in ABHD12 cause the neurodegenerative disease PHARC: an inborn error of endocannabinoid metabolism. Am J Hum Genet 87:410–417
[4] Ollis DL, Cheah E, Cygler M et al. (1992) The α/β hydrolase fold. Protein Eng 5:197–211
[5] Holmquist M (2000) Alpha beta-hydrolase fold enzymes structures, functions and mechanisms. Curr Protein Pept Sci 1:209–235
[6] Mochizuki S, Harada A, Inada S et al. (2005) The *Arabidopsis* WAVY GROWTH 2 protein modulates root bending in response to environmental stimuli. Plant Cell 17:537–547
[7] Mercker M, Kollath-Leiss K, Allgaier S et al. (2009) The BEM46-like protein appears to be essential for hyphal development upon ascospore germination in *Neurospora crassa* and is targeted to the endoplasmic reticulum. Curr Genet 55:151–161
[8] Berepiki A, Lichius A, Shoji JY et al. (2010) F-actin dynamics in *Neurospora crassa*. Eukaryot Cell 9:547–557

Korrespondenzadresse:
Prof. Dr. Frank Kempken
Christian-Albrechts-Universität zu Kiel
Abteilung Botanische Genetik und Molekularbiologie
Botanisches Institut und Botanischer Garten
Olshausenstraße 40
D-24098 Kiel
Tel.: 0431-880-4274
Fax: 0431-880-4248
fkempken@bot.uni-kiel.de
www.uni-kiel.de/Botanik/Kempken/fbkem.shtml

AUTOREN

Krisztina Kolláth-Leiß
1999–2002 Studium der Biologie, Eötvös Loránd Universität, Budapest, Ungarn. **2003–2008** Studium der Biologie an der Universität zu Kiel. Seit **2008** Dissertation bei Prof. Dr. F. Kempken.

Frank Kempken
1980–1985 Studium der Biologie an der Universität Bochum, **1988** Promotion bei Prof. Dr. Dr. h. c. mult. K. Esser, **1989–1990** Postdoc bei Prof. Dr. D. Pring, University of Florida, USA. **1996** Habilitation, **1996–2001** Hochschuldozent an der Universität Bochum. Seit **2001** Professur für Botanische Genetik und Molekularbiologie an der Universität zu Kiel, seit **2011** Vizepräsident der Gesellschaft für Genetik.